A high resolution record of ice-rafting from the Northeast Pacific

by

Antony Trevor Hewitt
B.Sc., University of Victoria, 1994

A Thesis Submitted in Partial Fulfillment of the
Requirements for the Degree of

MASTER OF SCIENCE

in the School of Earth and Ocean Science

We accept this thesis as conforming
to the required standard

[redacted]

Dr. B. D. Bronhold, Supervisor (Pacific Geoscience Centre)

[redacted]

Dr. E. Vanderflier-Keller, Departmental Member (School of Earth and Ocean Science)

[redacted]

Dr. A. J. Weaver, Departmental Member (School of Earth and Ocean Science)

[redacted]

Dr. P. T. Bobrowsky, Outside Member (British Columbia Geological Survey)

[redacted]

Dr. J. V. Barrie, External Examiner (Pacific Geoscience Centre)

Supervisor: Dr. Brian D. Bornhold

ABSTRACT

Ice-rafted debris (IRD) in marine sediments can provide considerable information on a number of aspects of the paleoenvironment, including the timing of continental ice advance and retreat, and also paleoceanography. In this study, five deep sea cores from the northeast Pacific were investigated, consisting of four from the Gulf of Alaska, and one from off northern Vancouver Island, British Columbia. The supply of IRD was evaluated in each of the cores based on the mass accumulation rate of coarse lithic material, and on Gamma Ray Attenuation Porosity Evaluator (GRAPE) density in one of the cores from the Gulf of Alaska. The provenance (source) and shape of IRD grains were also evaluated under a microscope. Together, the results provide a high-resolution, 800,000 year account of ice-rafting in the Northeast Pacific.

It was found that the Chugach and St. Elias mountains of Southern Alaska were the dominant source of IRD in the Gulf of Alaska cores, but at times there was an increased proportion of debris from southeastern Alaska and/or northwestern British Columbia (Alexander Archipelago - Queen Charlotte Sound). Such times are proposed to represent cold ocean conditions when a greater number icebergs calved from eastern sources survived melting to reach the more northerly core sites. Northwestern British Columbia (Queen Charlotte Sound) was the chief source of IRD in the core off northern Vancouver Island.

Periods of increased IRD flux in the Gulf of Alaska are concurrent with intervals of widespread continental ice advance in western North America during the last 40,000 years. This work suggests that many additional, older ice advance-retreat cycles occurred during the late Quaternary, and since the chronology extends beyond the range of radiocarbon dating it provides a detailed history of these events through the late Pleistocene. The single IRD event in the core off Northern Vancouver Island occurs out of phase with those recorded in the Gulf of Alaska cores, and in fact occurs during the initial stages of deglaciation of the shelf in that area. This may reflect a northward shift of the subarctic ocean gyre boundary, such that the surface ocean circulation favored iceberg transport over this core site during deglaciation, but not during full glacial conditions.

Fluctuations in IRD supply are concurrent between the four cores from the Gulf of Alaska, but in some cases the magnitude of IRD accumulation rates are quite different, in some cases. The close proximity of these core sites probably precludes paleoclimatic/oceanographic factors in producing this variability. Instead, it may be a result of random debris dumps off the top of icebergs.

Correlation between the IRD record and $\delta^{18}O$ record in Greenland ice (GRIP) reveals that IRD flux decreased markedly during especially long interstadials recorded in the GRIP core. These are the same interstadials that follow the North Atlantic Heinrich events. Correlation with the marine $\delta^{18}O$ isotope record (SPECMAP) shows that the 100,000 year cycle in ice volume, that dominates the SPECMAP record, is in phase with a 100,000 year cycle in IRD flux. The correlations with GRIP and SPECMAP suggest fluctuations in Laurentide ice volume and consequent forcing of the climate system are important factors controlling the timing of ice advance/retreat in northwestern North America on both 100,000 year time scales, and on suborbital time scales.

IRD was also deposited during several global interglacial intervals, including isotope stage 5e, but not during the Holocene. The shorter, higher frequency Dansgaard-Oeschger interstadials (those that occur between interstadials that follow the Heinrich events) have no correlative interstadials recorded in North Pacific IRD accumulation. There is also no IRD event associated with Younger Dryas time. These events likely have origins different from the climatic effects of ice volume oscillations.

Examiners:

[redacted]

Dr. B. D. Bronhold, Supervisor (Pacific Geoscience Centre)

[redacted]

Dr. E. Vanderflier-Keller, Departmental Member (School of Earth and Ocean Science)

[redacted]

Dr. A. J. Weaver, Departmental Member (School of Earth and Ocean Science)

[redacted]

Dr. P. T. Bobrowsky, Outside Member (British Columbia Geological Survey)

[redacted]

Dr. J. V. Barrie, External Examiner (Pacific Geoscience Centre)

[redacted]

TABLE OF CONTENTS

Abstract ii
Table of contents v
List of tables viii
List of figures ix
Acknowledgments x
I. Introduction 1
1. Lithic material in continental ice and icebergs 3
i.) Lithic material in continental ice 3
ii.) Debris content of icebergs 4
iii.) Iceberg deterioration and deposition of debris 6
2. Ice-rafted debris in the North Pacific: previous work 7
3. Late Quaternary glaciation in western North America 9
i.) Extent of glaciation 9
ii.) Chronology of glaciation 12
a.) Late Wisconsinan 12
b.) Middle Wisconsinan 13
c.) Early Wisconsinan 15
d.) Last interglacial 15
e.) Pre-Wisconsinan glaciations 16
4. The geology of coastal western North America 17
II. Methods 18
1. Evaluating the flux of IRD to the seafloor 19
2. GRAPE density approximation for the timing of IRD events 20
3. Petrology and shape of IRD grains 21
III. Results and Discussion 23
1. Unpredictable iceberg behaviour and its influence on IRD supply 25
2. Petrology and shape of IRD grains 26
i.) Petrology of IRD grains 26

ii.) Shape of IRD grains 31
3. IRD accumulation and implications for Alaska and British Columbia..... 35
i.) Chronology and extent of glaciation: Wisconsinan time 35
a). Glacial history inferred from cores in the Gulf of Alaska..... 35
b). Glacial history inferred from a core off northern Vancouver Island.. 40
ii.) Chronology and extent of glaciation: pre-Wisconsinan time 44
4. Paleoceanography..... 49
5. Global paleoclimatic implications: The last 115,000 years 54
i.) Previous work: globally synchronous suborbital climatic variability 55
ii.) Climatic variability in the Northeastern Pacific IRD record 58
a.) A mechanism for synchronous Northern Hemisphere
(and global) climatic events..... 59
b.) The core off northern Vancouver Island 69
c.) Comments on the glacial history of southern British Columbia 70
d.) The missing Younger Dryas and high frequency
Dansgaard-Oeschger cycles 71
iii.) Transmitting the climate signal to the Southern Hemisphere 72
6. The last interglacial period (isotope stage 5e) 76
7. The last 800,000 years 78
i.) Correlation of the IRD record to the SPECMAP isotopic record 79
ii.) A mid-Brunhes climatic transition 79
IV. Conclusions 80
Bibliography..... 85
Appendix A:
Mass of IRD (lithic debris in the size range 180-500 mm) in ODP-887..... 97
Appendix B:
Mass of IRD (lithic debris in the size range 180-500 mm) in PAR87A-01 98
Appendix C:
Mass of IRD (lithic debris in the size range 180-500 mm) in PAR87A-02 ...99
Appendix D:

Mass of IRD (lithic debris in the size range 180-500 mm) in PAR87A-10... 100

Appendix E:

Mass of IRD (lithic debris in the size range 180-500 mm) in PAR85-01..... 102

Appendix F: Petrology of IRD grains (500-5000 μm) in ODP-887..... 103

Appendix G: Petrology of IRD grains (500-5000 μm) in PAR87A-10..... 104

Appendix H: Petrology of IRD grains (500-5000 μm) in PAR85-01 105

LIST OF TABLES

Table 1. Percent composition of IRD grains in the >500 to <5000 μm size fraction in samples from ODP887 and from PAR87-10 (in the Gulf of Alaska) 28

Table 2. Percent composition of IRD grains in the >500 to <5000 μm size fraction in samples from PAR85-01 (off northern Vancouver Island) 29

Table 3. Petrology of pebbles (>5 mm) from cores PAR87A-1,2,10, and ODP 887, and cobbles from a dredge haul on Cowie Seamount (Gulf of Alaska) 30

Table 4. Grain shape of pebbles (>5 mm) and cobbles removed from the cores, and dredge hall from Patton-Murray seamounts in the Gulf of Alaska (see text for discussion) 34

LIST OF FIGURES

Figure 1. The study area, showing core locations and place names 2

Figure 2. The flux of ice-rafted debris to the northeast Pacific during the last 250,000 years 24

Figure 3. The percentage of granitic grains per sample (diamond markers) follows trends in total IRD concentration more closely than do other grain types 32

Figure 4. All grain types increase with increasing IRD flux 33

Figure 5. IRD mass accumulation rate (and GRAPE density in ODP-887) during the last 65,000 years 36

Figure 6. Major IRD events during the Early Wisconsinan 41

Figure 7. IRD events during the pre-Wisconsinan (135-250 ka BP) 46

Figure 8. Major interstadials during the last 250,000 years 47

Figure 9. Correlation between ODP-887 GRAPE density and the SPECMAP marine $\delta^{18}O$ record 48

Figure 10. The complete 800,000 year record of GRAPE density 50

Figure 11. The single short IRD event in PAR85-01 apparently occurs during an interval of reduced IRD accumulation in the Gulf of Alaska cores 52

Figure 12. Schematic diagram depicting the proposed paleoceanography 53

Figure 13. North Atlantic Heinrich events and correlation the GRIP ice core 55

Figure 14. Correlation of IRD mass accumulation rate (and GRAPE density in ODP-887) with GRIP $\delta^{18}O$ 60

Figure 15. Reorganization of atmospheric circulation during glacial maximum due the influence of large northern Hemisphere ice sheets 64

Figure 16. Correlation between IRD mass accumulation rate (and GRAPE density in ODP-887) with GRIP $\delta^{18}O$ during the last 250,000 years 76

ACKNOWLEDGMENTS

The author would like to express his appreciation to several individuals who have been especially helpful throughout the development of this work. First of all, my supervisor, Brian Bornhold, for his invaluable guidance and encouragement. I would also like to thank the other members of my thesis committee, Peter Bobrowsky, Eileen Vanderflier-Keller, Andrew Weaver, and Vaughn Barrie for their suggestions and review of the final work. Thanks are also extended to Darcy MacDonald for lending materials and results from his own work that made this work possible. Also to Tom Pedersen who allowed access to one of the cores for sampling.

Financial support to the author was from an NSERC grant to Brian Bornhold, a grant from the NOAA Scripps-Lamont Consortium on the Ocean's Role in Climate to Andrew Weaver, and Graduate Teaching Fellowships from the University of Victoria.

I. INTRODUCTION

Under favourable climatic conditions continental ice can extend to the coast where it may calve icebergs into the ocean. Some of the lithic debris originally entrained by glaciers on the continent can be 'rafted' out over the deep ocean and deposited as the icebergs drift and melt in the prevailing ocean currents. If the continental ice goes through phases of advance and retreat, there can be a corresponding increase and decrease in the flux of ice-rafted debris (IRD) to the seafloor, thereby indirectly reflecting the extent of glaciation. The nature of the marine terminus (tidewater glacier, floating ice tongue, or ice shelf) and surface ocean temperature also control the supply of IRD. Variations in the supply of IRD, and its provenance (i.e., its source location), can be evaluated in cores recovered from the deep ocean. This knowledge can then be related to the timing and extent of glaciation in regions that are thought to be likely sources for the debris, and ultimately it can provide information on the paleoclimate and paleoceanography of the region.

This work will present a high resolution record of ice-rafting from the Northeast Pacific, based on the mass accumulation rate of lithic material >180-500 μm, and on Gamma Ray Attenuation Porosity Evaluator (GRAPE) density. The cores investigated in this study were recovered from the Patton-Murray Seamount Group, in the Gulf of Alaska, and from a bathymetric high on the abyssal plain directly west of Explorer Ridge, off northern Vancouver Island (Figure 1). The results provide a detailed account of glaciation in coastal northwestern North America through the late Quaternary. The results are also compared to paleoclimatic and paleoceanographic records from the North Pacific and other parts of the world, including the $\delta^{18}O$ isotopic record in Greenland ice (GRIP) and in the marine sediment record (SPECMAP). Concurrent events between these records are proposed to be a result of forcing of the large scale ocean-atmosphere circulation by oscillations in the volume of the Laurentide ice sheet.

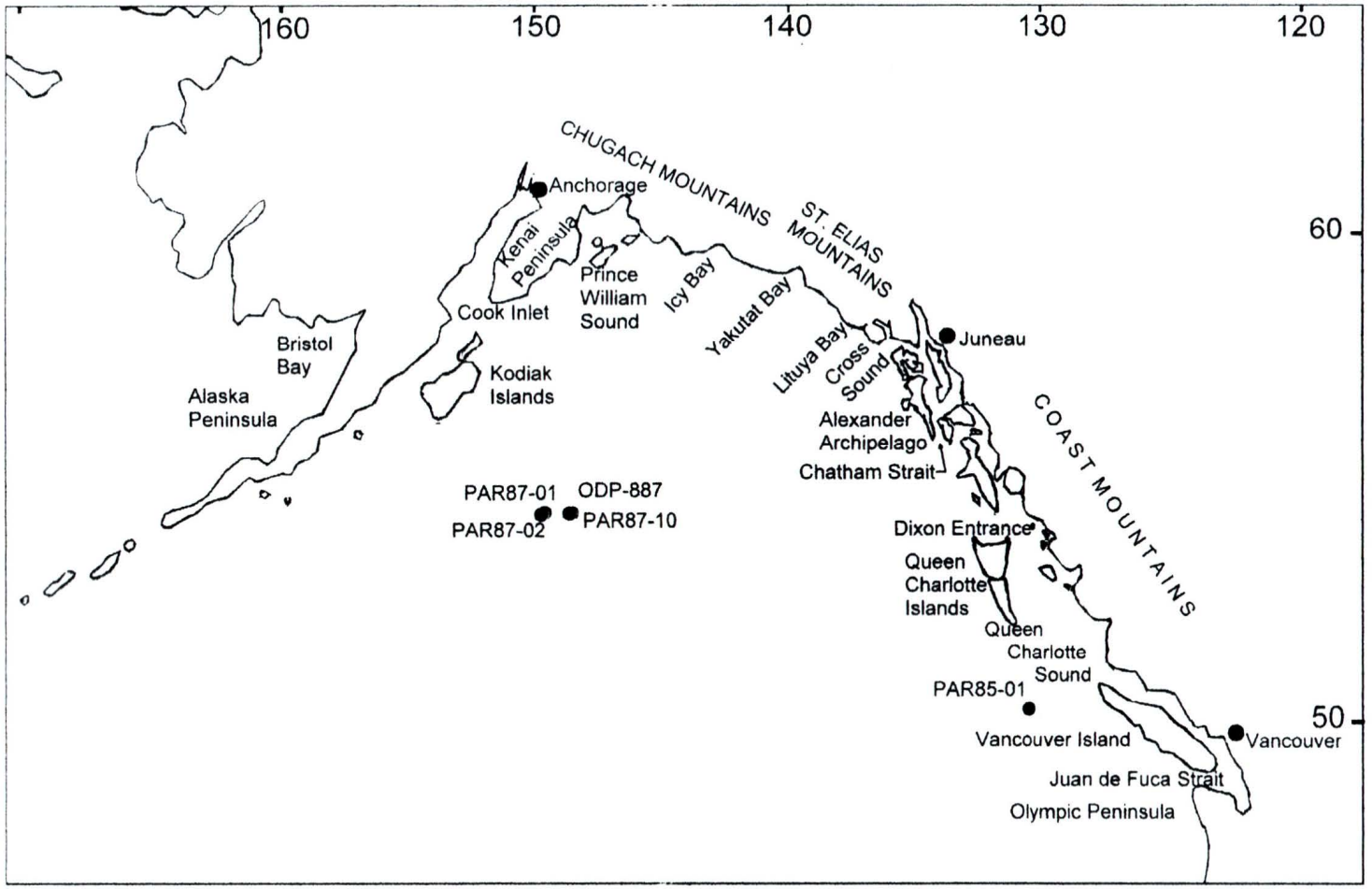

Figure 1. The study area, showing core locations (black circles) and place names referred to in text.

1. Lithic material in continental ice and icebergs

i.) Lithic material in continental ice

In glacier systems, sediment can be transported in a variety of ways: (1) in subglacial fluvial systems, (2) on and within the glacier ice, and (3) in deforming sediment below the ice. The relative importance of each depends on availability of debris and thermal conditions within the glacier system. In three modern Alaskan tidewater glaciers (temperate glaciers), Hunter *et al.* (1996) estimated sediment transport based on observations of the sediment distribution within the glaciers. In their study the most important is glaciofluvial transport (~$10^7 m^3$/year), followed by transport on and within the ice (up to ~$10^6 m^3$/year), and least important was transport in a layer of deformable sediment (~$10^5 m^3$/year). For ice-rafting, the most important path is the debris transported on and within the ice.

One process of debris entrainment into glacier ice is the freezing of basal water onto subglacial sediment. "Freeze-on" is dependent on the thermal regime at the base of the glacier and partly on the availability of debris. Extremes in thermal regime preclude high concentrations of basal debris; glaciers that are frozen to their beds are less erosive since there is no meltwater to allow freeze-on; hence, basal debris concentrations are low. Many Antarctic glaciers, for example, are frozen to their beds and observations have shown that they have low concentrations of debris (Warnke, 1970; Drewry and Cooper, 1981; Powell, 1984). On the other hand, ice streams, that feed ice shelves, and some glaciers in temperate climates have a very large area of basal melting. In this case, basal debris content is low because it is transported away by subglacial melt water (Alley *et al.*, 1989; Hunter *et al.*, 1996). Some present day glaciers in Glacier Bay, Alaska, have low concentrations of basal debris (Powell, 1984; Hunter *et al.*, 1996). A thermal regime between these two extremes, with alternate areas of melting and freezing, provides the largest volume of basal debris (Powell, 1984). Basal entrainment also depends on the nature of the geology underlying the ice. Clearly, easily eroded and/or poorly consolidated material is more readily entrained.

Debris can also be entrained supraglacially, that is, added to the top of glaciers through subaerial weathering of rock outcrops, and also from aeolian deposition. The

importance of supraglacial entrainment can be highly variable from one location to another, depending on the quantity and stability of rocks outcropping above the ice. In general, there are few outcrops above thick continental ice sheets, such as those covering Antarctica today, hence they contain relatively little supraglacial debris. On the other hand, the surfaces of alpine-valley glaciers are subjected to rock falls from valley walls, and can transport large volumes of supraglacial debris (Boulton, 1978). The proportion of supraglacial debris within the total debris content of glaciers depends on the width of the valleys through which the glacier flows and on the number of tributary glaciers that join the main flow (Hunter *et al.*, 1996). A narrow glacier, flowing through a narrow valley, will have a greater proportion of its surface covered by debris. The lateral moraines of tributary glaciers can be incorporated into the supraglacial and englacial debris loads where they join the main glacier.

At the glacier's terminus, supraglacial, englacial, and basal debris are released in a number of ways: most importantly (according to Hunter *et al.*, 1996) are the processes of melt out along the face of the ice cliff, dumping during calving, melt out along the terrestrial margins, and ice-rafting. In two of the glaciers studied by Hunter *et al.* (1996), 25% of the debris transported in the ice was removed via ice-rafting in one, and up to 96% in a second. Therefore, ice-rafting of debris is, and probably always has been, an important process in removing debris from glaciers in Alaska. Dowdeswell and Dowdeswell (1988) also observed high concentrations of supraglacial debris in icebergs calved from glaciers in Spitsbergen, in the high latitude North Atlantic.

ii.) Debris content of icebergs

The debris content of icebergs depends not only on the processes of entrainment and debris availability, discussed above, but also on the type of marine terminating ice mass from which the icebergs are released: floating ice shelves, floating ice tongues, and tidewater glaciers. Tidewater glaciers terminate in the tidal zone with the foot of an ice wall in contact with the seafloor. Ice shelves and ice tongues, on the other hand, are floating extensions of continental ice that extend beyond the grounding line. Ice floating on water spreads out rapidly under its own weight and eventually breaks up, allowing only small floating ice

tonuges to form, unless there are constraints on the rate of spreading. Powell (1984) and Alley *et al.* (1989) review a number of possible constraining factors that are thought to allow the formation of large ice shelves: (1) a confining embayment reducing lateral spreading; (2) topographic highs on the seafloor beneath the shelf can serve as "pinning points" where the ice is locally grounded; (3) particularly rapid flow from an inland ice sheet into the ice shelf to replenish mass lost through calving; and (4) cold temperatures that lead to ice with greater strength. Today, ice shelves and floating ice tongues are found only in polar latitudes, such as Antarctica and Greenland, but during Pleistocene glaciations they also occurred in subpolar latitudes. In contrast modern tidewater glaciers exist in both polar and subpolar climates, for example, in Antarctica, Alaska, Greenland, Norway, and Chile. Tidewater glaciers were also more common during Pleistocene glaciations.

In tidewater glaciers, calving occurs mainly through the breaking of slabs away from the face of the ice wall, caused mainly by the difference in hydrostatic pressure between ice and water at the calving front (Hughes, 1992). These slabs are roughly equal to the ice thickness in length, a few 10's of meters wide, and less than 10 m thick (Hughes, 1992). If the thickness is greater than the planar dimension, then the iceberg rolls over and quickly disintegrates into smaller bergs. In floating ice, the distribution of crevasses has an important control on calving. Fracture through crevasses typically leads to tabular icebergs that can be very much larger than the thin slabs that calve from tidewater glaciers. They typically have a thickness equal to ice thickness and much larger planar dimensions (Hughes, 1983).

Ice shelves may calve the largest bergs, but they contain relatively little debris (Warnke, 1970; Powell, 1984). This is due partly to the fact that the ice streams that feed them may be largely melted at the base with little freeze-on occurring (Alley *et al.*, 1989; Licht *et al.*, 1996), and because modern ice shelves are extensions of thick continental ice sheets which have few outcrops above the ice. It is also because ice shelves typically deposit most of their basal debris before the calving front due to net basal melting in the relatively warm ocean water within which they float (Powell, 1984). Consequently, the contribution of ice shelf bergs to the flux of IRD is relatively small. Conversely, both floating ice tongues and tidewater glaciers typically calve icebergs richer in debris than do ice shelves, since they

entrain more debris to begin with (previous section), and also because floating ice tongues are much smaller than ice shelves, and tidewater glaciers calve at the grounding line, both of which result in less basal melt out before calving. Tidewater glaciers may calve debris-rich bergs, but iceberg size is very much smaller than those calved from ice tongues. The small bergs melt more quickly releasing most of their debris close to their origin. Therefore, like ice shelf icebergs, the contribution to the flux of IRD in the open ocean from tidewater glaciers may not be that great either, depending on sea surface temperature, which also controls melting rate. Ice tongues, on the other hand, calve large, tabular, debris-rich bergs that survive in the open ocean for a long time, potentially providing the greatest contribution to the flux of IRD.

iii.) Iceberg deterioration and deposition of debris

In addition to the nature of the marine terminating ice mass, ocean and atmosphere temperature are also important controls on iceberg melting and the flux of IRD. When conditions are cold, iceberg melting and debris release is slower. Therefore, more icebergs are likely to have survived melting and drifting out into the middle of the ocean, and dropped more IRD into deep sea, during the cold stadials of a glaciation. Conversely, during relatively warmer interstadials, icebergs likely melted closer to their source and led to reduced IRD flux in the deep sea. The lowest supply of IRD is probably associated with interglacials, as in the Holocene, when more tidewater glaciers terminated within fjords, supplying few icebergs to the open waters. Furthermore, higher global sea level, and thus flooded continental shelves, increase the distance of warm water through which icebergs must travel in order to reach the deeper ocean.

As icebergs melt, debris can be released from the bottom, sides, and top. Debris is exposed on the surface and side walls as icebergs drift into regions where atmospheric temperature is >0°C. Below the water line waves and relatively warm water lead to accelerated melt out, supplying a quasi-steady rain of debris as the iceberg disintegrates. Melt out from the side walls also occurs as a semi-continuous rain out. Release from the top, however, is more episodic, characterized by periodic debris dumps when surface

accumulations become unstable, or when the iceberg rolls over as it deteriorates. Therefore, debris release from icebergs is irregular, with large episodic releases superimposed on a semi-continuous rain out; this behaviour may be important to the apparent supply of IRD to the seafloor. The close proximity of the cores on the Patton-Murray Seamounts allows an evaluation of the importance of this behaviour.

2. Ice-rafted debris in the North Pacific: previous work

The application of IRD as a paleoenvironmental indicator in the North Pacific has been rather limited, and most of the earlier work was concerned with establishing the long term trends in the flux of IRD over the last few million years. For example, in the 1970's work was done on DSDP leg 18 cores by Kent *et al.* (1971), followed by Creager and Scholl (1973), and Kulm *et al.* (1973). Rea and Schrader (1985) reanalyzed the early cores with application of a more rigorous chronology, based on diatom stratigraphy and paleomagnetism. The later studies place the date for the first occurrence of IRD at 4.5 Ma, and record a marked increase after 2.5 Ma.

The Ocean Drilling Program returned to the North Pacific in 1992 (ODP leg 145) and recovered cores from several sites. Preliminary results from these cores indicate ice-rafting was most intense in the eastern and western Pacific but less so in the mid-ocean (Rea *et al.*, 1993). In the west it appears that IRD was in greatest concentration near the entrance to the Sea of Okhotsk, indicating a Siberian and Kamchatka source (Rea *et al.*, 1993).

A few investigations of ice-rafted debris have concentrated on the late Quaternary: Griggs and Kulm (1969) identified IRD deposited in cores from as far south as the Cascadia basin off Oregon (several cores between 46-44°N). They did not quantify the IRD concentrations or develop a chronology, but they did find that the IRD petrology matched that of rocks in the coast mountains of southern British Columbia and Washington. The only likely source for this IRD is the Strait of Juan de Fuca, where an ice lobe terminated a the edge of the continental shelf during glacial maximum.

Von Huene *et al.* (1973,1976) concentrated on the last 800 ka in cores from the Gulf of Alaska. The quality of these early cores was not particularily good for paleoceanographic

work as they were recovered from the abyssal plain and continental slope, where turbidites are common. Also, the chronostratigraphy was poor, with only seven age control points through the last 800 ka. Despite these problems Von Huene *et al.* (1973, 1976), were able to make some interesting correlations.

Von Huene *et al.* (1976) identified 13 major intervals of increased IRD deposition, during the last 800 ka. In the first 250 ka there were 6 major intervals. They compared IRD abundance to other long records from around the world that existed at the time, and noted a general agreement between their record and European glacier advances, lake level fluctuations in California, SST reconstructions from the Gulf of Mexico, Caribbean oxygen isotope fluctuations, and the Camp Century ice core from Greenland (references in Von Huene *et al.*, 1976). Based on this, Von Huene an colleagues suggested that fluctuations in ice advance inferred from the IRD curve reflected increased northern hemisphere ice accumulation, on timescales of 10-15 ka.

Von Huene *et al.* (1973) examined 115 pebbles from gray muds recovered from the abyssal plain, and found that 95% were slate and graywacke, and the remainder were granitoid, schistose, and metavolcanic rocks. Kulm *et al.* (1973) described pebbles from one of these cores; 38% were slate, 20% medium sandstone and graywacke, 17% fine-grained sandstone, 17% quartzite, 4% amphibolite, 4% granodiorite. From a core on the continental slope, Von Huene *et al.* (1973) looked at 200 coarse sand grains and pebbles (<6 mm). Again, sedimentary grains, mostly slate and graywacke, predominated (70%), with fewer quartz grains, volcanics, metavolcanics, and granitoid rocks. Von Huene *et al.* (1973) and Kulm *et al.* (1973) found that the IRD petrology fit description of rocks from the Chugach-St. Elias Mountains.

Excluding Von Huene *et al.*'s (1976) work, there have only been two other IRD studies covering the Late Pleistocene in the North Pacific region. Blaise *et al.* (1990) recovered one core from ~200 km west of central Vancouver Island. This core was re-investigated in this study for the purpose of providing a clearer comparison between southern Alaska and western British Columbia. Kotilainen and Shakleton (1995) present a GRAPE density approximation of IRD abundance for the last 95 ka from the western North Pacific.

Their chronology was poor but their data do contain variability at a frequency similar to that seen in the $\delta^{18}O$ record from the GRIP ice core.

3. Late Quaternary glaciation in western North America

i.) Extent of glaciation

During the Late Pleistocene, glaciation in much of inland Alaska was alpine-valley in nature (Hamilton, 1994). The Cordilleran ice sheet, a mass of interconnected valley and piedmont glaciers, was confined mainly between the Coast and Rocky mountains of British Columbia, where, in some areas, it may have reached a thickness in excess of 2 km during glacial maxima (Clague, 1989). Along the coast, in both Alaska and British Columbia, individual glaciers flowed down valleys onto the continental shelf; in some locations these glaciers coalesced to form larger complexes that crossed to the shelf edge, but did not form a marine ice sheet. An exception may have been along the southwestern Alaska Peninsula where equilibrium line altitudes near sea level allowed individual glaciers that originated on mountain peaks to cover the narrow continental shelf (Mann and Peteet, 1994). East and south of the Alaska Peninsula, there were many ice-free areas on the shelf.

East of the Alaska Peninsula, glaciers flowed into upper Cook Inlet from the surrounding mountains, and at times these glaciers calved into tidewater, either as individual glaciers or a coalesced complex; however they never filled the inlet during the Wisconsinan (Hamilton, 1994). Subdued moraines in Cook Inlet beyond the limit of Wisconsinan advances are thought to have been deposited prior to isotope stage 5e (Hamilton, 1994). East of Cook Inlet ice reached the shelf edge in major valleys (now submarine valleys) cut by large glaciers during low sea level stands (Carlson *et al.*, 1982). The lack of evidence for ice erosion on the upland areas between these valleys suggests that much of the shelf was ice-free during the Pleistocene, or at least, had a non-erosive ice cover (Molnia, 1986; Mann, 1986a). The reason for this is likely two-fold. First, the high relief in coastal areas resulted in concentration of ice into discrete valleys forming a few outlet glaciers which traversed the shelf (Mann, 1986a). Secondly, the presence of unglaciated, or thinly glaciated, areas on the

shelf also indicates that temperatures were not cold enough for these regions to be important accumulation areas. In the eastern Gulf of Alaska, in the islands of the Alexander Archipelago, field data suggest that a Late Pleistocene glacier system was formed by outlet glaciers flowing from mainland ice onto the shelf through the fjords that dissect the archipelago today, and also through Dixon Entrance (Mann, 1986a; Barrie and Conway, 1993). Small mountain ice caps on the inner islands of the archipelago may have coalesced with mainland ice, but in the outer islands local uplands and parts of the shelf probably remained ice-free; glaciers only reached the shelf edge through the major fjords (Mann, 1986a).

On the Queen Charlotte Islands, the provenance of tills is predominantly of island origin, suggesting local ice was of great importance during glaciation. At times, however, mainland ice did impinge on the east coast (Warner *et al.*, 1984). From there, ice flowed around the islands out to the shelf edge, through Dixon Entrance to the north, and Queen Charlotte Sound to the south (Barrie and Bornhold, 1989; Luternauer and Murray 1983; Barrie and Conway, 1993). Dixon Entrance is a wide, glacially cut valley between the Alexander Archipelago and the Queen Charlotte Islands. In Queen Charlotte Sound grounded glaciers carved three troughs through the continental shelf out to the shelf break (Luternauer and Murray 1983; Josenhans *et al.*, 1993). It is not certain if the banks between the troughs in the sound show evidence of glaciation (Josenhans *et al.*, 1993). At the shelf break icebergs were calved into open waters. Luternauer and Murray (1983) and Barrie and Bornhold (1989) identified iceberg scours in Queen Charlotte Sound and Hecate Strait, indicating ice retreated in contact with the ocean as eustatic sea level rose during the early stages deglaciation.

In southern British Columbia, Cordilleran ice flowed into Georgia Strait and was at times thick enough to flow over Vancouver Island in places. For example, Howes (1981, 1983) has described glaciation on central-northern Vancouver Island. There, during glacial maxima, mainland ice coalesced with and overtopped local ice as it flowed west to the coast. South of Queen Charlotte Sound, and north of Juan de Fuca Strait, there are no troughs cut to the shelf edge, or other unequivocal evidence of glaciation, suggesting the outer shelf was

unglaciated (Bornhold and Barrie, 1991). On southern Vancouver Island, till is dominated by debris of local origin, but there is also a low percentage (2 - 4%) of material from the mainland, indicating that during glacial maxima mainland ice flowed over southern Vancouver Island (Alley and Chatwin, 1979). On the shelf, large glaciers flowed out of what are now Barkley Sound and Juan de Fuca Strait. At least once during the late Quaternary these glaciers coalesced and carved a trough out to the shelf edge (Herzer and Bornhold, 1982). A second lobe of Cordilleran ice in southern British Columbia, the Puget Lobe, flowed southward into the Puget Lowlands of northern Washington, but there was no tidewater glaciation at the edge of the continental shelf south of Juan de Fuca Strait.

Very little is known about the glacial history of Kamchatka, Northeastern Siberia, and the region of the Bering Sea that was exposed during low sea level stands. Mapping of glacial deposits in Northeastern Russia, and a lack of isostatically uplifted shorelines in Northwestern Alaska, Chukotka, or on St. Lawrence Island indicate that no large ice sheets were present, and that glaciation was probably limited to small mountain glacier complexes isolated in upland areas (Heiser *et al.*, 1995). Glaciers extended to tidewater in Kamchatka, and their history would certainly be important for IRD studies in the west Pacific (for example, Kotilainen and Shackleton, 1995). However, it is highly unlikely that even the largest icebergs calving from Kamchatka glaciers would reach the eastern Pacific since predominant ocean currents would first take them south through increasingly warmer waters.

Based on the above discussion, it is likely that there was an extensive length of at least quasi-continuous calving ice fronts along the Alaskan Peninsula. However, it is unlikely that this region supplied as much IRD to the Gulf of Alaska core sites as did sources farther east, since ice on the peninsula was calving into waters "down stream" from their location. The fast flowing Alaska Stream would have carried icebergs to the west. Elsewhere along the Late Pleistocene coastline of western North America, calving fronts were narrower and separated by unglaciated regions. If ice only reached the edge of the continental shelf in a few valleys in the coastal regions east and south of the Alaska Peninsula, then it is of special relevance to this study: the glaciers flowing through these valleys are likely to have been main sources of icebergs in the Northeast Pacific, and it follows that debris entrained from the terrain through which the parent glaciers flowed will

characterize the ice-rafted debris at the core sites.

ii.) Chronology of glaciation

a.) Late Wisconsinan

Dates from numerous glacial deposits in coastal Alaska suggest the late Wisconsinan glaciation began after 29,000 radiocarbon years ago ("29 ka-^{14}C-BP"), and major advances across the shelf were underway by 23 ka-^{14}C-BP (Denton, 1974; Hamilton, 1994; Mann, 1986a; Mann and Peteet, 1994). Glaciers reached their maximum extent before 16 ka-^{14}C-BP, and were retreating sometime thereafter (Mann, 1986a, Mann and Peteet, 1994). Along the southern Alaska Peninsula, glaciers had retreated from the outer shelf by 14.7 ka-^{14}C-BP (Mann and Peteet, 1994). Glaciers had completely retreated off the shelf throughout Alaska by 10 ka-^{14}C-BP (Molnia, 1986). During deglaciation, a brief, but widespread readvance after ~13.5 ka-^{14}C-BP is recognized in Alaska. For example, end moraines deposited during a late advance in the Brooks Range dated from 13-11.5 ka-^{14}C-BP (Hamilton, 1994), and a late advance before 11.5 ka-^{14}C-BP is recognized in the mountains of Seward Peninsula (Hamilton, 1994). The event is also preserved in coastal areas. For example, Mann and Peteet (1994) describe two sections that contain evidence of an advance on southern Kodiak Island at 13.4 ka-^{14}C-BP. They suggest this event is associated with a readvance of the local ice cap on Kodiak Island. In Cook Inlet, end moraines of a final advance date between 14.7-11.7 ka-^{14}C-BP (Schmoll *et al.*, 1972). Raised beaches south of Glacier Bay and near Juneau record a period of reduced isostatic rebound beginning around 13.4 ka-^{14}C-BP (Hamilton, 1994), and Mann (1986a) describes a lateral moraine that includes a log dated at 12.4 ka-^{14}C-BP from the Lituya Bay area.

The Queen Charlotte Islands and northern Vancouver Island shared a glacial history similar to that experienced by Alaska's southern coast. According to Blaise *et al.* (1990) Cordilleran ice crossed to the Queen Charlotte Islands between 23-21 ka-^{14}C-BP, reached its maximum extent before 16 ka-^{14}C-BP, and was retreating thereafter. Ice had completely retreated from Dixon Entrance and Queen Charlotte Sound by 13.6-12.9 ka-^{14}C-BP (Barrie

and Conway, 1993; Luternauer *et al.*, 1989a, 1989b). Hebda (1983) also found that parts of northern Vancouver Island were ice-free by 13.6 ka-^{14}C-BP. There is no record of a deglacial readvance of glaciers in this area at around 13.5 ka-^{14}C-BP.

A chronologic record exists for the late Wisconsinan glaciation in southwestern British Columbia and northern Washington (called the Fraser Glaciation in that area). Three distinct ice advances during the Fraser Glaciation are recognized; they are the Evans Creek advance, the Vashon advance, and the Sumas advance. The Evans Creek advance reached its maximum after 22 ka-^{14}C-BP and retreated before 18 ka-^{14}C-BP (Easterbrook, 1992). During the Vashon advance, ice reached its late Wisconsinan maximum in this area, at ~15 ka-^{14}C-BP (Hicock *et al.*, 1982; Easterbrook, 1992). The Sumas advance was a short readvance during deglaciation at 11.3-10 ka-^{14}C-BP (Easterbrook, 1992). There are other dates for late readvances throughout British Columbia. For example, Alley and Chatwin (1979) proposed an advance, or at least a halt in retreat, on southern Vancouver Island before 13 ka-^{14}C-BP. However, many of the other deglacial readvances in the south occurred at different times, such as the Sumas advance.

b.) Middle Wisconsinan

Throughout northwestern North America, there is abundant evidence for a lengthy interstadial interval during the middle Wisconsinan, locally called the Olympia Nonglacial Interval, and a considerable number of radiocarbon dates give some indication of its history. In many areas glaciers retreated out of lowlands, where nonglacial sediments were deposited. The event is recognized on Graham Island (the more northerly of the Queen Charlotte Islands) where a peat layer dating from 45.7-27.5 ka-^{14}C-BP is bracketed by till (Warner *et al.*, 1984). Nonglacial deposits on northern Vancouver Island date between 40.9-25.2 ka-^{14}C-BP (Howes, 1981, 1983), and in southern British Columbia glaciation may have begun before 50 ka-^{14}C-BP (Alley and Chatwin, 1979, Clague *et al.*, 1980). Pollen assemblages on the Olympic Peninsula indicate an interstadial between >47-28 ka-^{14}C-BP (Heusser, 1977). The event is recognized in many areas of British Columbia, including the Rocky Mountains (Jackson *et al.*, 1989; Bobrowsky and Rutter, 1992).

According to Hamilton (1994), extensive ice advances of the late Wisconsinan obliterated most middle Wisconsinan glacial deposits in southern Alaska, but some areas may have remained glaciated throughout Wisconsinan time, including the Olympia interval. There are, however, a few indications of an interstadial; for instance, in interior regions of Alaska, a period of ice retreat is recognized (Hamilton, 1994, and references therein). In coastal regions, evidence for ice retreat in the mid-Wisconsinan is more sparse, but near Juneau a peat bed beneath glaciomarine deposits is >39 ka-^{14}C-BP and may have been deposited during an interval when glaciers retreated from inner fjords (Mann, 1986a). Mann (1986a) also identified three Wisconsinan drifts near Lituya Bay. The oldest drift overlies peat with an interglacial pollen content. The peat dates to >72 ka-^{14}C-BP (enriched radiocarbon date), and the drift is therefore assigned to the early Wisconsinan. The second and third advances are both late Wisconsinan (<30 ka-BP). Farther west, Goethcheus (1995) describes a paleosol preserved beneath tephra (not drift or till) on the northern Seward Peninsula, dated to >42-30 ka-^{14}C-BP. Lea *et al.* (1991) described a sequence containing two interstadial layers deposited beneath loess in southwestern Alaska, in the Bristol Bay area. There are no absolute dates, but the faunal and floral evidence indicates these interstadial layers were deposited during intervals cooler than present. Therefore, Lea *et al.* (1991) suggest they occurred after isotope stage 5e.

A few studies have proposed ice advances during Olympic time in British Columbia and Washington, but they are all single accounts from one locale (see Clague, 1981). For instance, Easterbrook proposed an advance in the Puget Lowlands, but there is no record of advance in southern British Columbia at this time (see discussion by Fulton *et al.*, 1976, and reply by Easterbrook). Given the variable climate of the time, advances and retreats in alpine areas were likely, but there is little evidence for such an event, probably because the deposits of such advances have been thoroughly eroded by the Fraser advances. Blaise *et al.* (1990) noted a minor IRD layer dated at ~37 ka-^{14}C-BP in a deep sea core off Northern Vancouver Island, representing tidewater glaciation somewhere on the continental shelf, presumably in Queen Charlotte Sound, during Olympia time. There are several tills preserved beneath the latest Wisconsinan till in Queen Charlotte Sound, suggesting earlier advances, but they remain undated (Josenhans *et al.*, 1993).

The climate of this mid-Wisconsinan nonglacial interval has been reconstructed based on pollen and other biostratigraphic evidence (reviews by Clague, 1977, 1981). Although it is generally considered to be an interstadial period, it was apparently characterized by marked swings in climate: at times it was as cold as during full glacial conditions, and at other times almost as warm as present. Therefore, northwestern North America, like many other parts of the world, was characterized by significant oscillations in climatic conditions during middle Wisconsinan time. The record of IRD flux presented here will provide a chronology of these oscillations.

c.) Early Wisconsinan

At least one early Wisconsinan advance was widespread throughout western North America (Reviews by: Clague, 1989; Jackson *et al.*, 1989; Bobrowsky and Rutter, 1992; Easterbrook, 1992; Hamilton, 1994). Although Hamilton (1994) noted that in some places it appears that the last major advance before the Late Wisconsinan occurred prior to isotope stage 5e (therefore pre-Wisconsinan), in most places investigators have assigned deposits of a major advance to stage 4. There were apparently two phases of advance at this time in the central Brooks Range, Alaska (Hamilton, 1994), and in the Alaska Range (Thorson, 1986; Kline and Bundtzen, 1986). Kaufman *et al.* (1996) present a chronology based on several dating techniques, in addition to stratigraphic evidence, for the Bristol Bay region, on the north side of the Alaska Peninsula. They dated a major early Wisconsinan advance thought to have occurred sometime between 75-90 ka-BP. The extensive advances older than this were likely deposited prior to isotope stage 5e (Kaufman *et al.*, 1996).

d.) The last interglacial

Marine isotope stage 5 (~75-135 ka-BP) is a period in the Late Pleistocene during which global ice volume was relatively low compared to stage 4 and 6. Stage 5e (~115-135 ka-BP) corresponds to the last interglacial maximum. A few continental deposits of 5e age contain information on conditions in Alaska at that time. For example, Brigham-Grette and

Hopkins (1995) describe beach terraces on Alaska's northeastern coast that are thought to date from the high sea level stand of stage 5e. Mollusk and ostracod assemblages indicate temperatures were warmer than present in coastal waters, and peat layers, interbedded with the beach deposits, contain pollen that suggest continental temperatures warmer than present. Furthermore, ice deformation features that develop in Holocene beach deposits are only found ~150 km farther north in 5e deposits. From Siberia, Lozhkin and Anderson (1995) provide a synthesis of palynological data that indicate forests expanded inland and northward, and coastal Siberia experienced summer temperatures 4-8°C warmer than present. Winter temperatures, on the other hand, were similar or only slightly warmer than present. Precipitation was probably slightly higher than today, and the expansion of one tree, *Larix dahurica*, indicates deeper snow cover. Hicock (1990) reviewed evidence for proposed stage 5e deposits in southern British Columbia and Northern Washington, where abundant Douglas Fir pollen indicates a 5e climate similar to present.

Information about 5e interglacial conditions is also provided by the GCM of Harrison *et al.* (1995), which simulates Northern Hemisphere climate. Harrison *et al*'s. (1995) experiment was chiefly a sensitivity study on the effect of insolation changes. At the beginning of 5e, summer insolation was higher, and winter insolation lower. At the end of stage 5e the situation reversed: summer insolation was lower, and winter insolation higher. With this prescribed insolation trend, Harrison *et al.*'s model suggests a climate for southern Alaska at the beginning of stage 5e, in which winters were 1-2°C warmer than present, and summers 1-2°C warmer (inferred from their figure 3), and precipitation was reduced in western Alaska. The latter half of stage 5e, on the other hand, had a cooler, wetter climate than the earlier half; winter temperatures were about the same, summers were 2°C cooler, and precipitation was more like today's. In so far as glacier mass balance is concerned, precipitation similar to present, and cooler summer temperatures, might lead to more extensive glaciers at the end of stage 5e.

e.) Pre-Wisconsinan glaciations

Clague (1989), Jackson *et al.* (1989), Bobrowsky and Rutter (1992), Easterbrook,

(1992), and Hamilton (1994) have all reviewed evidence of proposed pre-Wisconsinan advances in western North America. All these authors caution readers that there is little chronostratigraphic control on the timing of these early advances and so many correlations between areas are speculative. According to Jackson *et al.* (1989), confident correlations are also hampered by the discontinuity of drift sheets, even over short distances, resulting in "considerable disagreement and confusion regarding the number of glaciations". Nevertheless, some similarities between regions are apparent: in most areas there were two or more pre-Wisconsinan advances during the Pleistocene. In some cases these advances seem to be concurrent with Laurentide advances. The oldest major pre-Wisconsinan advance during the Pleistocene is pre-Brunhes-Matayama (>750 ka-BP) and is, therefore, early Pleistocene in age (Jackson *et al.*, 1989; Hamilton, 1994). Various techniques have produced dates that converge on the middle Pleistocene (400-500 ka-BP) for the younger pre-Wisconsinan advance (Jackson *et al.*, 1989; Hamilton, 1994).

The large uncertainty in assigning the age of these older drifts, and the likely incompleteness of the records, suggests that there could have been many glacial advances within the general time frame of the pre-Wisconsinan glaciations. Von Huene *et al.* (1973, 1976; section I.2.) recorded many fluctuations in the concentration of IRD from the Pleistocene in deep-sea cores from the Gulf of Alaska. The continuous and well dated record of ice-rafting to be presented here should help resolve the timing of late Quaternary glacial history in coastal western North America.

4. The geology of coastal western North America

The likely source of IRD grains recovered from the northeast Pacific would be the rocks seaward of the paleo-ice divides in the coastal mountain ranges of southern Alaska and western British Columbia. Therefore, a brief summary of the geology in these regions is appropriate.

Plafker *et al.* (1994) and Gehrels and Berg (1994) have recently reviewed the geology of southern Alaska, concluding that it is predominantly constructed from accreted terranes, namely the Chugach, Prince William, Ghost Rocks, and Yakutat terranes. Farther east, the

geology of the Alexander Archipelago and northwestern-most British Columbia is dominated by the Alexander terrane, and the Coast Plutonic Complex (Coast Mountains Batholith).

The Ghost Rocks Formation outcrops in a 10 km wide belt along the south coast of the Kodiak Islands. It underlies a total onshore and offshore area of about 6000 km^2. The lithology comprises an assemblage of deformed sandstone, mudstone, volcanics, and minor pelagic limestone (upper Cretaceous-Paleocene). Prince William terrane is made up of deep-sea-fan flysch, subordinate oceanic volcanics (15-20% of the total area), and minor hemipelagic mudstone (upper Paleocene-middle Eocene). It outcrops in a belt more than 100 km wide and extends from western Prince William Sound to directly east of the Copper River, and across the continental shelf between these points. The Chugach terrane (Mesozoic) is 60-100 km wide and extends 2,100 km around the Gulf of Alaska from the Alaska Peninsula to Catham Strait in the Alexander Archipelago. The most common rocks in this terrane are classified as flysch and oceanic basalt, both metamorphosed to variable extents. There is also a lesser amount of melange. The flysch and basalt make up approximately 90% of the area of the Chugach terrane. Basalt is relatively uncommon, but the proportion of basalt versus flysch increases from west to east. Basalt is uncommon west of the Chugach mountains, where flysch dominates, but increases in proportion toward the eastern Chugach mountains. The flyschoid rocks consist of slope, fan, and deep sea sediments. These rocks are relatively unaltered west of Kodiak Island, but to the east the extent of metamorphism increases progressively. Other rock types include subordinate amounts of argillite, tuff, tuffaceous argillite, siliceous argillite, chert, and gray carbonates, all metamorphosed to varying degrees. The Yakutat terrane consists mainly of continent-derived sedimentary rocks (Cenozoic), minor coal, and some marine sediments.

Gehrels and Berg (1994) reviewed the regional geology of southeastern Alaska and the adjacent regions of British Columbia. The geology is comprised of a variety of sedimentary, plutonic, and volcanic rocks, metamorphosed to different extents. The main difference between the geology of this region and geology of southwestern Alaska is the much greater proportion of granitoid rocks. The geology in the coast mountains is dominated by the Coast Plutonic Complex, or Coast Mountains Batholith as it is called in the United

States. Metavolcanics and metasedimentary rocks comprise about 20% of the complex whereas rocks of granoditoid composition make up most of the remaining 80% (Gehrels and Berg, 1994). West of the Coast Mountains lies the heavily glaciated Alexander Archipelago. In the northern archipelago, suites of Cenozoic plutonic rocks dominate. They are predominantly of granodioritic composition, but monzonite, quartzdiorite, diorite, and gabbro are also present. The Chugach terrane that dominates southwestern Alaska outcrops in a few locations in northern Alexander Archipelago, but is absent south of Catham Strait. In the southern archipelago the Alexander terrane dominates, although it also outcrops north of Catham Strait. Rocks of the Alexander terrane (Paleozoic and Mesozoic in age) include metamorphosed rhyolite, andesite, and basaltic volcanic rocks. Rhyolitic rocks are less common in the northern islands whereas mafic-intermediate rocks are more common farther south. Argillite and metasedimentary rocks are also widespread throughout the terrane. Along the western flank of the Coast Plutonic Complex are small outcrops of the Gravina and Taku terranes. The Gravina terrane consists mainly of upper Jurassic to mid-Cretaceous argillite, graywacke, andesitic, and basaltic rocks, along with lesser amounts of quartz diorite, dunite, and peridotite. Taku terrane is comprised of metarhyolite, metabasalt, and metasedimentary rocks (Mesozoic).

Two conclusions of potential importance to IRD provenance can be gleaned from the review of the regional geology. (1) Granitic rocks are relatively uncommon west of Alexander Archipelago, whereas they are very common in western British Columbia. Granitic material, therefore, may be expected to dominate the petrology of IRD grains in cores off Vancouver Island. (2) West of the Alexander Archipelago the geology is predominantly composed of fine grained sedimentary and metasedimentary rocks, and fewer volcanic and metavolcanic rocks. These would likely dominate the petrology of IRD grains deposited on the Patton-Murray Seamount Group.

II. METHODS

Four of the cores studied in the course of this work were recovered from the Patton-Murray Seamount Group: PAR87A-01, PAR87A-02, PAR87A-10, and a composite of ODP

site 887 cores (ODP leg 145). A thorough chronostratigraphy has been established for these cores, based on radiocarbon dates, oxygen isotope and carbonate stratigraphies (MacDonald, 1996, and also in Zhan *et al.*, 1991). PAR87A-01 extends to a depth corresponding to ~150 ka, PAR87A-02 was investigated only to a depth corresponding to ~30 ka, PAR 87A-10 extends to ~110 ka, and the chronology in ODP 887 extends to ~800 ka. Samples of 10-16 cm^3 were removed from these cores every ~5 cm along their entire length using a syringe 25 mm in diameter and 8 cm^3 cubes. The exception was ODP 887 which was sampled every ~5 cm for the last 250 ka. A fifth core, PAR85-01, recovered from just west of Explorer Ridge, off the coast of northern Vancouver Island, was previously analyzed for IRD flux by Blaise *et al.*, (1990). The samples from this core were re-examined for the purpose of comparison, although the record only covers the last 60 ka. There are no $\delta^{18}O$ data for this core and the chronostratigraphy is based solely on six radiocarbon dates. At depths older than the range of radiocarbon dating the age model was extrapolated to ~55 ka-^{14}C-BP assuming a constant sedimentation rate.

1. Evaluating the flux of IRD to the seafloor

In order to quantify the amount of IRD, each sample was sieved to separate the coarse, most likely ice-rafted grains, from the finer material. This alleviates the problem of having to determine the origin of the finest material. Discounting the finest material will not effect stratigraphic occurrence and still allows a relative measure of IRD flux at different levels within the core. The remaining coarse material is the ice-rafted fraction and can be represented quantitatively in a number of ways. For example, as mg/g, lithic grains/g, grains/cm^2/ka, or g/cm^2/ka (mass accumulation rate). Biogenic material (diatoms, foraminifera, and radiolarian tests), that often fall into the sand size range, must be removed in order to use a representation that involves determining the mass of IRD.

The mass accumulation rate of IRD was chosen for this study. This technique has been described by Keany *et al.* (1976). Samples were first washed through a 180 μm sieve, to remove the fine material, sonicated, then acid washed to remove foraminifera. This procedure, along with discounting material <180 μm, removes all foraminifera and virtually

all diatoms and radiolarians, leaving behind the coarse lithic material. The samples were then dried and resieved at 500μm and 180 μm. The material retained within the size range of 180μm-500μm was weighed and the value taken as the mass of IRD used to calculate mass accumulation rate as follows: **A = M / (V/R)**. Where **A** = mass accumulation rate ($g/cm^2/ka$), **M** = grams of ice-rafted debris. **V** = sample volume (cm^3), **R** = sedimentation rate (cm/ka). The reason for not considering the material >500 μm in the calculation is that large pebbles that are encountered in cores would distort the within core variation in mass accumulation rate (Keany *et al.*, 1976) i.e., a few large grains in one sample would result in a large mass, and consequently an unrealistically high accumulation rate.

2. GRAPE density approximation for the timing of IRD events

GRAPE (Gamma Ray Attenuation Porosity Evaluator) density was determined on board during ODP leg 145. Kotilainen and Shackleton (1995) have shown at ODP sites 882 and 884 that GRAPE density might be a useful approximation of ice-rafting in the western North Pacific. The technique measures the attenuation of gamma rays passed through the core at 3 cm intervals and relates it to density. Attenuation is determined by grain density and size, and sediment porosity. Coarse lithic grains are dense and therefore result in greater attenuation and greater GRAPE density. Fine muds with relatively few plankton tests also have low porosity and may also produce high GRAPE density. This might lead to relatively high GRAPE density in the interglacial northeast Pacific, when coarse terrestrial input to the core sites was greatly reduced. The highest values of GRAPE density occur where coarse grains lie within a muddy matrix with few plankton tests; i.e., layers rich in IRD. To test the accuracy of the approximation, the GRAPE density time series was compared with the mass accumulation rate results of the first 250 ka-BP. This may reveal that GRAPE density can serve as a high resolution proxy for ice-rafting that could be used to continue the IRD record to 800 ka-BP in ODP 887 without the time consuming process of a grain size analysis.

3. Petrology and shape of IRD grains

The lithology of the coarsest IRD found within the cores was determined and compared to descriptions of continental rocks around the North Pacific. This was carried out under a microscope on 116 pebbles (>5 mm diameter) that were individually extracted from the cores, and on >18,000 grains in the >500-5000 μm size fraction from subsamples in PAR85-01, PAR87A-10, and ODP 887. In addition, there was a dredge haul conducted on the Patton-Murray Seamounts at the time of core recovery and 20 large cobble sized dropstones were obtained.

Material in the >500-5000 μm size fraction from 60 subsamples in ODP-887 was separated into the following categories: (1) quartz grains, (2) feldspar grains, (3) basalt fragments, (4) other volcanics and metavolcanic fragments (occasional glass, pumice, tuff, green stone, and andesite or rhyolite), (5) dark gray to black slate and argillite, (6) coarser sedimentary and metasedimentary rock fragments (dark colored siltstone to medium sandstone, and more rarely phyllitic and mica-schist fragments), (7) quartzite fragments, and (8) plutonic rock fragments (virtually all granodiorite in composition, although other plutonic rocks cannot be ruled out in the smaller fragments). In addition, material in the >500-5000 μm size fraction from 35 subsamples in PAR87-10 was separated into: (1) quartz grains, (2) feldspar grains, and (3) other grains. Only samples with more than 100 grains (>200 on average) were included in the analysis. There was insufficient course material in PAR85-01 to allow this kind of analysis.

Boulton (1978), Domack *et al.* (1980), and Dowdeswell and Dowdeswell (1988) have shown that roundness of debris entrained in a glacier, and therefore icebergs, is characteristic of its entrainment and transport position within the glacier (i.e., basal or supraglacial). Basal debris is subject to more abrasion and is generally more rounded (subrounded and may have striations) than supraglacial debris (more angular). Therefore, the proportion of angular clasts versus subrounded ones can be used as a proxy for the dominant mode of entrainment, supraglacial or basal (Dowdeswell and Dowdeswell, 1988). This has a bearing on the supply of debris, and on ice thickness.

In this study, the degree of roundness was determined, using the classification scheme of Powers (1953), in the 20 cobbles from the dredge haul, and 116 pebbles (>5 mm) removed from the cores in the Gulf of Alaska. There was insufficient large material in the core off

Vancouver Island to allow its inclusion in the analysis. Based on their roundness, these IRD grains were separated into 2 categories: (1) Angular and subangular clasts, assumed to be supraglacially entrained since this material experiences little abrasion; any clasts with lichen still attached were also assumed to be supraglacially entrained. (2) Subrounded grains are most likely entrained and transported at the base, where they experienced more abrasion. Rounded and well rounded clasts are not typical of ice transport processes, and are therefore likely to be fluvial in origin. They were probably entrained at the base from interglacial river deposits as the ice advanced over them. Any rocks with polished or striated surfaces are also assumed to be entrained at the base of the ice.

III. RESULTS AND DISCUSSION

The down-core variation in mass accumulation rate of lithic material in the size range between 180-500 μm is presented in Figure 2. A number of features of this record are particularly apparent: (1) the fluctuations in IRD supply are characterized by maxima lasting several thousand years, separated by shorter minima, (2) in general the 'peaks' in ice-rafting are concurrent between cores, but the magnitude of peaks are, in some cases, somewhat different. Likewise, the magnitude of the reduction in IRD flux between peaks is also variable between cores, and (3) there is only one significant IRD event in the core off northern Vancouver Island (PAR85-01).

The GRAPE density record from ODP 887 (Figure 2) shows that in general GRAPE density values are high when there is IRD, but high values of GRAPE density do not always correspond to a proportionally high mass accumulation rate. Fluctuations in the GRAPE density record are also at a higher frequency than in the mass accumulation rate time series. This is probably becuase GRAPE cannot distinguish a dense layer produced by one large grain from a dense layer produced by a high concentration of grains. A single large clast may register as an especially dense level in the core, but does not have any more significance than a small grain in so far as regards the intensity of ice-rafting; i.e., it is not the size of an IRD grain that is important, but rather the amount of IRD. Nevertheless, even if GRAPE

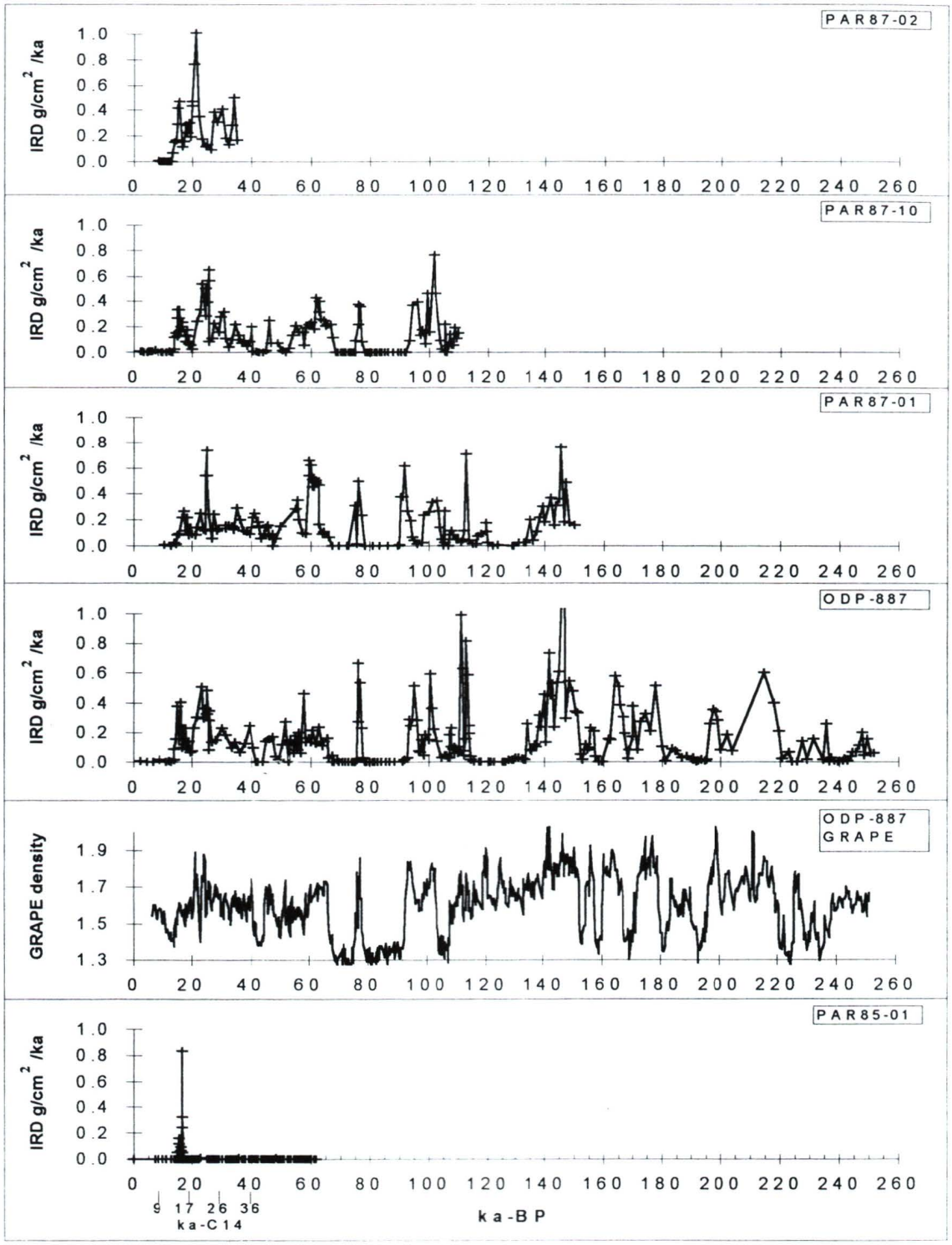

Figure 2. The flux of ice-rafted debris to the northeast Pacific during the last 250,000 years. IRD flux is quantified as the mass accumulation rate ($g/cm^2/ka$) of lithic material in the 180-500 μm size fraction, and also GRAPE density in core ODP-887. Periods of increased IRD accumulation are inferred to be stadials when tidewater glaciers advanced and ocean temperatures were colder, providing more icebergs and greater iceberg survivability. Note that despite the very close proximity of the four cores from the Gulf of Alaska there are differences in the accumulation rate during intervals of equivalent age; this is proposed to be a result of random debris dumps off the top of icebergs.

density does not provide a proxy for the intensity of ice-rafting, it may provide a useful means of identifying time periods when ice-rafting occurred. With this limitation in mind, a high resolution record was constructed for the entire length of ODP 887 (to ~800 ka) based on GRAPE density.

There are differences in the down core petrology of IRD grains in the Gulf of Alaska sites, and also in the petrology of grains between the Gulf of Alaska sites and the core off Vancouver Island. Also, most of the IRD is angular in shape with relatively little subrounded and rounded grains. The significance of these observations listed above will be discussed in the following sections.

1. Unpredictable iceberg behaviour and its influence on IRD supply

If a debris dump off the top of an iceberg were to occur over a core site then, potentially, it would lead to a greater supply of IRD at that particular moment in time, in that particular core, than at nearby sites. Consequently, the difference in accumulation rates between two sites may not be related to paleoceanographic/paleoclimatic factors, but instead to unpredictable iceberg behaviour. This behaviour may be important if differences in the paleoceanography and paleoclimate between two regions are to be inferred based on the amount of IRD at some level in a core, especially if only one core is investigated from each site.

The influence that unpredictable iceberg behaviour might have is likely dependent on the supply of icebergs over the area of study. In an area where iceberg supply is plentiful, the distribution of debris dumps is likely to be more uniform over time, as would the distribution of IRD, consequently there would be less difference in IRD flux between nearby cores. On the other hand, in areas where the supply of icebergs is less, unpredictable iceberg behavior would potentially be of greater importance. The supply is also likely to change with time, such that entry and exit from periods of intense ice-rafting might be characterized by the most uneven distribution. This would also depend on how sudden is the transition in and out of the ice-rafting events.

The supply of icebergs required to assure a more or less even distribution of debris

cannot be quantified since there are no known quantitative models of debris release from icebergs through time. There are models of iceberg melting (review in Drewry, 1986), but to create a model of debris release would require a detailed knowledge of debris content and location within typical icebergs from the area of study; a reliable knowledge of past ocean circulation patterns, paleo-temperature gradients, and information on insolation absorbed by the bergs surface.

In the North Pacific, Rea *et al.* (1993) found that IRD concentrations were generally higher in the east and west Pacific, with significantly less in the middle regions. This suggests that iceberg supply was not uniformly distributed in the glacial North Pacific. It also suggests that temperatures were important in controlling the survivability of icebergs. Study of Figure 2 reveals that the magnitude of IRD flux during concurrent peaks, and concurrent minima, between the Gulf of Alaska cores is often quite different, as are the details of the time of entry and exit from periods of increased IRD flux. Therefore, unpredictable iceberg behaviour was probably of importance to IRD flux in the Gulf of Alaska, especially during interstadials, when icebergs melted quickly, perhaps before many of them reached the cores sites. Hence, the first appearance of IRD is, in some cases, diachronous between core sites; this, unfortunately, hampers age determination for the beginnings and endings of interstadials.

The issue of random iceberg behavior and its potential influence on IRD records has not, to the my knowledge, ever been addressed in any of the literature concerning North Atlantic Heinrich events. Iceberg distribution was probably more even in the North Atlantic since there were more potential sources, but it may still be an issue worth addressing in light of the more detailed analysis of Heinrich layers that is currently underway (for example, Gwiazda *et al.*, 1996).

2. Petrology and Shape of IRD grains

i.) Petrology of IRD grains

The similarity in lithologies around the coastal regions of the Gulf of Alaska would

result in assignment of IRD grains to specific sources equivocal, so this was not attempted. However, grains tend to match the general description of rocks in the coastal ranges of southern Alaska, namely the Chugach and St. Elias mountains.

Identification of IRD grains in the >180-500 μm fraction in 60 core samples (6,875 grains) from ODP 887 yielded the results presented in Table 1. The proportion of quartz and feldspar grains versus other grain types, determined from PAR87A-10 in 35 samples (7,551 grains), resulted in percentages that were essentially the same as in ODP-887: quartz 20.3 %, feldspar 1.5% (Table 1). In the core off northern Vancouver Island, very low concentrations of debris compared to the Gulf of Alaska sites only allowed 476 grain counts yielding the results in Table 2. The main difference is the much larger proportion of quartz (63.2%) and feldspar (8.6%) in the core off Vancouver Island compared with the Gulf of Alaska. This reflects the fact that granitic rocks are far more common in southeastern Alaska and British Columbia than they are farther west along Alaska's southern coast. Identification of 136 pebbles and cobbles (>5 mm) extracted from the cores and the dredge haul in the Gulf of Alaska yielded the results in Table 3.

During glaciations, it is reasonable to surmise that more icebergs calved from eastern glaciers (in Alexander Archipelago, Dixon entrance, and possibly Queen Charlotte Sound) would be found over the Gulf of Alaska core sites under two possible environmental conditions: (1) during periods when climate is coldest and more icebergs survive melting, and (2) during glacial maximum conditions, when more glaciers reach the shelf edge and calve more icebergs. Neither condition is exclusive of the other; in fact, it is most likely they would work together to provide a greater supply of icebergs from the east. It follows, that during such times, debris characteristic of the geology in the east should comprise a greater proportion of IRD grains. To test this hypothesis the down-core variation in the proportion of "granitic material" (quartz + feldspar + granitoid grains) was determined in the >500-5000 μm size fraction in the 35 samples from PAR87A-10 and 60 samples from ODP-887. The percentage of granitic material was compared to the concentration of IRD (g of IRD/cm^3) in the >180-500 μm fraction from these same samples. Results yielded a weak positive correlation (simple correlation coefficients of 0.32 in PAR87A-10 and 0.37 in ODP-887

Table 1. Percent composition of 6,875 IRD grains in ODP-887, 7,551 IRD grains in PAR87-10, in the >500-5000 μm size fraction

ODP-887	IRD grain type	Average %
	quartz	21.9
	feldspar	1.5
	granitic	0.9
	basalt	2.0
	other volcanics & metavolcanics	6.6
	slate (and argillite)	19.3
	quartzite	10.9
	other sediments & metasediments	31.2
PAR87-10	IRD grain type	Average %
	quartz	20.3
	feldspar	1.5
	other grain types	78.2

Table 2. Percent composition of 467 IRD grains in the >500-5000 μm size fraction in samples from PAR85-01 (off northern Vancouver Island).

IRD grain type	Average %
quartz	63.2
feldspar	8.6
granitic	0.9
basalt	2.1
other volcanics & metavolcanics	4.7
slate (and argillite)	2.1
quartzite	9.6
other sediments & metasediments	8.8

Table 3. Petrology of 116 Pebbles (>5 mm) from cores PAR87A-1, 2,10, and ODP 887, and 20 Cobbles from a dredge haul on Cowie Seamount (Gulf of Alaska).

Pebbles:	Number of grains
Basalt	16
Metavolcanics	9
Argillite (dark gray-black)	18
slate (dark gray-black)	22
Quartzite	13
Graywacke and sandstone	33
Granodiorite	5
Dredged cobbles:	
Basalt	3
Mica schist	1
Granitic	9
Serpentine	2
Quartzite (white-gray)	1
Graywacke	1
Limestone (gray)	2
slate	1

; significant at the 95% and 98% level respectively), shown graphically in Figure 3. In other words, this suggests the percentage of granitic material is, indeed, highest during periods of increased ice-rafting in the Gulf of Alaska (Figure 3). This is not just because the greater supply of IRD is caused by an increased amount of granitic material, since all grain types increased with increasing IRD concentration (Figure 4). Since more icebergs from eastern sources survived melting and reached the Gulf of Alaska core sites, it lends support to the assumption that ice-rafting is greatest during coldest periods (= glacial maxima) in the Gulf of Alaska. This result also has paleoceanographic implications that will be discussed in following sections.

ii.) Shape of IRD grains

The grain shape analysis of the 116 pebbles and 20 cobbles yielded the results in **table 4**. The majority were angular and subangular, 45% and 26% respectively, and therefore 71% were likely supraglacially entrained. Conversely, 19% were subrounded and 10% rounded, and therefore only 29% were likely entrained at the base of glaciers. Five of the large cobbles retained lichen, suggesting supraglacial entrainment, and six of the subrounded pebbles had polished and striated surfaces, suggesting entrainment at the base. In conclusion, supraglacially entrained debris was the most important component of glacially transported debris in the Gulf of Alaska, whereas freeze-on was of relatively less importance. Since supraglacial entrainment (rock falls) was always an important processes in Alaska, it is therefore unlikely that Alaskan glaciers were ever starved of debris, and it is unlikely that major variations in IRD flux could be an artifact of debris availability. This lends support to the usefulness of the IRD record as an indicator of the timing of ice advance and retreat. The material in PAR85-01 was too small to determine proportions of abraded versus angular clasts.

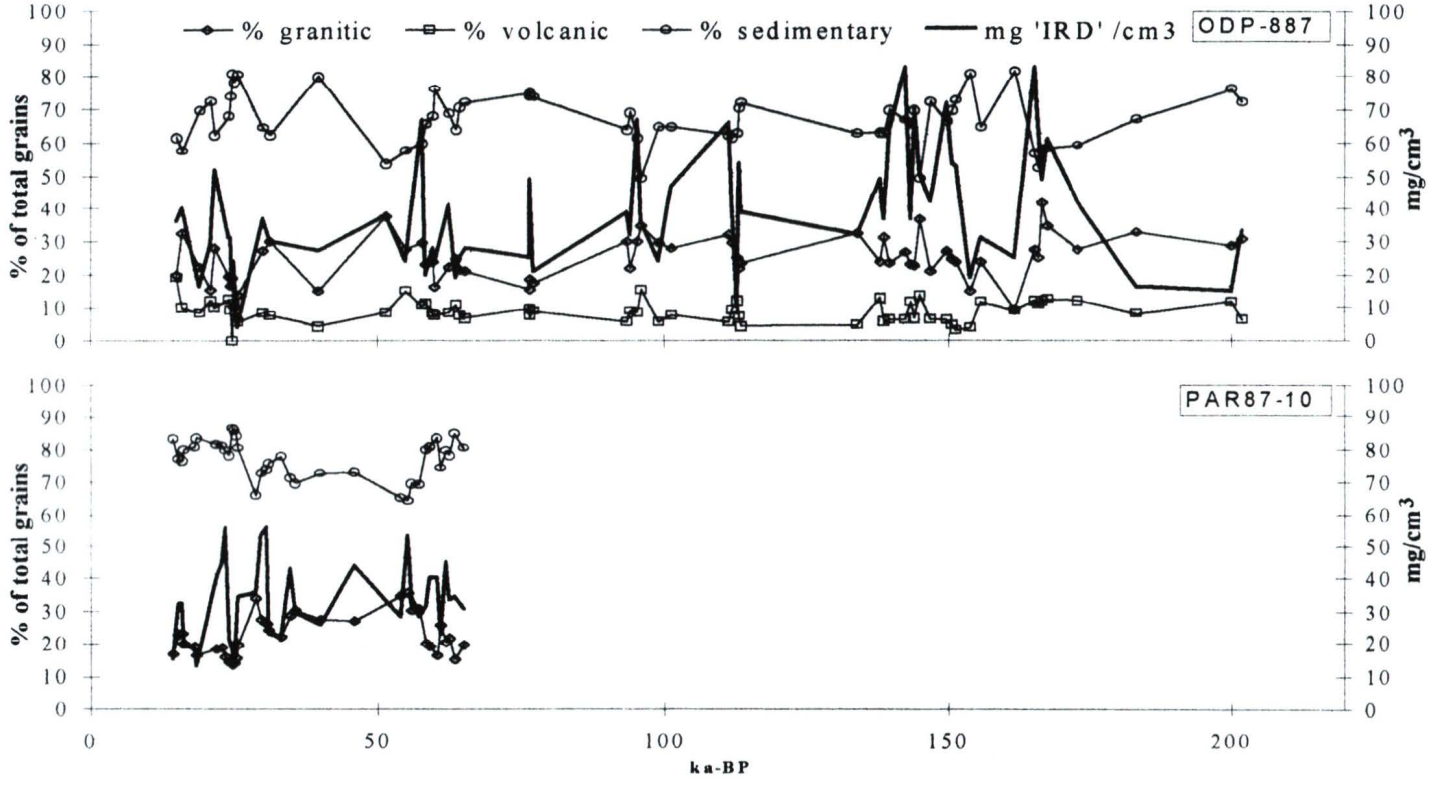

Figure 3. The percentage of granitic grains per sample (diamond markers) follows trends in total IRD concentration (heavy line) more closely than do the other grain types. This suggests more icebergs from eastern source regions (Alexander Archipelago to Queen Charlotte Sound) survive melting to reach the Gulf of Alaska core sites during times when IRD accumulation is highest, and these are, in turn, inferred to be periods of coldest ocean temperature and most extensive tidewater glaciation. Simple correlation coefficients for this comparison were weak, however (0.37 for ODP-887 and 0.32 for PAR87-10; significant at the 98% and 95% level respectively), possibly due to random iceberg behaviour. On the other hand, the correlation exists not just because the increased amount of granitic material leads to a greater supply of IRD, since all grain types increased with increasing IRD concentration (see figure 4).

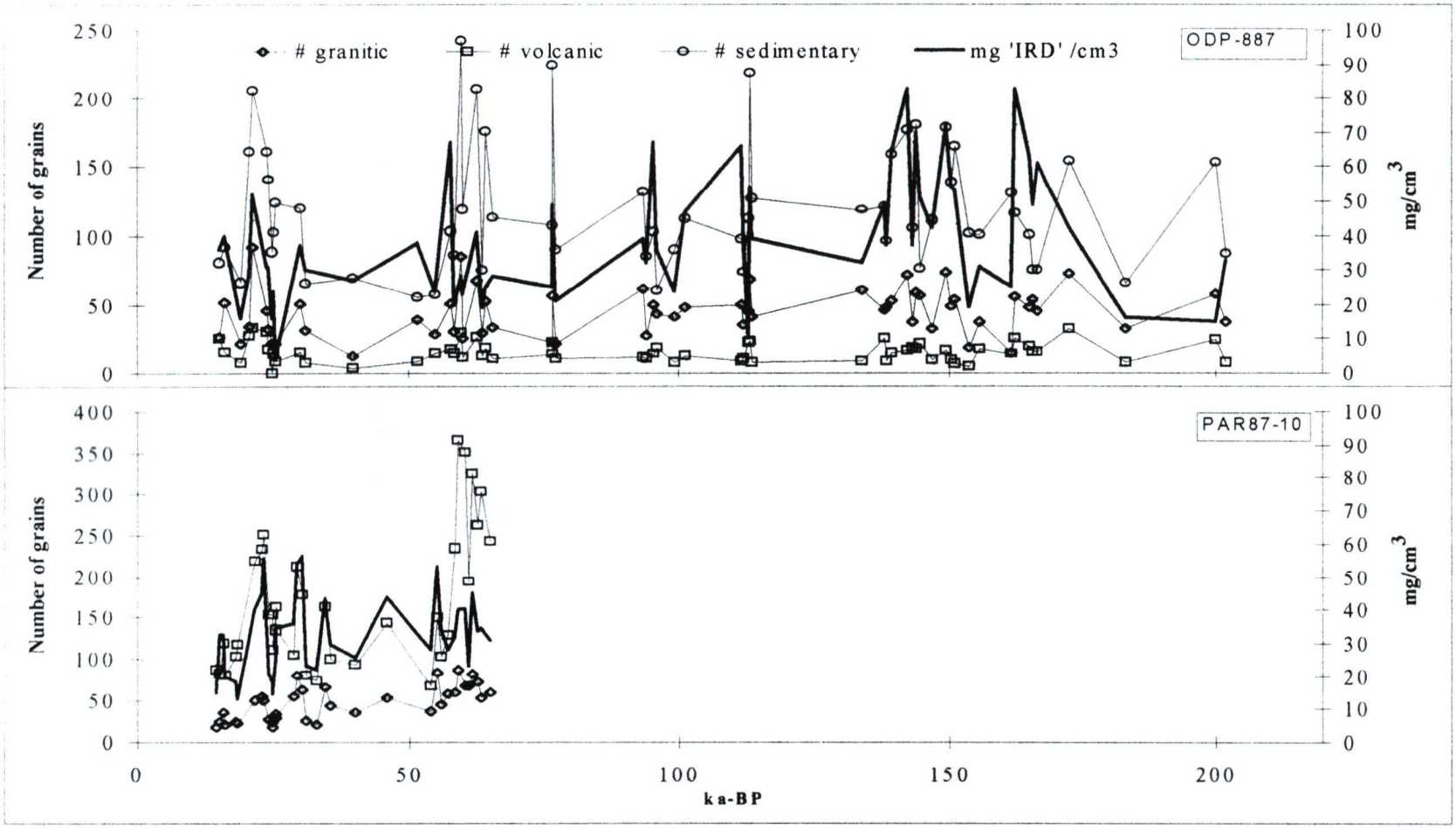

Figure 4. All grain types increase with increasing IRD flux

Table 4. Grain shape of 116 pebbles (>5 mm) and 20 cobbles removed from the cores, and dredge hall from Patton-Murray seamounts in the Gulf of Alaska (see text for discussion).

	Angular	Subangular	Subrounded	Rounded
Pebbles	43	33	26[a]	14
Cobbles	18[b]	2	0	0

[a] 6 of the subrounded grains showed evidence of polishing and striations.

[b] 5 of the large cobbles retained lichen preserved on their surface.

3. IRD accumulation and implications for glaciation in Alaska and British Columbia

The continental stratigraphic record of glacial history is incomplete, especially for pre-late Wisconsinan time. This problem arises due to a number of factors: (1) datable material in a stratigraphic position that allows tight constraints on timing of events may be sparse; (2) alternative methods of dating deposits older than the limit of the radiocarbon method have large errors (several 1000's of years); (3) a more recent ice advance may destroy, or be indistinguishable from the record of an earlier one; and, (4) much of the record is on the continental shelf, now below sea level, and subjected to erosion. Deep sea cores, on the other hand, can potentially contain a more continuous record of paleoenvironmental conditions, and thorough chronostratigraphies can be established based on foraminifera $\delta^{18}O$. Of course, the stratigraphic occurrence of IRD in deep sea cores should correspond to times of marine glaciation on the continental shelf - where it is known. The following sections will show that this relationship exists for the latest Wisconsinan ice advances, for which there is a reasonably complete and well dated continental record. It follows that the IRD record of earlier periods should provide a more complete chronology of glaciation around the Gulf of Alaska than is possible from continental stratigraphy. IRD has recently been used in a similar application by Baumann *et al.* (1995) for western Scandinavia. They found that peaks in IRD flux were concurrent with dated glacier advances in Norway. From this they were able to establish an improved chronology for glacier advances through the last 150 ka.

i.) The chronology and extent of glaciation: Wisconsinan time

a.) Glacial history inferred from cores in the Gulf of Alaska

Deposition of ice-rafted debris over the core sites in the Gulf of Alaska had essentially ceased by 12 ka-^{14}C-BP (Figure 5), but up until this time the IRD record suggests there was tidewater glaciation on the continental shelf, in places at least, throughout the

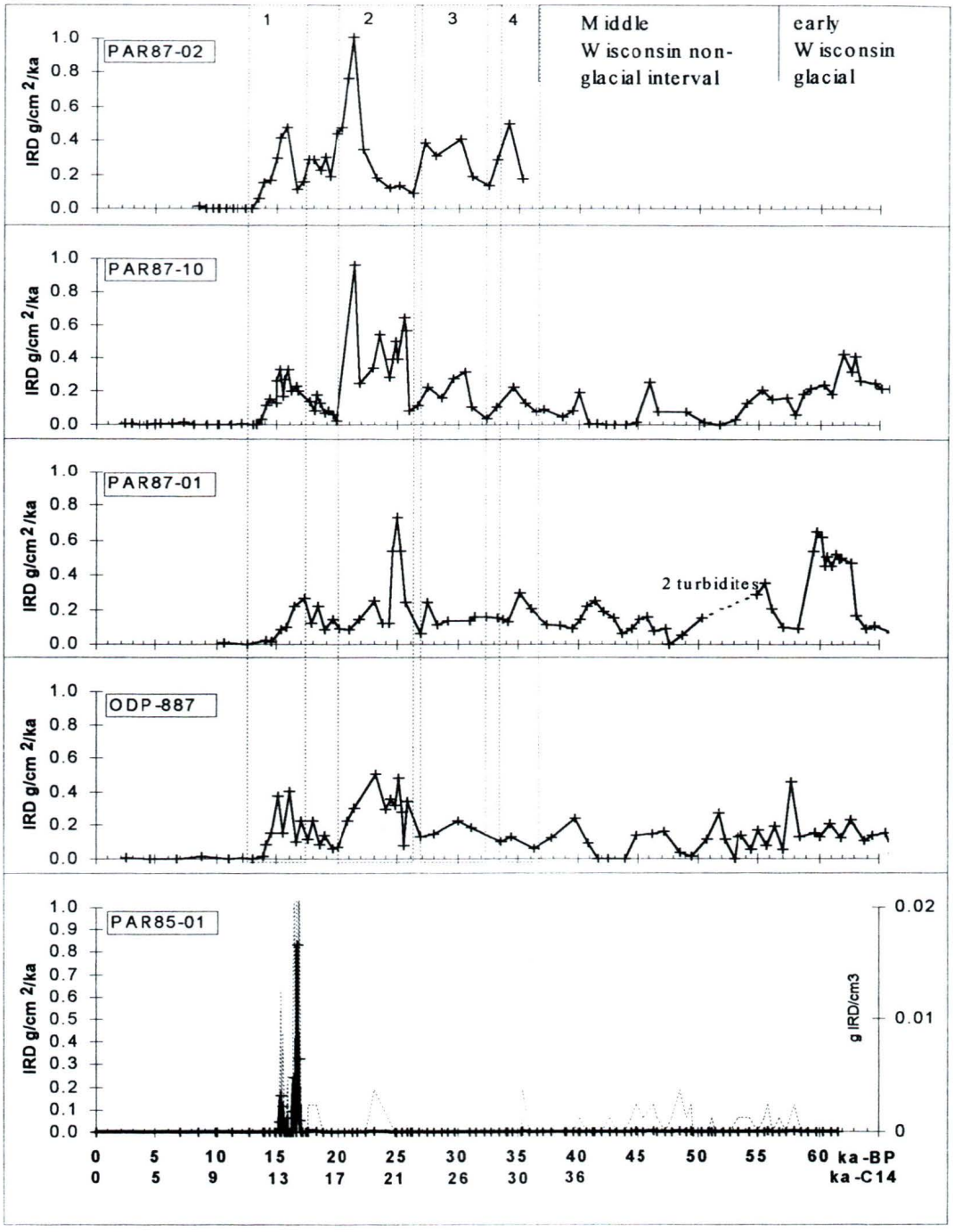

Figure 5. IRD mass accumulation rate, and GRAPE density in ODP-887, during the last 65,000 years. The age scale is given in both radiocarbon and corrected calendar years before present. There were apparently 4 IRD events in the late Wisconsinan (1-4 above). Prior to this was an interval characterized by lower amplitude fluctuations in IRD accumulation, compared to the late Wisconsinan. This interval corresponds to the middle-Wisconsinan non-glacial interval (Olympia non-glacial interval) identified in continental deposits from western North America. The dashed line in PAR85-01 represents grams of IRD/cm^3, which provides a representation of IRD flux without taking into consideration the sedimentation rate. This is given in order to expose older, minor IRD events that were identified by Blaise *et al.* (1990) during their original investigation of this core. When the sedimentation rate is taken into account, when determining the IRD mass accumulation rate, it reveals that these events are insignificant in comparison to the event at 15,000 radiocarbon years BP.

entire Wisconsinan (Figure 5 and 6). The exceptions are two intervals in the early Wisconsinan when IRD flux was zero. There are also significant fluctuations in IRD accumulation throughout this time.

The intervals of maximum IRD flux are interpreted as stadials, when: (1) more glaciers advanced to the shelf edge; some may have advanced beyond the mouths of the fjords they occupied, and may even have developed floating ice tongues; the result was an increased supply of icebergs, and in the latter case increased size of icebergs calving from ice tongues. (2) Temperatures were colder, resulting in improved iceberg survivability in open ocean waters, so that more icebergs reached the core sites before melting completely. Conversely, the intervals of reduced IRD flux are interpreted as interstadials, when floating ice tongues broke up and more tidewater glaciers terminated within fjords; the result was reduced size and supply of icebergs. Also, temperatures were warmer, resulting in reduced iceberg survivability.

In the Alaskan cores a final IRD peak occurs between ~13-14.5 ka-^{14}C-BP. Continental records (the reader is directed to section I.3.ii. where the continental work was reviewed) indicate a widespread readvance after 13.5 ka-^{14}C-BP, which may be correlative with this IRD event.

There is apparently no widespread deglacial readvance of glaciers at ~13.5 ka-^{14}C-BP preserved in British Columbia. There were readvances, but they appear diachronous (Clague, 1989). Clague (1989) suggests these events are probably only local, and probably controlled by local climate conditions, rather than a change in global climatic conditions. It probably should not be expected that the details of the time of advance and retreat would agree everywhere since changes in the volume and extent of the Cordilleran glaciers will themselves influence local precipitation patterns. However, changes in the large scale circulation should be expected to control the general trends of ice advance and retreat. Therefore, since the late readvance at ~13.5 ka-^{14}C-BP in Alaska was apparently widespread it suggests a significant change in the climate system at this time.

In continental records the last major phase of advance across the continental shelf began ~23 ka-^{14}C-BP and by 16 ka-^{14}C-BP ice was retreating off the shelf again. This is in excellent agreement with IRD accumulation which was increasing markedly after 23 ka-^{14}C-

BP and decreasing again by 17 ka-^{14}C-BP. Ice was retreating off the shelf by 16 ka-^{14}C-BP, again in good agreement with decreased IRD accumulation at this time. This IRD event represents the late Wisconsinan maximum. Prior to this there was an earlier late Wisconsinan IRD event which began after 29 ka-^{14}C-BP and ended before 23 ka-^{14}C-BP. A distinct advance during this interval is not well preserved in continental records from coastal Alaska. However, since the late advance after 23 ka-^{14}C-BP was more extensive, the occurrence of an earlier advance, the evidence of which has since been overridden and submerged, cannot be ruled out. In interior regions of both Alaska and British Columbia, some investigators have identified three late Wisconsinan advances, the earliest of these occurred around 28 ka-^{14}C-BP, and therefore may be correlative with the concurrent event in the IRD record. Another late Wisconsinan IRD event began ~32 ka-^{14}C-BP, but accumulation rates are relatively low compared with the younger events, and I am unaware of any documented ice advances in continental records at this time, with the exception of one date of 34,340 ^{14}C from Alaska (in Hamilton, 1994).

In summary, the IRD record presented here suggests four stadials during the late Wisconsinan (numbered 1-4 on Figure 5) when conditions were favourable for ice-rafting. During these events increased mass balance led to increased calving and, in combination with colder ocean temperatures, resulted in greater flux of IRD to the sea floor. The three youngest events are correlative with continental glacier advances. Whereas the fourth event was relatively minor and there is no major continental advance documented at this time, although minor alpine advances cannot be ruled out. Between these events are interstadials when glacier mass balance was reduced due to warmer temperatures and/or reduced precipitation. In conclusion, correlations between IRD flux and continental records, suggest that the North Pacific IRD record, is indeed, a useful indicator of the time of stadials/interstadials and glacier advance/retreat in Alaska, and thus, can be used to reliably reconstruct the chronology of older glaciations.

Prior to the late Wisconsinan, there was a lengthy middle Wisconsinan 'non-glacial' interval (Olympia non-glacial interval in British Columbia and Washington). Clearly, IRD flux was reduced during this time compared to the late Wisconsinan, but never fell to zero in all the cores at the same time (Figure 5). This suggests glaciers never retreated completely

from fjord mouths during the middle Wisconsinan in Alaska. This is not too surprising since glaciers terminated at fjord mouths at times during the Holocene, including the beginning of this century (historical accounts reviewed by Molnia, 1983; Mann, 1986b). During the middle Wisconsinan sea level was still relatively low and so glaciers terminated at fjord mouths closer to the core sites; this, in combination with temperatures that were at times colder than during the Holocene, resulted in significant deposition of IRD, whereas there has been essentially none deposited during the Holocene.

The fluctuations in IRD accumulation during the middle Wisconsinan are generally concurrent between cores, and therefore have environmental significance beyond simply unpredictable iceberg behaviour, although this factor probably had considerable influence given the low supply of icebergs at the time. These fluctuations are proposed to be a result of the climatic fluctuations of the middle Wisconsinan documented in biostratigrapic studies throughout western North America. From this study a chronology of these fluctuations was possible, and is summarized below and in Figure 5.

There was an interstadial between 32-34 ka-^{14}C-BP, although accumulation rates remained significant. This event followed a stadial, from 34-37 ka-^{14}C-BP. During this event maximum IRD flux occurs earlier in PAR87-01(~37 ka-^{14}C-BP) than in ODP 887 or PAR87-10 (~35 ka-^{14}C-BP), suggesting unpredictable iceberg behavior has some influence on IRD accumulation at this time. Likewise, the next earlier interstadial spans 36-41 ka-^{14}C-BP in PAR87-10, 37-41 in ODP887, and >39-41 ka-^{14}C-BP in PAR87-01. The date of this interstadial agrees closely with the few continental records that show glacier retreat in coastal Alaska during the middle Wisconsinan (for example, Mann, 1986a; see section I.2.ii.). (Beyond the range of radiocarbon dating the chronology is based on the oxygen isotope chronostratigraphy, and so dates are now given as calendar years before present "ka-BP"). Another IRD event lasted from 44-48 ka-BP. In cores PAR87-01 and ODP887 this IRD event followed an interstadial between 48-49 ka-BP, which, in turn, followed another IRD event between 49-52.5 ka-BP. In PAR87-10, however, this event is missing, instead the previous interstadial lasted from 48-53 ka-BP. All the Gulf of Alaska cores show increasing IRD accumulation prior to this event, indicating the start of the extensive early Wisconsinan glaciation which has been inferred from numerous continental sites, where it is recognized as

a till or drift stratigraphically underlying mid-Wisconsinan organic deposits with infinite radiocarbon dates and biological remains that indicate a climate cooler than present (i.e. younger than the last full fledged interglacial). Beyond the range of radiocarbon dating there are few absolute dates and those that do exits have large errors, rendering the timing and number of advances during the early Wisconsinan to remain questionable.

According to the IRD record, there are, in fact, five distinct IRD events in the early Wisconsinan, 55-115 ka-BP (numbered 1-5 on Figure 6), suggesting five continental advances. IRD accumulation rates during these events are comparable to those of the late Wisconsinan, and each stadial is separated by a distinct interstadial, also comparable to those of the late and middle Wisconsinan. During two of these early Wisconsinan interstadials (EWI1 and EWI2 on Figure 6) there was apparently no IRD deposited at all; the younger event spanned the interval from 68-74 ka-BP, and the older one from 79-91 ka-BP. The older event is comparable in duration to the last interglacial (isotope stage 5e). However, the duration of these interstadials is probably exaggerated by unusually high sedimentation rates in this interval. In the cores these interstadial layers are comprised of diatomaceous ooze with very little background terrestrial input. It may be that these layers were deposited much faster than age control currently predicts. John Crusius at the University of British Columbia has produced some initial ^{230}Th (excess) data that suggest these layers were deposited 3 - 6 times faster than the intervening mud layers. When the data collection is completed the age model will require correction in these intervals. Increased sedimentation rates in this interval would shorten the length of the interstadials and broaden the IRD events. Nevertheless, they still will represent periods of IRD flux lower than at any other time during the Wisconsinan, and may represent particularly warm interstadials.

b.) Glacial history inferred from a core off northern Vancouver Island

In the core off northern Vancouver Island, there is only one very brief IRD event within the last 55 ka-BP, occurring at ~15 ka-^{14}C-BP (Figure 5). In their original study of this core Blaise *et al.* (1990) counted grains of IRD and observed two additional, although minor, IRD peaks at ~23 ka-^{14}C-BP and at ~ 37 ka-^{14}C-BP. These peaks are absent in the

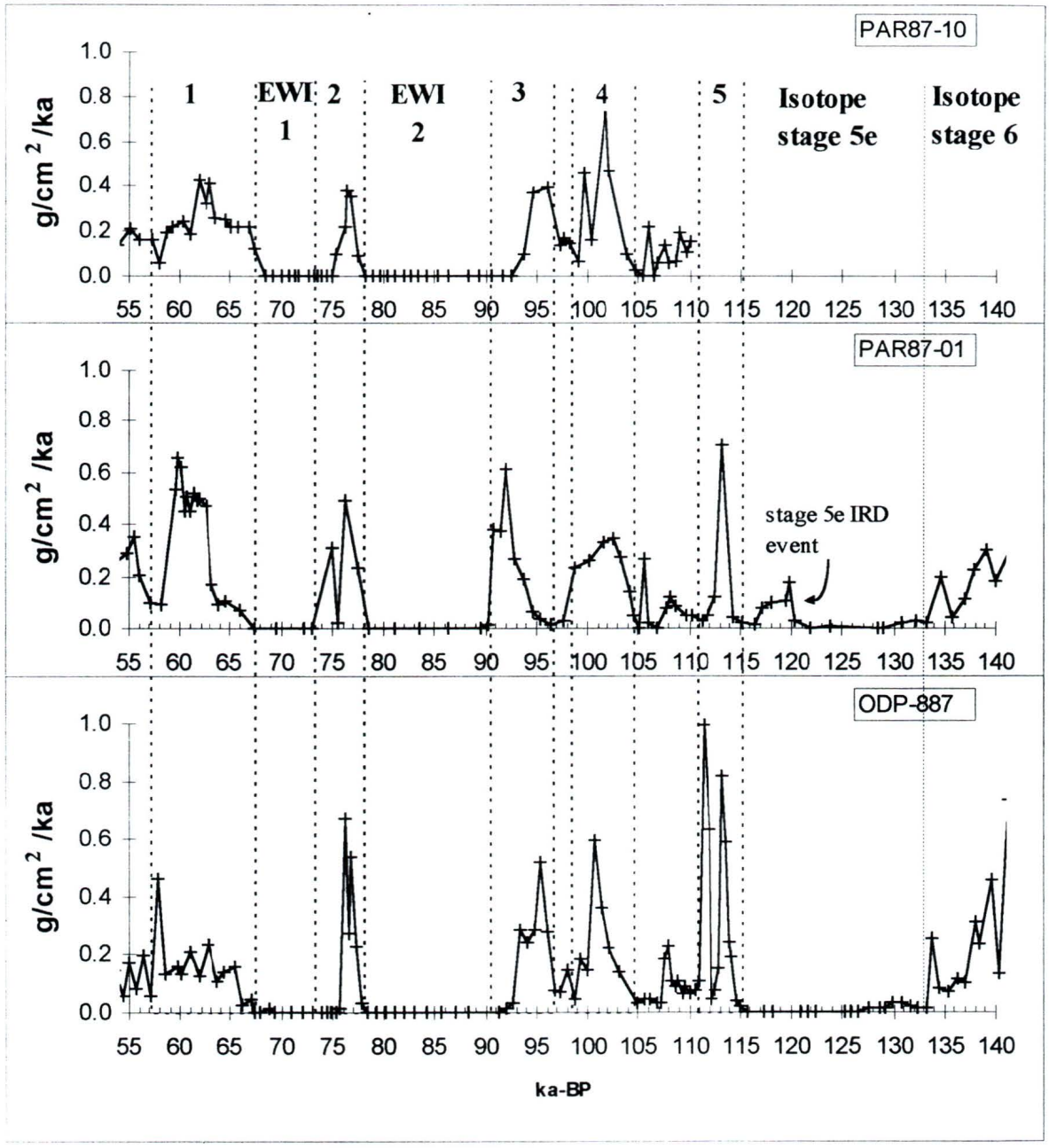

Figure 6. There are five major IRD events during the early Wisconsinan (numbered 1-5 above) separated by interstadial intervals when IRD accumulation was much lower. IRD accumulation was insignificant during two of these early Wisconsinan interstadials (EWI1 and EWI2 above). EWI2 appears to be comparable to the last interglacial (isotope stage 5e) in its duration. However, the duration of EWI1 and EWI2 may be exaggerated by the extremely rapid deposition of the diatomaceous ooze that comprises these intervals. Presently, data are being collected that will soon allow correction of the age model in this interval (John Crusius, University of British Columbia). There is a small, but significant IRD event during that later half of isotope stage 5e in PAR87-01, suggesting tidewater glaciation at fjord mouths and a period of colder ocean temperature at this time.

record presented here because when the sedimentation rate is accounted for it reveals that IRD accumulation rates were insignificant at these times compared with the 15 ka-^{14}C-BP event (the earlier events are shown in Figure 5, PAR85-01, by the dashed line which represents the concentration of IRD in g IRD/cm^3 rather than accumulation rate). It is generally agreed that ice was retreating from Queen Charlotte Sound and the Queen Charlotte Islands by 15 ka-^{14}C-BP. Therefore, the IRD peak apparently occurs during the initial stages of deglaciation in this area, rather than during glacial advances, as it does in Alaska. Blaise *et al.* (1990), suggested the IRD maximum occurred at this time, because of increased calving due to grounding line retreat as sea level began to rise during deglaciation. Such a process can account for the observed pattern in IRD records from around Antarctica (Keany *et al.*, 1976; Bornhold, 1983). There, sea level rise may cause a considerable increase in calving from ice shelves as they become detached from pinning points and break up. Consequent streaming due to steeper ice slopes between the new grounding line and inland ice may also lead to increased calving. Furthermore, with less extensive ice shelves, less debris is melted out before calving, resulting in icebergs richer in debris. These factors, in combination with SST's that remained cold during interglacials around Antarctica, allowed the increased IRD to occur. There are, however, a few problems with applying this model to western North America, and there are a number of factors that would favour increased calving during glacial maxima in the Northeast Pacific.

In Alaska, east of the Alaska Peninsula, and in western British Columbia, glaciation did not reach a marine ice sheet stage of development. As reviewed previously, ice was mainly confined to a number of major U-valleys on the continental shelf. Sea level rise may still have caused calving retreat of glaciers, but they would have retreated into these valleys, and this, in combination with warming temperatures, would result in few icebergs surviving to reach the open sea. Instead, the situation would have been much like the present day, when most icebergs melt within fjords. Another factor which might dampen the effect of a deglacial increase in ice-rafting is the very high flow rate of Alaskan glaciers (see Hunter, *et al.*, 1996, for example). When glacier flow rate is high, it is less likely that any additional

supply of icebergs, due to grounding line retreat, will overwhelm the ambient supply and dominate the IRD record. Also, during times of increased snow accumulation (presumably during stadials), glaciers terminating at fjord mouths will thicken and attempt to flow beyond the fjord mouth, farther out into the ocean. The positive mass balance will be countered by increased calving outside the confines of the fjord (Mann, 1986b). Finally, it has already been shown that highest IRD accumulation rates in the Alaskan cores did, indeed, occur during glacial advances inferred from continental records, and were lowest during intervals of ice retreat. There is no apparent reason why the situation should be different in Queen Charlotte Sound.

Disagreement with the deglacial increase interpretation of the IRD peak in PAR85-01 does not change the fact that it occurs when the northern British Columbia shelf and islands were being deglaciated. So why does this IRD peak occur out of phase with peaks in the Gulf of Alaska? After all, coastal Alaska and the Queen Charlotte Islands underwent a similar glacial history. This could simply be an artifact of poorer chronostratigraphy in PAR85-01, or the fact that only one core was investigated from this site. However, assuming the chronostratigraphy and previously published dates for ice retreat from the Queen Charlotte area are true to each other, then some other factor that effects iceberg supply at this core site must be involved.

The occurrence of IRD in PAR85-01 prior to the latest Wisconsinan advances (dashed line in Figure 5), even though accumulation rates were insignificant, suggests that somewhere in Queen Charlotte Sound there was tidewater glaciation during the middle Wisconsinan despite the general consensus that British Columbia, including the Queen Charlotte Islands, experienced a widespread nonglacial interval at this time. There is no more likely source for this debris other than Queen Charlotte Sound. It cannot be floating from Juan de Fuca Strait, even if the glacial Alaska Current were that far south, since the Olympia nonglacial interval is best documented in the south. The only other possibility is that a few rare icebergs floated south from Alaska, into the transition zone, survived melting and floated back to the east. The number of grains representing these IRD layers in PAR85-01 was to few to allow elimination of Alaska as a potential source based on the petrology of the >500 μm size fraction. However, examination of the finer fraction (180-500 μm) in

samples of equivalent age from the Gulf of Alaska cores and PAR85-01 reveals they are distinctly different. Immediately obvious is that the samples from the Gulf of Alaska are much darker in color than the PAR85-01 samples. No grain counts were carried out, but examination under a microscope shows that the darker color in ODP887 samples is due to smaller fragments of the dark slates and fine grained sedimentary rocks that dominate the coarser fraction. In PAR85-01, samples are virtually all quartz, with much fewer darker grains. Therefore, it is unlikely that the icebergs that dropped this debris came from anywhere but Queen Charlotte Sound. The occurrence of these minor events appears to coincide with the major IRD events (stadials) in the Gulf of Alaska cores (Figure 5). Perhaps, a few glaciers at fjord mouths on the mainland calved icebergs into the open waters of the sound, and when temperatures were favourable, a few floated out over the core site.

If the age model to the bottom of PAR85-01 is valid, then an early Wisconsinan advance that supplied significant IRD occurred sometime before 55 ka-BP (i.e., beyond the bottom of the core). Therefore, the tills preserved beneath the latest Wisconsinan till in Queen Charlotte Sound (Josenhans *et al.*, 1993) are probably early Wisconsinan or older.

ii.) Chronology and extent of glaciation: pre-Wisconsinan time

Only PAR87-01 and ODP887 extend through the last interglacial (isotope stage 5e). This is clearly a time of reduced IRD accumulation comparable to the Holocene. IRD accumulation rates are high again immediately after stage 5e and also at the end of stage 6 (Figure 6). Interestingly, there is also a small IRD event during the later half of stage 5e in PAR87-01, but not in ODP 887 (Figure 6). This suggests glaciers were at fjord mouths at this time, and probably temperatures were colder than present in order to allow icebergs to survive melting as they traveled across the continental shelf to the core sites.

Prior to the last interglacial (isotope stage 5e) there was an interval comparable to the late Wisconsinan in both duration and IRD accumulation. In fact, accumulation rates during this interval appear slightly higher in PAR87-01. Some continental investigations record evidence of an extensive glaciation that occurred stratigraphically below interglacial deposits, some of which contain biotic evidence suggesting temperatures similar to those of

the present day. On this basis the underlying till or drift has been assigned to stage 6.

Between 135-250 ka-BP there are as many as seven IRD events with intervening interstadials (Figure 7). Mass accumulation rates are often higher than they were in the late Wisconsinan, suggesting a greater extent of older glaciations, and/or colder stadials in Alaska. Of special significance is a lengthy interstadial between 180-195 ka-BP, where IRD accumulation is reduced, although not as low as during the Holocene, the early Wisconsinan interstadials, or stage 5e. Like stage 5e, and the oldest early Wisconsinan interstadial, this event also follows a period of particularily high IRD accumulation (i.e., between 195-220 ka-BP). Therefore, there are five apparent occurrences of long interstadials following long stadials (I1-I5 on Figure 8), and all occur beyond the range of radiocarbon dating. This then suggests caution should be used when making correlations between supposed interglacial sections on land, and also between the land and interglacials in the IRD record, especially when there may have been an interval of cooler climate during stage 5e.

Prior to 220 ka-BP is a period of reduced IRD accumulation. This interval corresponds to another interglacial episode (isotope stage 7), when global ice volume was reduced. According to IRD accumulation rates, the interval of maximum interglacial conditions at this time was not as long as it has been during the Holocene already, or isotope stage 5e, or possibly even the early Wisconsinan interstadials. This suggests that this interglacial period, and isotope stage 5e, both experienced intervals when climate was colder and glaciers more extensive than during the Holocene.

The GRAPE density account of IRD events during the last 250 ka-BP is presented in Figure 5. The reliability of GRAPE density as a proxy for ice-rafting apparently fails during periods of low global ice volume; evidenced by the high GRAPE values during the Holocene and the last interglacial (isotope stage 5e), when there is no IRD present. There are also high GRAPE values during some of the earlier periods of low global ice volume (Figure 9). These peaks in GRAPE density might represent ice-rafting during interglacial periods, or alternatively periods of only deposition of very fine, low porosity sediments like during the Holocene, and most of stage 5e. This can be resolved with an evaluation of the amount of IRD from the cores. Subsamples (>150 μm size fraction)

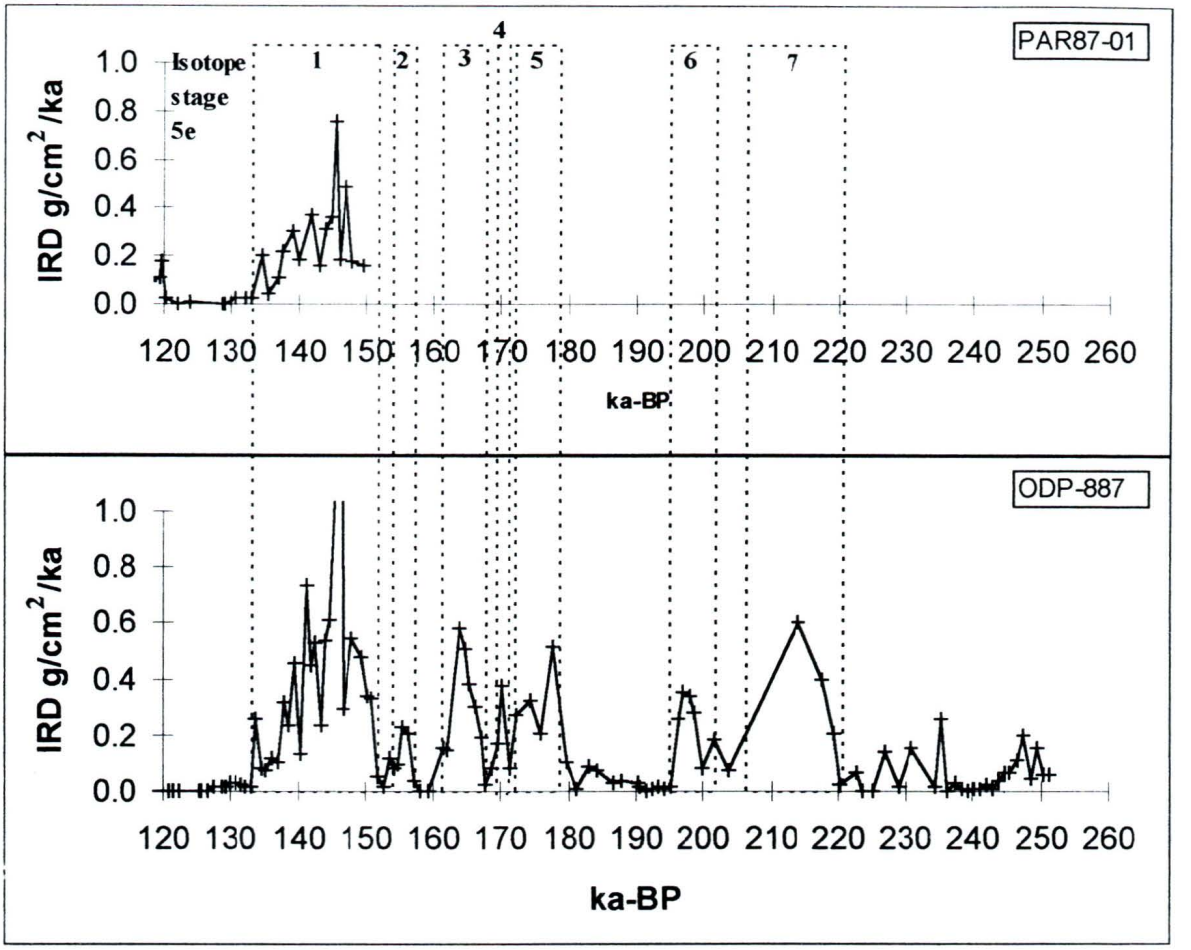

Figure 7. IRD events during the pre-Wisconsinan (135-250 ka BP). The events are numbered 1-7 above.

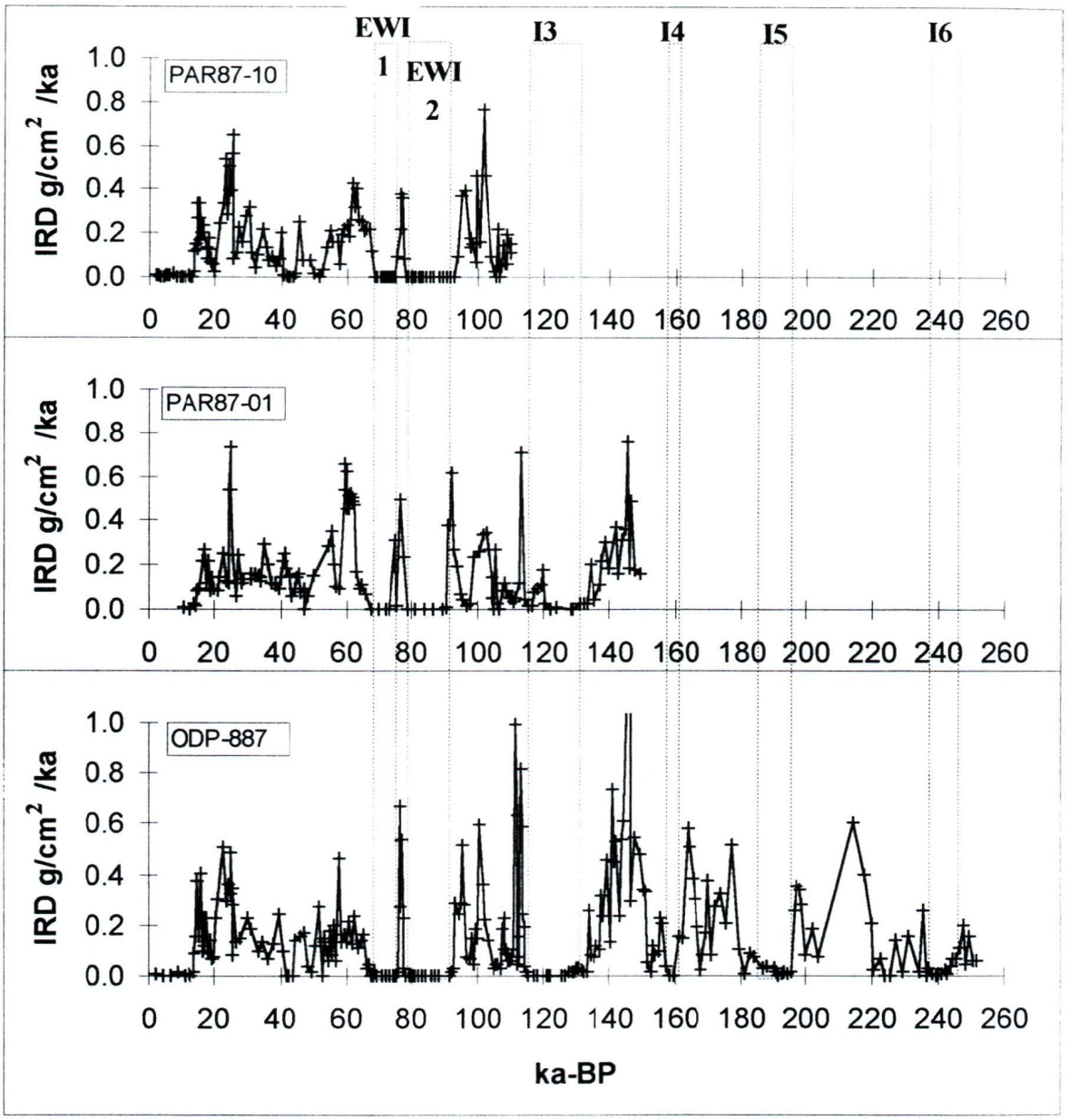

Figure 8. Major interstadials during the last 250,000 years. There were apparently five interstadials when IRD accumulation was insignificant (EWI1, EWI2, & I3-I6 above). Each of these events is older than the range of radiocarbon dating, suggesting caution should be used when making correlations between proposed interstadial deposits based on stratigraphic and geomorphic evidence without absolute age control.

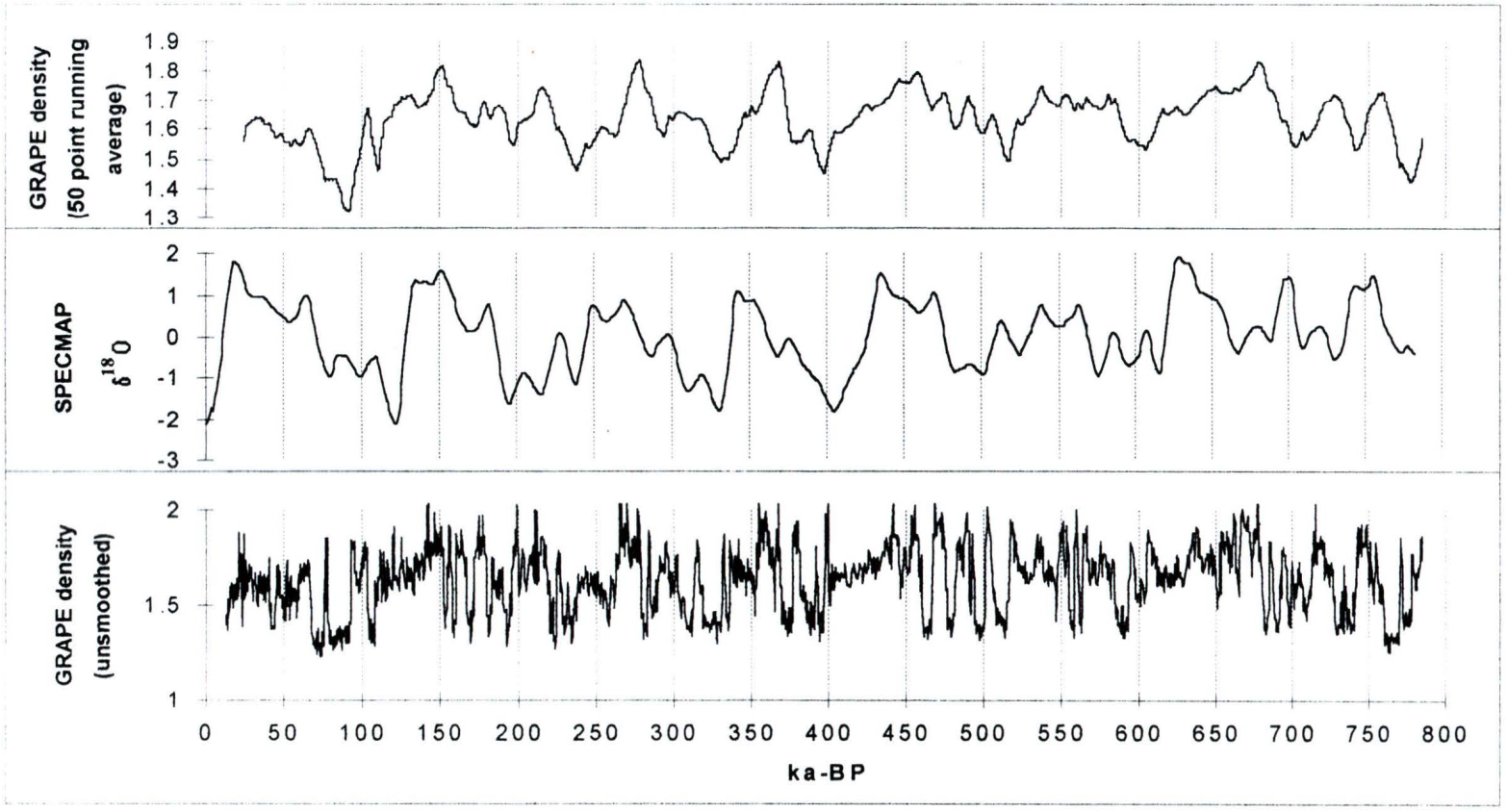

Figure 9. Correlation between ODP-887 GRAPE density and the SPECMAP marine $\delta^{18}O$ record. The 100,000 years cycle in ice volume recorded in the SPECMAP record is also clearly evident in the smoothed (50 point running average at top) GRAPE density record. Evidently fluctuations in ice-rafting on suborbital time scales (unsmoothed series at bottom) have also been a reoccurring characteristic of glaciations through the last 800,000 years. Note the greater contrast between glacial-interglacial extremes in the last 400 ka compared to the earlier half of the record. This "Mid-Brunhes Climatic Event", as it has been called by other investigators (Jansen, 1986, for example), is a global phenomenon.

removed every 10-30 cm from these depths in ODP-887 were borrowed from Darcy MacDonald at the University of British Columbia. Visual estimation of the amount of IRD was carried out in these samples, and from examination of the cores. This allows, in combination with the GRAPE data, which does reliably predict the presence of IRD during glacial periods on time scales greater than 1-2 ka, is a high resolution chronology of the timing of ice-rafting during the last 800 ka, comparable to that constructed for the first 250 ka (Figure 10). This was done without the time consuming process of dense sampling, preparing samples, and weighing or counting IRD grains. The only major piece of information that is lost in doing this is a measure of the intensity of ice-rafting, but in only one core this is probably of limited value anyway, due to unpredictable iceberg behavior. From this record it is evident that the older glaciations, like those in the first 250 ka-BP, have been characterized by marked high frequency advance-retreat cycles (stadial/interstadial oscillations) throughout the late Pleistocene. Furthermore, in some instances, significant IRD was deposited during several interglacials.

4. Paleoceanography

There is some evidence that the North Pacific subarctic transition zone was located farther south during glacial maxima (Moore, 1973; Sancetta and Silvestri, 1986; Morley *et al.*, 1987; and possibly Thunnel and Mortyn, 1995). The mean location of the bifurcation point of the Alaska and California currents was probably also shifted south, away from its present location off the southern Queen Charlotte Islands. This would result in icebergs calved from Queen Charlotte Sound to be carried northward in the Alaska Current, away from PAR85-01 during glacial maxima. At the same time, any icebergs calved from Juan de Fuca Strait were probably still carried southward in the California current. In this scenario the core site off northern Vancouver Island was sheltered from a large amount of ice-rafting during glacial maxima due to the lack of a favourable ocean current. Only during deglaciation, when oceanographic conditions reverted to a more interglacial configuration, were icebergs carried over the cores site, and then only for a very brief time before waters

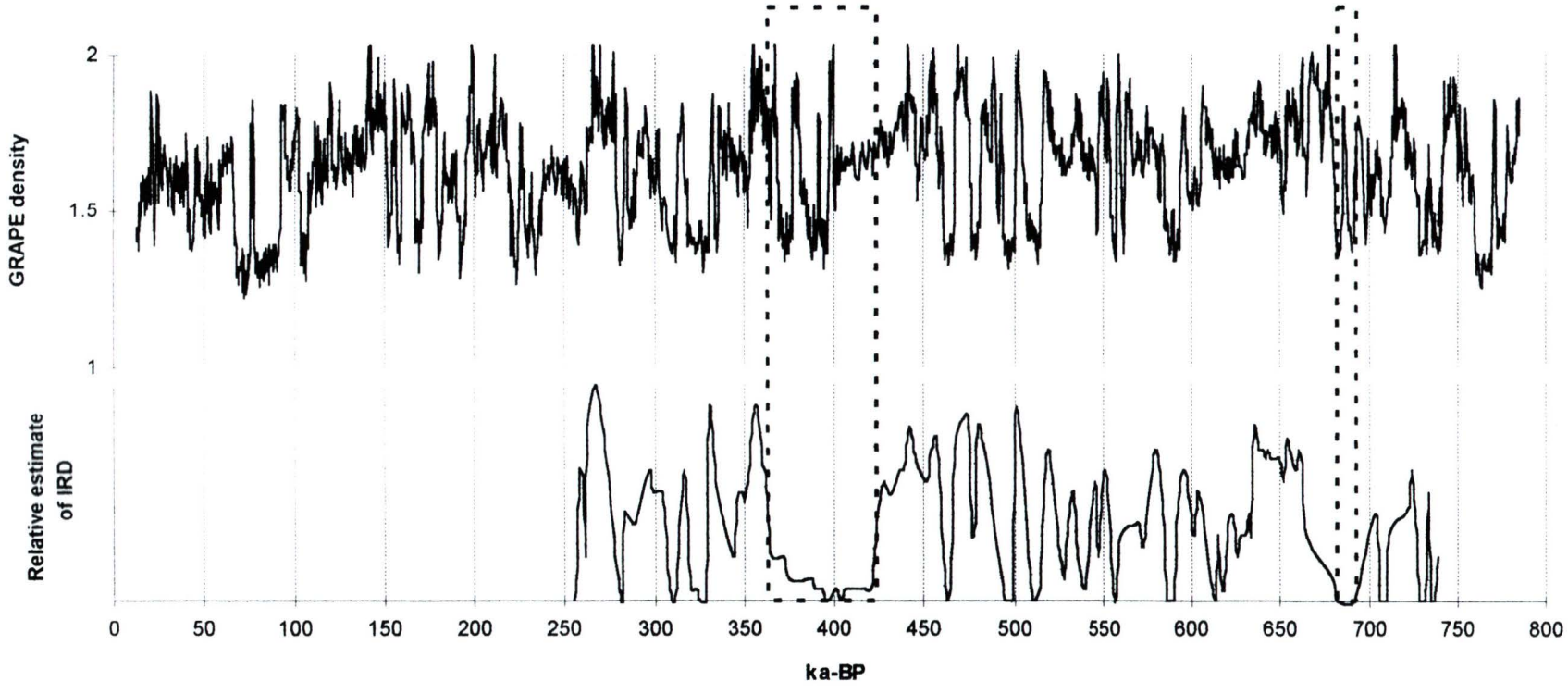

Figure 10. The complete 800,000 year record of GRAPE density from ODP-887 compared to a visual estimate of IRD concentration in samples older than 250,000 years. Note, that like the 250 ka-BP record (figure 6), there are times when GRAPE density is high even though there was little or no IRD deposited (represented by the dashed lines).

became too warm, and before ice had retreated off the northern shelf altogether. The short duration of the IRD event, and low overall concentration of IRD in PAR85-01, compared to concentrations of IRD in the Gulf of Alaska cores, is consistent with this scenario (Figure 11). The scenario is also consistent with the increase in the percentage of granitic material deposited in Alaskan cores during stadials, which could reflect a greater supply of icebergs floating northward from Queen Charlotte Sound (Figure 12). However, the increase in granitic material might just as easily be supplied from Dixon Entrance or the Alexander Archipelago. Finally, abundant IRD in cores off Oregon, investigated by Griggs and Kulm (1969), is also consistent with this model.

Griggs and Kulm (1969) identified IRD in cores from the Cascadia Basin, off Oregon, they did not establish a detailed chronology of IRD deposition. The only date of 37 ka-^{14}C-BP underlies the only IRD layer (~10 cm thick) in one of the more southerly cores. This layer was likely deposited around 15 ka-^{14}C-BP, since this is the time frame of glacial maximum in southern British Columbia (section I.3.ii.). The cores south of this contain no IRD, whereas a thick sequence (5.7 m in one core) containing layers rich in IRD is described in the northerly cores. Griggs and Kulm proposed that this entire thick sequence was equivalent in age to the ~10 cm thick layer deposited after 37 ka-^{14}C-BP. However, it is now well documented that the only time ice advanced down Juan de Fuca Strait to the shelf edge after 37 ka-^{14}C-BP was during the Vashon advance of the Fraser glaciation, ~15 ka-^{14}C-BP. The thick, 570 cm sequence of IRD layers was not likely deposited in ~1000 years, and Griggs and Kulm described the sequence as follows: "The IRD layers were 1-4 cm thick interbedded with laminated clays containing little coarse material." This suggests intermittent deposition of IRD in distinct events, and the thick sequence probably represents several glacial advances to the shelf edge in Juan de Fuca Strait sometime during the Late Pleistocene, but before the mid-Wisconsinan. Griggs and Kulm did not quantify the IRD concentration in any way, but according to their descriptions of the IRD layers the cores contained high concentrations and a large number of pebbles, up to 7 cm in size, some with striations. A similar description would fit the cores from the Gulf of Alaska. This is in marked contrast to the low concentrations off northern Vancouver Island, thus supporting the hypothesis that PAR85-01 was sheltered from ice-rafting.

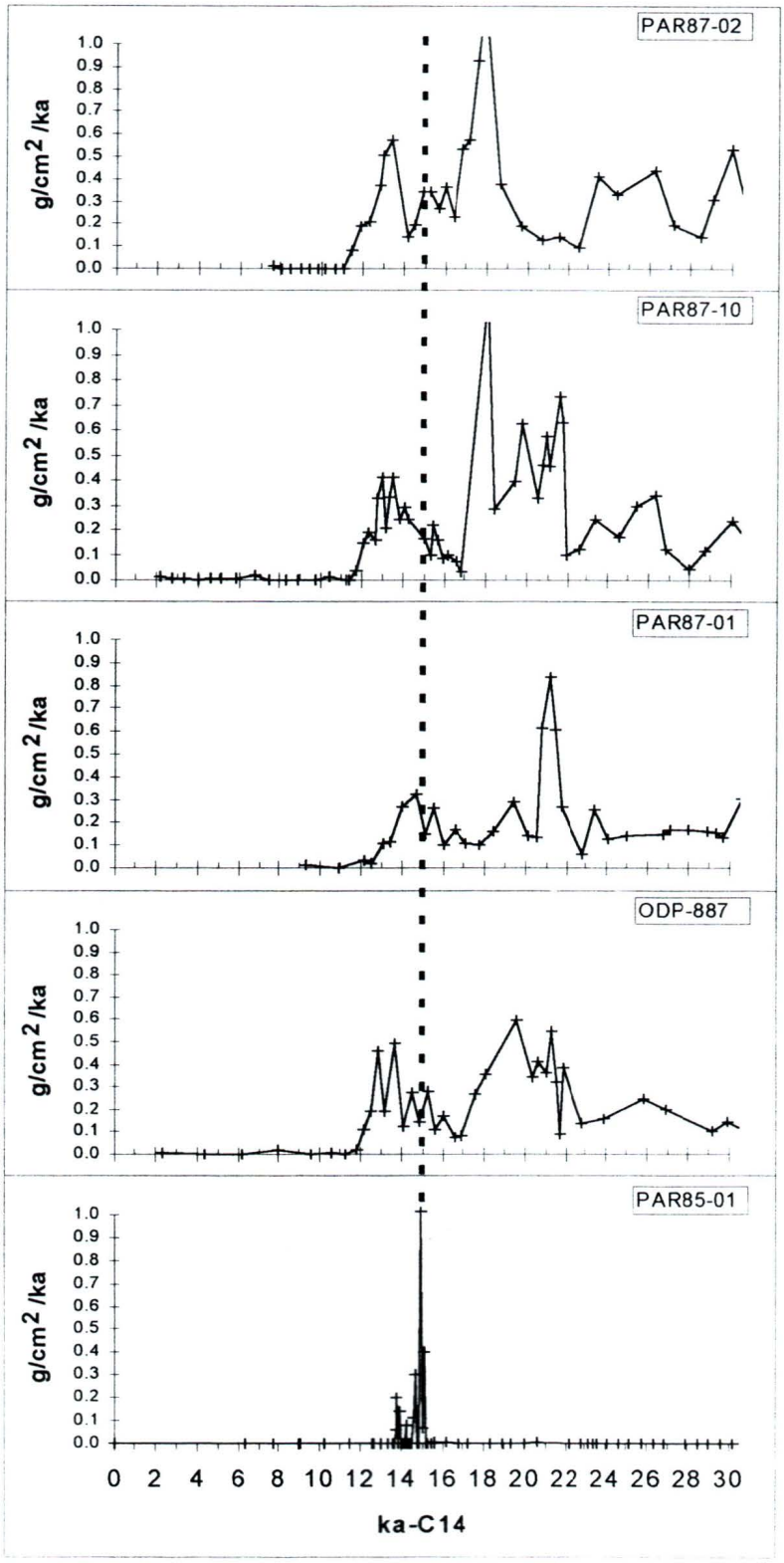

Figure 11. The single short IRD event in PAR85-01 apparently occurs during an interval of reduced IRD accumulation in the Gulf of Alaska cores (indicated by the heavy dashed line). IRD events in the Gulf of Alaska cores occur during dated intervals on continental advance. On the other hand, the event in PAR85-01 occurs during the initial stages of deglaciation of Queen Charlotte Sound (the source region for this debris). This is proposed to be a result of changes in the oceans surface circulation at the time (see text and figure 12).

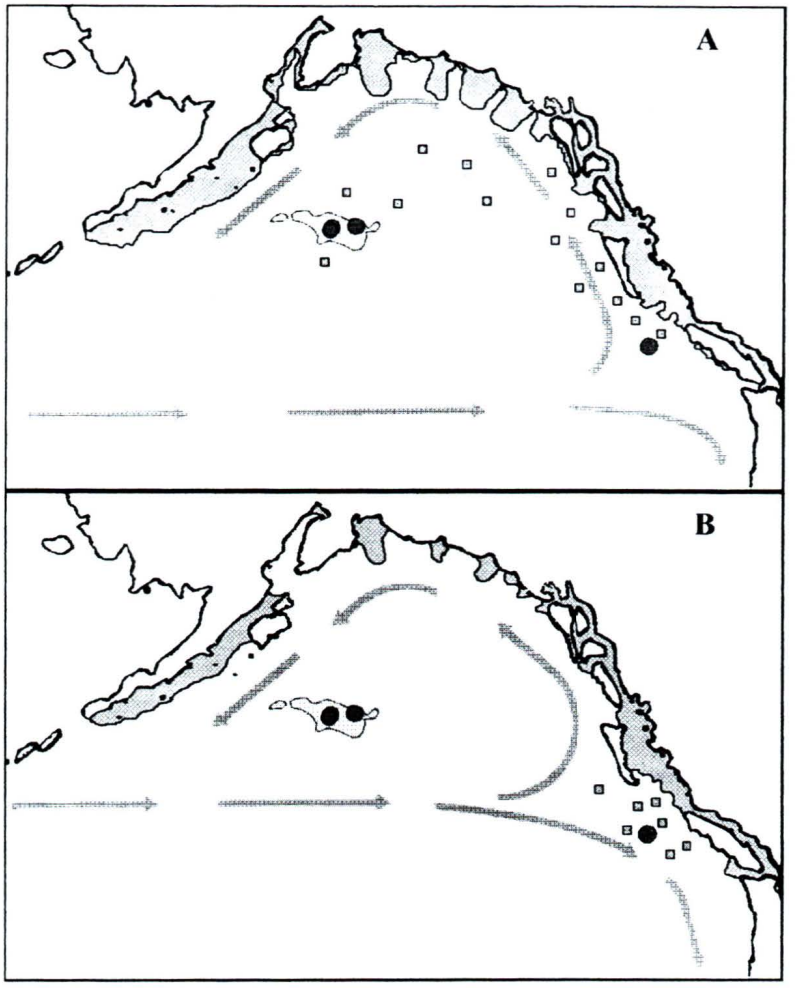

Figure 12. Schematic diagram depicting the proposed paleoceanography. The small squares represent the distribution of icebergs calved from glaciers at the shelf edge in Queen Charlotte Sound, during full glacial conditions (**A**), and during the initial stages of deglaciation (**B**). Many more icebergs calved from other sources are not shown. The shaded areas along the coast indicate ice extent on the continental shelf during glaciations; i.e. the important sources of icebergs (roughly drawn in (**A**) based on: Hamilton, 1994; Barrie and Bornhold, 1991; Bornhold and Barrie, 1991). The ice extent in (**B**) is mainly speculative. During full glacial conditions, surface ocean circulation patterns (heavy lines with arrows) were such that icebergs calved from Queen Charlotte Sound were carried northward away from the core site off northern Vancouver Island (dark circles), possibly over the more northerly core sites on the Patton-Murray Seamounts. During deglaciation surface currents would have tended to carry more icebergs from Queen Charlotte Sound southward along the coast into warmer waters. The paleocirculation patterns indicated in (**A**) are speculative, but represent a possible configuration that is consistent with the apparent distribution of ice-rafted debris in the Northeast Pacific. A full discussion of this hypothesis is given in section III.3.i.b.

In summary (see Figure 12), it is proposed that the small, short peak in IRD flux in PAR85-01 occurs during the initial stages of deglaciation because only then were ocean currents favourable for transport over this core site. It therefore records the waning supply of icebergs from a previously important source during glacial maxima when icebergs were carried northward, possibly even over the Alaskan core sites.

5. Global paleoclimatic implications: the last 115,000 years

i.) Previous work: globally synchronous suborbital climatic variability

It is has been recognized for some time that the last glaciation was characterized by marked climatic oscillations that occurred on time scales shorter than insolation cycles, and it has further become accepted that some of these events were global in influence, as evidenced by a number of long (~40 ka or longer), continuous paleoclimatic records from around the world (discussed below). A number of additional shorter records point to the occurrence of a cold climatic episode in western North America during the Younger Dryas chronozone (Engstrom *et al.*, 1990; Mathews *et al.*, 1993; Reasoner, 1994; Kunz and Reiner, 1994; Hu *et al.*, 1995, Patterson *et al.*, 1995; Gosse *et al.*, 1995; Davis, 1994).

In Greenland ice core $\delta^{18}O$ records there are stadial-interstadial climatic oscillations called Dansgaard-Oeschger cycles (see Dansgaard *et al.*, 1993). The Dansgaard-Oeschger cycles got progressively colder until there was an especially long, warm interstadial, which initiated the next series of Dansgaard-Oeschger cycles (Figure 13). Many of these longer interstadials followed events of major iceberg discharge into the North Atlantic, called Heinrich events (Heinrich, 1988; see Bond *et al.*, 1992). Each such package of Dansgaard-Oeschger cycles and one Heinrich event has been termed a Bond cycle (Broecker, 1994), these definitions are adopted here.

In the North Pacific a few early works realized rapid climatic oscillations were more frequent than orbitally induced insolation cycles. For example, the work by Von Huene *et al.*

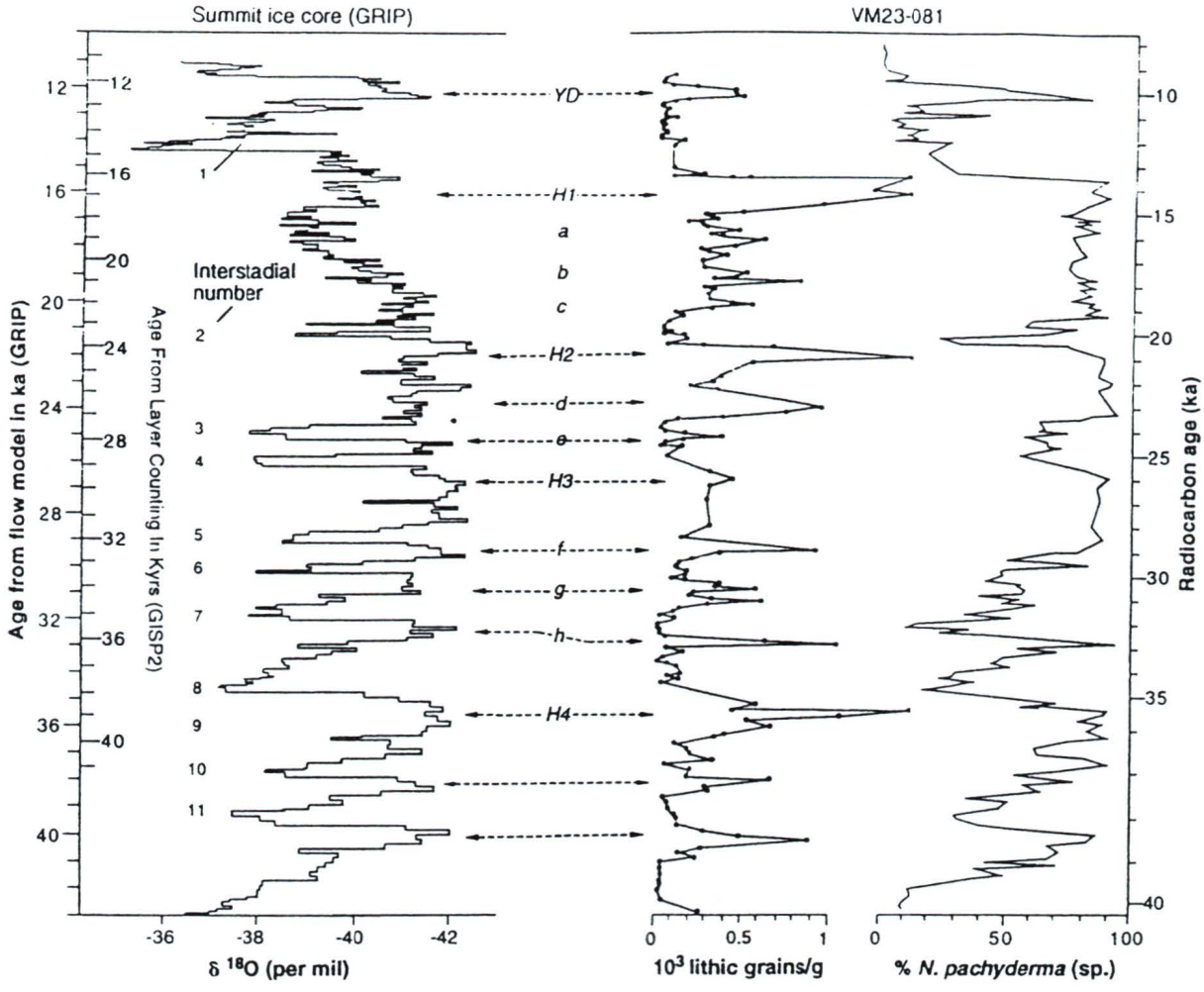

figure 13. Correlation between North Atlantic Heinrich events and and the Greenland icecore (GRIP) from Bond and Lotti (1995)

(1976), discussed earlier, noted fluctuations in IRD abundance at the 10-15 kyr frequency dominated their record. Despite, questionable core quality and chronostratigraphy, Von Huene *et al.* (1976) were able to show some similarities between their IRD curve and the Camp Century Greenland ice core.

Heusser (1972) reported multiple reversals in the dominant pollen type in a ~70 ka record from western Washington. The record is interpreted as showing that tree pollen (representative of interstadials) alternated with shrub tundra (stadials) eight times during the last 70 ka.

Moore (1973) investigated radiolarian assemblages in the North Pacific and found that the assemblage that now characterizes the Alaskan Gyre was once found off the coast of Oregon during the last glaciation. During deglaciation this assemblage moved progressively farther north, replaced first by a central subarctic assemblage, and then a transition zone assemblage. Superimposed on the glacial portion of the record were oscillations lasting up to several thousand years. Moore's (1973) interpretation of this was: "... in the climatic mode of a full glacial interval the intervals of slight warming must represent a northward movement of the oceanographic boundaries and should correlate approximately with the retreat of glaciers."

More recently, Thunell and Mortyn (1995) and Mortyn et al. (1996) have reported a similar conclusion to that of Moore (1973). They found high frequency variations in the number of sinistral *Neogloboquadrina pachyderma* (cold water foraminifera) in cores off the coast of southern California. Mortyn et al. (1996) suggest these may be correlative with the first three Heinrich events. During phases of Laurentide surge, the ocean-atmosphere system responded by producing a more southerly Subarctic Front in the North Pacific, which led to a colder California Current over their core sites. The colder water supported increased numbers of sinisteral *N. pachyderma*. When the ice sheet retreated, the gyre boundary shifted north once again resulting in warmer waters in the California Current, and thus fewer sinistral *N. pachyderma*..

Clark and Bartlein (1995) correlated records of mountain glacier advance in the western United States with North Atlantic Heinrich events 1, 2, 4, and 5, and also a minor Younger Dryas advance. The absence of H3 is attributed to a more extensive advance at the

time of H2, that consequently destroyed the record of a postulated less extensive H3 advance. They attribute the advances to oscillations in Laurentide ice sheet volume and the effect this would have in leading to colder temperatures in the areas south of the ice sheet.

Liu *et al.* (1996) used microlaminations in rock varnish to infer trends in the aridity of climate in Death Valley, California. They found that manganese-rich layers (wet periods) alternated with manganese-poor layers (dry periods). The manganese-rich layers, or wet climates, correlate with the Younger Dryas, and Heinrich events 1 through 6, presumably as a result of shifting precipitation belts.

Kotilainen and Shackleton (1995) present a GRAPE density approximation of ice-rafting in the western North Pacific, which they correlate to the GRIP core, but due to poor chronological control the correlation is not convincing. Nonetheless, there are similarities between the from the GRAPE record curve and the GRIP ice core curve.

Other studies in lower latitudes in the Northern Hemisphere and in the Southern Hemisphere have also claimed climatic oscillations associated with Heinrich events. Palynological studies from Florida show distinct cold periods recorded in lake sediments (Grimm *et al.*, 1993; Watts and Hansen, 1994). In China, Porter and Zhisheng (1995) report increased grain size in loess deposits correlative with the Heinrich events. Lowell *et al.* (1995) constructed a composite record of glacial advances from Chile and New Zealand that correlate with the Younger Dryas and Heinrich events. Liu (personal communication) believes rock varnish in the arid regions of the Southern Hemisphere records a similar pattern to that in California. Bender *et al.* (1994) correlated the Vostok ice core with the GISP2 Greenland ice core, and found that of the 22 interstadials recorded in Greenland ice during the last 105 ka-BP, only the 9 longest (>2 ka) occur in the Vostok ice core. In the Greenland ice cores, these long, especially warm interstadials follow the older Heinrich events (Bond and Lotti, 1995), but shorter interstadials, like the Dansgaard-Oeschger cycles, are absent. Well defined interstadials after Heinrich events 1 and 2 are not apparent in the Antarctic ice cores. Antarctic cores show a more steady decline in $\delta^{18}O$ after 22 ka-BP, whereas GRIP and GISP2 cores are interrupted by marked returns to colder conditions associated with Heinrich event 1 and the Younger Dryas. Some Antarctic cores do show an oscillation around the same time as the Younger Dryas, although of much smaller amplitude

in the $\delta^{18}O$ record (for example, Jouzel *et al.*, 1995; Sowers and Bender, 1995).

In the low latitude western Pacific, Linlsey (1996) correlated a foraminifera oxygen isotope record with the GRIP ice core. Several of the long interstadials they suggest are concurrent with the those in the GRIP core are similar to the ones identified by Bender *et al.* (1994) in the Vostok ice core, and Bond and Lotti (1995) following the Heinrich events.

The higher frequency Dansgaard-Oeschger cycles, between the major Bond cycle interstadials, have been recorded in the high latitude North Atlantic deep-sea sediments (Figure 13) (Bond and Lotti, 1995; Fronval *et al.*, 1995), but the paleoenvironmental records discussed above, from outside the North Atlantic, only show climate related events that can be clearly correlated with the Younger Dryas and North Atlantic Heinrich events, but not with the higher frequency Dansgaard-Oeschger cycles. Only two studies (Phillips et al, 1994; and Behl and Kennett, 1996) suggest a correlation between the Dansgaard-Oeschger cycles and proxy records outside the northern North Atlantic.

Phillips *et al.* (1994) correlated salt layers in pluvial-lake Searles to interstadials in the GRIP ice core. Between the salt layers are mud layers representing high lake levels during wetter stadials, presumably due to shifts in dominant precipitation patterns. The evaporite layers may have been deposited during Laurentide retreat when storms were tracking farther northward. However, the correlations made by Phillips *et al.* (1994) were admittedly ambiguous in some cases.

Behl and Kennett (1996) correlated anoxic/oxygenated intervals in Santa Barbara Basin with interstadial/stadials in the GISP2 ice core, respectively. The core displays laminated sediments deposited during anoxic periods and massive (bioturbated) sediments that are deposited during oxygenated periods. Behl and Kennett (1996) attribute greater oxygenation to stadial conditions, when they propose there was either: (1) increased production of intermediate water in the North Pacific; or else (2) a missing component of NADW in the North Pacific due to a reduction in thermohaline circulation in the North Atlantic. The missing NADW component (old and O_2 depleted) is replaced by younger more O_2 enriched Pacific Intermediate Water.

ii.) Climatic variability in the Northeastern Pacific IRD record

To further support the hypothesis of globally synchronous Bond cycle climatic oscillations this study presents a high-resolution record of the flux of ice-rafted debris to the seafloor of the Northeast Pacific. Correlation of this record with the GRIP ice core $\delta^{18}O$ record (Figure 14) reveals that accumulation of IRD was increasing in the North Pacific several thousand years prior to the North Atlantic Heinrich events (as defined in Bond and Lotti, 1995; Figure 13). During and after the Heinrich events IRD flux in the North Pacific is greatly reduced, concurrent with the major interstadials that follow the termination of each event in the GRIP ice core. Some of these are the same interstadials Bender *et al.* (1994) identified in the Vostok ice core, namely interstadials 8, 12, 14, and 16.

IRD events correlative with the more frequent Dansgaard-Oeschger cycles between the Heinrich events are apparently absent in the IRD accumulation rate time series. There is a higher frequency of variability in the GRAPE record similar to that of the Dansgaard-Oeschger cycles, however, as many of these more frequent peaks are concurrent with Dansgaard-Oeschger cycles as are not. For this reason, and for the reason discussed previously to explain imperfect agreement between GRAPE and mass accumulation rate, IRD minima concurrent with the shorter, more frequent, Dansgaard-Oeschger interstadials are not proposed. A younger Dryas equivalent IRD event is also entirely absent.

As was discussed in III.3.i.b. the more southerly core site (PAR85-01), shows only one prominent IRD event which apparently is out of phase with any of those in the Alaskan cores.

a.) A mechanism for synchronous Northern Hemisphere (and global) climatic events

A popular theory for the origin of the Dansgaard-Oeschger cycles recorded in Greenland ice cores are fluctuations in the strength of North Atlantic Deep Water (NADW) formation (see for example, Broecker *et al.*, 1990). The basis of this theory is that when NADW formation is weak, less of the warm surface water transported from lower latitudes into the North Atlantic is required to replace the deep water that leaves under conditions of strong NADW formation. The reduced northward flow of warm surface waters leads to a

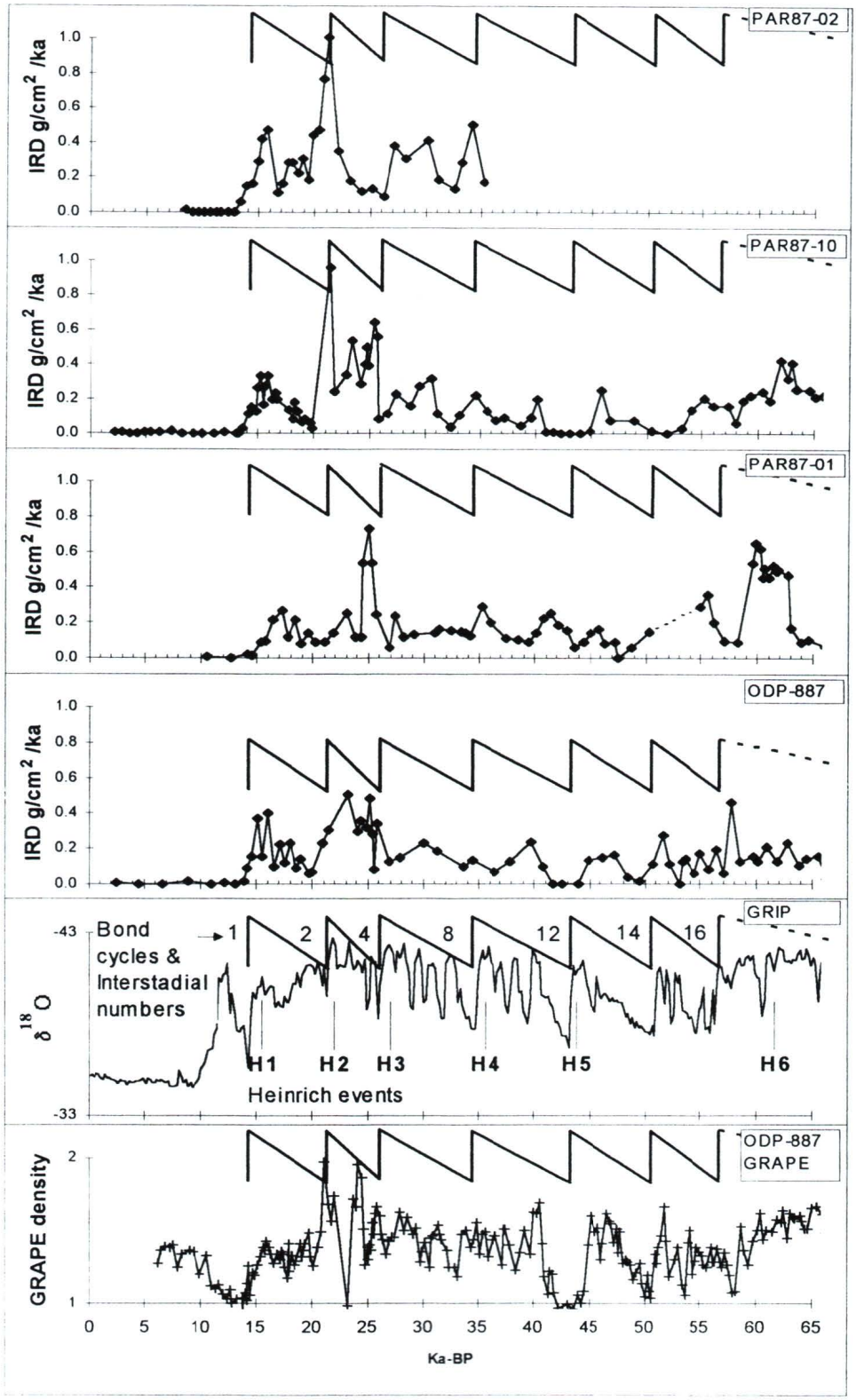

Figure 14. Correlation of IRD mass accumulation rate (and GRAPE density in ODP-887) with GRIP $\delta^{18}O$. The ramps represent the Bond cycles (Bond *et al.*, 1993). Interstadial numbers are from Dansgaard *et al.* (1993), and the Heinrich events (H1-H6) are from Bond *et al.* (1993), and Bond and Lotti (1995). IRD accumulation in the Northeast Pacific is high several thousand years before the Heinrich events and decreases shortly thereafter.

reduction in high latitude sea surface temperatures, therefore reduction in heat released to the atmosphere, and hence, colder climate. Now that high frequency climatic events have been documented outside the North Atlantic, investigators have suggested that oscillations in the intensity of the thermohaline circulation might account for the events in these areas also. One dynamic model (Fanning and Weaver, 1996) produced a 2.4°C cooling in the North Pacific due to reduced NADW formation during the Younger Dryas. This is considerably less cooling than occurred in the North Atlantic, however. A short coming of the NADW theory is that it does not explain the progressive cooling of Dansgaard-Oeschger events packaged in each Bond cycle.

A few investigators who have noted synchroneity in climate proxies between western North America and the circum North Atlantic, have considered the effect that oscillations in the Laurentide ice sheet volume might have on western North American climate (Clark and Bartlein, 1995; Thunell and Mortyn, 1995). They adopt the results of GCM's that have simulated the effect of ice sheets on various aspects of glacial climate (For example, Cook and Held, 1985; Cook, 1990; Kutzbach and Guetter, 1986; Manabe and Broccoli, 1985; Broccoli and Manabe, 1987a, 1987b; Rind, 1987; COHMAP, 1988). It was proposed that a displaced transition zone and colder ocean temperatures in the North Pacific (Thunell and Mortyn, 1995; and Mortyn *et al.*, 1996), and mountain glacier advances south of the Laurentide ice sheet (Clark and Bartlein, 1995), would accompany periods of ice sheet growth, whereas warmer SST's and glacier retreat would accompany Laurentide retreat. Here I propose that major oscillations in ice sheet volume may also account for the IRD record presented here: periods of ice sheet growth had direct and indirect effects that led to colder temperatures, increased precipitation, glacier advance, and ultimately increased ice-rafting from sources in southern Alaska. Ice sheet collapse, on the other hand, resulted in warmer temperatures, glacier retreat, and decreased ice-rafting.

The GCM simulations (listed above) and a more recent one by Hall *et al.* (1996) have indicated that the Laurentide ice sheet had a profound effect on glacial atmospheric circulation. The North Pacific High was displaced southeastward, and the strongest flow in the Westerlies was split around the ice sheet, with jets to the north and south; the stronger jet to the south. As a result storm tracks were also farther south, and the Aleutian Low was

displaced southeastward. During deglaciation COHMAP (1988) showed that when the ice sheet began to retreat, glacial circulation patterns were replaced by interglacial conditions. These models either only consider a glacial maximum condition or else glacial maximum followed by uninterrupted deglaciation. They do not consider the effect of ice sheet collapse and re-growth throughout the span of the last glaciation. Nevertheless, one can envisage that if an ice sheet went through oscillations in thickness and extent then so might its effect on atmospheric and oceanic circulation. The result would be concurrent fluctuations in climate between the North Atlantic and North Pacific - if the volume of ice involved during the collapse and growth cycle was sufficient.

In Rind's (1987) simulation he explores the direct effect of ice sheet elevation on the glacial climate. He found that an ice height of 3 km caused substantial cooling beyond that induced by just the area covered by ice alone. The reason for this was the reduced mass of the atmosphere above the ice sheet, which results in less long wave absorption and hence greater radiative cooling of the atmosphere; i.e., reduced Greenhouse Effect. Rind (1987) also presents two positive feedbacks associated with this cooling that increase albedo: (1) in winter 3 km thick ice allows greater snow cover around the ice sheet, and greater sea ice cover in the adjacent oceans; and, (2) 3 km thick ice also allows more snow cover on the ice sheet itself during summer (new snow albedo is ~85% whereas ice has an albedo of only 50%). Additional feedbacks might arise through effects on the hydrologic cycle. For example, in the present climate, the largest negative cloud radiative forcing (cooling) occurs in cloud systems associated with cyclonic activity and the extensive stratus cloud decks found over the oceans in the mid-high latitudes (Ramnathan *et al.*, 1989). Ramnathan and colleagues suggested that due to southward migration of the storm tracks during the last glacial maximum, this region of greatest negative cloud radiative forcing would also have shifted southward, perhaps amplifying Northern Hemisphere glaciation.

Oscillations in the ice sheet may also have influenced NADW formation. According to the glacial GCM's (listed above), cold winds blowing off the ice sheet, and ice sheet induced northerly winds out of the Arctic, would have cooled the North Atlantic ocean surface. MacAyeal (1993) postulated that colder SST's, leading to reduced evaporation (or even a cap of sea ice over areas of deep sinking), may have suppressed NADW formation.

When the ice sheet fails the cold winds it induced are not as severe, sea ice retreats, the polar front moves north, allowing more warm water to be brought in the high latitudes, where increased evaporation would allow NADW formation to intensify. One might think it more intuitive to have melting icebergs leading to reduced salinity and hence a reduction in NADW at the time of the Heinrich events, but Oppo and Lehman (1994) provide evidence that suggests NADW formation was reduced long before the cold SST's associated with the Heinrich events, and there was no apparent further reduction in intensity during or following the events. In addition, Bond and Lotti (1995) present mircofossil evidence that suggests surface warming occurred immediately after the Heinrich events, this is also when the major warming occurs in the ice cores (Bond and Lotti, 1995; Figure 13). Dokken and Hald (1996) provide microfossil evidence that suggests that sea ice retreated after the Heinrich events.

Hall *et al.* (1996) ran a higher resolution GCM than previous studies, which also included a seasonal cycle. Like the older models, it predicts a major influence on Northern Hemisphere climate due to the presence of large ice sheets during glacial maxima (Figure 15). In the North Pacific summer, the North Pacific High was shifted southeast, and the low level northerlies that dominate summer winds at present were weakened. In the North Pacific winter, the Aleutian Low is shifted to the southeast. This results in a more southerly low level flow over the eastern edge of the Pacific, which draws more tropical air into western North America. In some previous models this southerly flow produced a slight warming during the last glacial maximum in Alaska. But now, the higher resolution in Hall *et al.*'s (1996) model shows that cold winds draining (cold out-breaks) from the Laurentide ice sheet actually provides a net cooling in Alaska. Hall *et al.*'s (1996) model also predicts increased precipitation as snow fall in Alaska during both winter and summer, due largely to the southerly inflow of warm moist air.

Without the cold outflow off the Laurentide ice sheet, Hall *et al.* (1996) state that the warm southerlies might lead to a warmer climate in Alaska in their model, much as the older models predicted. An interesting possibility arises from this conclusion: Since the cold drainage is sensitive to ice height, a reduction in height might lead to warming in Alaska. Furthermore, the absence of the cold inflow might cause less of the precipitation to fall as

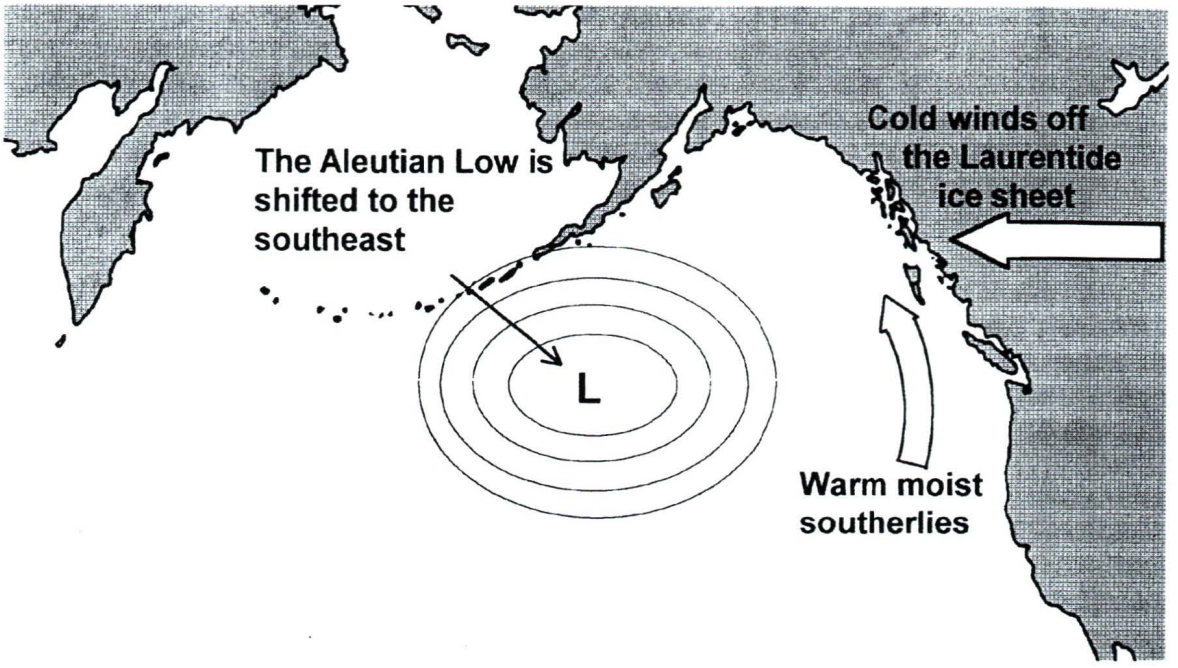

Figure 15. Schematic diagram highlighting the reorganization of atmospheric circulation during glacial maximum due to the influence of large Northern Hemisphere ice sheets (based on results of Hall *et al.*'s., 1996, general circulation model). The Laurentide ice sheet produces cold, low level winds draining off its surface (cold out-breaks). The Aleutian low is farther south and east from its interglacial position, inducing southerly flow of warm moist air along the west coast of North America. These changes lead to decreased temperature and increased precipitation in Alaska in Hall *et al.*'s model. If the Laurentide ice sheet were reduced in height (perhaps due to massive surging at the time of the North Atlantic Heinrich evetns) then so would its affect on atmospheric circulation; i.e., temperature would increase and precipitation would decrease. This suggests a possible link between Laurentide ice sheet height and glacier advance and retreat in Alaska, and may, thus, explain the correlation between major interstadials recorded in IRD flux and major interstadials recorded in Greenland ice cores (see text for discussion, and Figure 14).

snow. It is conceivable that these two factors, working together, would reduce glacier mass in Alaska when the ice sheet was reduced in height.

The major problem of an ice sheet height oscillation theory is whether or not the reduction in ice height is large enough during phases of failure. The identification of IRD-rich layers in North Atlantic deep-sea cores suggests a large scale increase in the calving rate from continental ice masses surrounding the North Atlantic, suggesting that massive surges from the eastern portions of the Laurentide ice sheet did, indeed, occur (Heinrich, 1988; Bond *et al.*, 1992). It has been recognized for some time that it is possible for ice sheets to go through such periodic surging on a massive scale, controlled by internal processes (Budd and McInnes, 1979; Boulton and Jones, 1979), and MacAyeal (1993) presented a model that suggests such large scale internal oscillations in ice sheet volume, rather than reduced temperatures, are responsible for the Heinrich events. Furthermore, Clark (1994) has suggested that failure of the Laurentide ice sheet was continent-wide based on major advances in places along the southern margin of the ice sheet concurrent with the first two Heinrich events. In MacAyeal's (1993) model the sediment underlying the ice cycles between periods when it is frozen and shorter periods when it melts. When the base is frozen ice flow velocity is small, as are iceberg calving rates. During this phase the ice sheet increases in thickness through net accumulation at the surface. However, thick ice keeps the base near the pressure melting point and the insulating effect allows geothermal heat to build until the base melts. When the sediment melts, pore-water pressure in the sediment approaches that of the overburden pressure, clast-clast contact forces are reduced, and eventually a threshold level is reached beyond which the ice sheet rests on a layer of low strength material. This low strength material reduces basal traction allowing greatly accelerated sliding through sediment deformation. The result is that the effected portions of the ice sheet start to stream and drawdown ice height. Surging along the marine margins results in Heinrich events. After a relatively short period of collapse [~250 years in MacAyeal's model, and generally <1000 years according to determinations of sedimentation rates during the Heinrich events (Francois and Bacon, 1994; Thomson *et al.*, 1995)] the ice sheet thins to such an extent that the base of the ice refreezes causing the surge to cease, along with the Heinrich event, until sufficient thickness is once again built up. Others agree

that such a mechanism is plausible (Orelemans, 1993; Fowler and Johnson, 1995).

During ice sheet collapse, sea level begins to rise, providing an additional mechanism that could facilitate further rapid collapse. For instance, ice shelves stabilize marine ice sheets by confining the ice streams that feed them. But one of the requirements for extensive iceshelves are pinning points (high points where the ice is grounded locally) which provide traction and slow the spread of the ice. If sea level rises, iceshelves can be floated off their pinning points causing the ice to spread and thin over the water, and ultimately the ice shelf to break up. Less extensive iceshelves along the marine margin increase the steepness of the surface slope between the grounded inland ice and the floating portion. The increased surface slope and less confined ice streams result in increased flow into the ocean and consequent thinning of the inland ice. The thinned ice at the grounding line is now susceptible to floating, and thus ice sheet collapse could be self-perpetuating (Weertman, 1974). The slope of the seafloor under the ice is therefore important to this kind of ice sheet decay. On a flat ocean floor, or one sloping down toward the ice, Weertman's (1974) numerical model showed that this process would lead to total deterioration of an unconfined ice sheet. Whereas a seafloor sloping seaward eventually stops the thinning.

Blanchon and Shaw (1995) proposed that catastrophic sea level rise (up to 13.5 m) accompanied the Heinrich events. In their conceptual model sudden draining of proglacial reservoirs caused a rise in sea level of sufficient magnitude that it destabilized the ice sheet margins, causing collapse (Heinrich events). The influx of freshwater from both draining lakes and melting icebergs was enough to drown Caribbean corals; the terraces that form as a result serve as Blanchon and Shaw's sea level indicator. The assumption that the volume of water drained from proglacial reservoirs was sufficient to raise sea level enough to destabilize marine ice sheets, may be problematic. In Shaw (1989) an out-burst flood that formed extensive drumlin fields in North America was estimated to have had sufficient volume to cause a sea level rise of only 23 cm. It also seems unlikely that proglacial lakes would be largest during the coldest phase of Dansgaard-Oeschger cycles prior to the Heinrich events, since this is when the ice sheet elevation was greatest, and thus its surface and surrounding area coldest, which would lead to reduced runoff. Instead, it seems more likely that the Laurentide ice sheet became unstable and collapsed due to internal processes, as

discussed earlier.

Proglacial lakes may still have played a part in the collapse of the Laurentide ice sheet. When the ice sheet became unstable and started to surge along its marine margins, causing Heinrich events, it may also have started surging along its southern margins, perhaps into proglacial lakes in places. Mickleson *et al.* (1981) suggested that calving into proglacial lakes could have been an important process in the rapid deglaciation of the Laurentide ice sheet at the end of the last glaciation since an increase in lake depth could accelerate failure the same way sea level rise would along marine margins. By analogy, surging and calving into proglacial lakes concurrent with the Heinrich events could accelerate failure of the ice sheet. Eventually the lakes would drain, perhaps catastrophically, as new routes to the ocean were uncovered by retreating ice. Draining of the lakes might then play a role in bringing about the end of a phase of ice sheet collapse, since the ice could readily readvance over the drained lands.

Sea level rise at the time of the Heinrich events is likely, and is one possible candidate for destabilization of other marine ice sheets and glaciers in the North Atlantic, and therefore might explain the concurrent increased ice-rafting from a number of sources that has been documented (Bond and Lotti, 1995; Fronval *et al.*, 1995). However, there is no convincing evidence for a sea level rise at the time of the Heinrich events; Blanchon and Shaw's (1995a) date (12,200 ka-^{14}C-BP) for catastrophic sea level rise occurs too late to be the cause of Heinrich event 1. Glacier advances from smaller bodies of ice, more icebergs, and increased iceberg survivability are also likely candidates if it could be shown that IRD from non-Laurentide sources lay stratigraphically below Laurentide sourced IRD. Bond and Lotti (1995) suggest that deposition of IRD grains composed of basaltic glass, from Iceland, and hematite coated grains, from sources in the North Atlantic other than Hudson Strait, increase before the Heinrich layers are deposited (carbonate rocks around the Hudson Strait are thought to be the source of the detrital carbonate grains that comprise the Heinrich layers). Then, suddenly, during the Heinrich events, they appear to decrease again. This decrease is probably entirely due to dilution of basaltic and hematite coated grains by increased supply of detrital carbonate during the Heinrich events (Bond and Lotti, 1995), but advancing glaciers, and cold ocean temperatures before the Heinrich events may still account

for the increase from these sources at this time. Fronval *et al.* (1995) also noted that IRD deposition increased in the Norwegian sea when Greenland air temperatures decreased. They also found that periods of increased IRD flux were concurrent with glacier advances in Scandinavia, as did Baumann, *et al.* (1995), and Haflidason *et al.* (1995) noted IRD flux followed trends in Norwegian Sea surface temperatures very closely during deglaciation.

If internal processes within ice sheets, rather than climatic processes, can govern their susceptibility to failure (MacAyeal, 1993), and if continental ice along the west coast of North America was in the form of a similar continental ice sheet, then it would not respond quickly to the shifts in climate as described above. It may still have responded to global sea level rise. However, glaciation in coastal British Columbia and Alaska was not of true continental ice sheet scale. Consequently the coastal glaciers, would have responded more quickly to climate than the Laurentide ice sheet. In reality there is a lag in glacier response. According to Mann (1986b) fjord glaciers will equilibrate with climate in ~500 to <1000 years. However, in deep-sea cores this lag may not be discernible, due to the limitation of temporal resolution that is attainable given typical sedimentation rates. Although, in some cases in Figure 14 the interstadials in the Alaskan cores do reach a maximum slightly after the maximum interstadial conditions in the GRIP core.

In summary, it is possible that the Laurentide ice sheet went through massive failure on a continent-wide scale at the time of the Heinrich events. Therefore, the relation between North Pacific and North Atlantic IRD events, and hence a coupled North Atlantic-North Pacific climate at the Bond cycle frequency, is proposed to be primarily a result of internal oscillations between massive failure and re-growth of the Laurentide ice sheet. This had direct and indirect effects on the ocean and atmospheric circulation, including the oceans thermohaline circulation. Ultimately the indirect effects may have been most important in producing the observed global climate changes, but the ice sheet oscillations serve as the trigger. Henceforth, the two extremes in the model are referred to as *Laurentide maxima* and *Laurentide minima*. During Laurentide maxima the Laurentide ice sheet was at a maximum in volume and had its greatest effect on climate. Cold winds (out-breaks) induced by sinking over the ice sheet led to reduced temperatures in the North Pacific. Atmospheric pressure systems were displaced south and east, resulting in warm moist air flowing into western

North America, and increased snow fall. Greater snow and sea ice cover increased albedo and enhanced the cooling. Displacement of atmospheric pressure systems and geologic data suggest the subarctic gyre was farther south, which would have reduced northward heat flux. Associated with the displacement of the mid-latitude jet stream south of the ice sheet, was a southward shift of the storm tracks, which may have led to an increased albedo of the atmosphere and lower temperatures in the subtropics.

Given conditions of colder temperature and increased snow fall, glacier equilibrium line altitudes were lower in western North America, glacier mass balance increased, more glaciers advanced to tidewater on the continental shelf, and some may have developed floating ice-tongues. The result was increased number and size of icebergs calving into the Gulf of Alaska, and colder temperatures led to increased iceberg survivability, hence the increased flux of IRD to the core sites. During Laurentide minima, the ice sheet had recently failed (producing a Heinrich event in the North Atlantic) and the ocean-atmosphere circulation reverted to interstadial conditions (although not interglacial conditions). This brought warmer atmospheric and ocean temperatures to the Gulf of Alaska, causing rapid break-up of the floating ice tongues, and reduced iceberg survivability. In addition, snow fall was reduced and ice retreated from the shelf edge. Under these conditions IRD flux was greatly reduced at the core sites. This was followed by an increase again during the cooling phase of the Bond cycles, as the Laurentide ice sheet started to rebuild itself and push the climate system toward its Laurentide maximum conditions.

b.) The core off northern Vancouver Island

The out-of-phase relationship in IRD flux between the Alaskan cores and the core off northern Vancouver Island (Figure 11) can also be explained within this model: If the debris came from Queen Charlotte Sound, then only during the initial stages of deglaciation, when ocean circulation patterns had reverted to a more interglacial configuration, were conditions favourable for transport of icebergs over this core site (Figure 12), and then only for a short while since the shelf was being deglaciated during warming climate. Prior to this, the glacial Alaskan current, that originated farther south at the time, carried icebergs away from this

core site, perhaps over the Alaskan sites.

c.) Comments on the glacial history of southern British Columbia

Low elevations in southwestern British Columbia and northern Washington experienced an interval of ice retreat around 18 ka-^{14}C-BP, despite temperatures ~8°C colder than present (Hicock *et al.*, 1982). Hicock *et al.* attributed this to insufficient precipitation in this area during global glacial maximum conditions. They went on to suggest the reason for the final advance (the Vashon advance) was that precipitation increased "as a result of northward shift of zonal weather patterns associated with the initial decay of the Laurentide ice sheet." This advance could also be viewed as occurring after Heinrich event 2. Likewise the earlier advance (the Evans Creek advance) follows Heinrich event 3. A missing advance after Heinrich event 1 is conspicuous, unless the Sumas advance (Easterbrook, 1992), or the advance in Juan de Fuca Strait (Alley and Chatwin, 1979), can be accounted for in this way. Alternatively, given increasing Northern Hemisphere insolation at this time, temperatures may have been too warm and precluded an ice advance after Heinrich event 1. Therefore, glacial advances out of phase with northern coastal British Columbia and Alaska may be a recurring phenomenon in southwestern British Columbia and northern Washington. This region is then a special case that might be fit into the model as follows: During both Laurentide Maxima and Laurentide Minima conditions were unfavourable for ice advance in the south; it was drier during Laurentide Maxima, and simply too warm during Laurentide Minima. Instead glacial maxima in this area was brief, and only reached during the earlier stages of cooling associated with Bond cycles: As the Laurentide ice sheet began recovering after failure, temperatures decreased, but conditions were still wet enough such that more precipitation fell as snow, and so ice advanced in southern British Columbia and Washington. However, as the storm tracks were pushed farther south precipitation was reduced (i.e., now nearing Laurentide Maxima conditions) and the Juan de Fuca and Puget lobes could not maintain the same extent despite the cooler temperatures at the time, and therefore they retreated out of the lowlands shortly before glacial maxima in the Gulf of Alaska, whereas IRD accumulation in the Gulf of Alaska did not reach a minimum until

after the Heinrich events.

d.) The missing younger Dryas and higher frequency Dansgaard-Oeschger cycles

In the North Atlantic there is an IRD event concurrent with the Younger Dryas. However, an equivalent Younger Dryas IRD event is entirely absent in the Northeast Pacific. There are no records of glacier advance in Alaska at this time, and the almost total absence of IRD after 14 ka-BP suggests glaciers were terminating within fjords. This absence of a Younger Dryas IRD event is not necessarily in contradiction with other studies (those cited in III.i.a.) that record a Younger Dryas equivalent. Glaciers may have readvanced in some parts of western North America at this time (Reasoner *et al.*, 1994, shows evidence that they did in the Rocky Mountains), they simply did not readvance to fjord mouths to provide a calving front in open waters before the end of the Younger Dryas, so there were few icebergs despite colder temperatures. On the other hand, it is conspicuous that other mountain ranges in British Columbia and Alaska do not record a Younger Dryas time readvance.

The higher frequency Dansgaard-Oeschger interstadials could be missing from the North Pacific IRD record because they were too short to cause a retreat, but the increased temperatures would have reduced iceberg survivability, and this may have been detectable. The Dansgaard-Oeschger cycles are also missing from the works of other investigators, reviewed previously, with the exception of Behl and Kennett's (1996) very high resolution core from Santa Barbara Basin. This may indicate most of the other records are of insufficient sensitivity, or insufficient resolution to record them. However, this is not likely the case for the Vostok ice core (Bender *et al.*, 1994) and possibly the long pollen records in Florida (Grimm *et al.*, 1993), which do not record all the Dansgaard-Oeschger cycles. Even if Behl and Kennett's (1996) record of anoxia in Santa Barbara basin does correlate with the GISP2 ice core, it does not provide a proxy for temperature or precipitation, and it may be possible that oxygen-rich events correlative with Dansgaard-Oeschger cycles occur there because Santa Barbara Basin was just particularly sensitive. Indeed, Behl and Kennett (1996) suggest it was very sensitive. Furthermore, it has not yet been shown how a missing component of NADW in the North Pacific would effect climate in the North Pacific. It is

unlikely that perturbation of global thermohaline circulation, perhaps driven from the North Atlantic, would have *no* effect on the North Pacific. The model by Fanning and Weaver (1996) simulated the affect of reduced NADW formation at the time of the Younger Dryas on global climate. It only produced a cooling of only 2.4°C in the North Pacific, suggesting the Younger Dryas, and perhaps by analogy the high frequency Dansgaard-Oeschger events, may have been subdued outside the North Atlantic such that they are not felt by less sensitive recorders, like ice advance, and ocean temperatures were not reduced enough to effect iceberg survivability. If this were the case, then the North Pacific Ocean only warmed appreciably during the longer Dansgaard-Oeschger interstadials that occurred after Heinrich events, but not the higher frequency ones.

Variability in North Atlantic thermohaline circulation is one likely cause of localized climate oscillations in the Greenland ice cores. Bond and Lotti (1995) do note a temperature increase after some of the Dansgaard-Oeschger cycle IRD layers (non-detrital carbonate layers) comparable to the temperature increase after Heinrich events. Re-intensification of NADW formation, which may also have reduced sea-ice cover, might then explain the Dansgaard-Oeschger interstadials. Perhaps some sort of "salt oscillator" was in operation like that described in Broecker *et al.* (1990), superimposed on the Bond cycles.

Therefore, it is conceivable that the Dansgaard-Oeschger cycles were of dominantly local origin and influence in the North Atlantic, with little effect in other parts of the world. These warm intervals were superimposed on a general cooling trend (a Bond cycle) that was ultimately caused by increasing global ice volume. Each period of ice growth culminated with a Heinrich event that marks the transition into the following long interstadial. The effects of this growth and failure were felt very strongly throughout the Northern Hemisphere, and perhaps, also transmitted to the Southern Hemisphere.

iii.) Transmitting the climate signal to the Southern Hemisphere

Lowell *et al.* (1995) have presented evidence of Southern Hemisphere ice advance concurrent with the North Atlantic Heinrich events, and Bender *et al.* (1994) have correlated the interstadials in the Vostok ice core with major interstadials in the GRIP core, and these

also follow the earlier Heinrich events (there is no oscillation correlative with Heinrich event 1). It has been suggested (Bender *et al.*, 1994) that increased production of NADW would warm Antarctica, through increased upwelling in the ocean around it, which would release heat to the atmosphere and surface waters, and also reducing winter sea ice cover, which further amplifies warming by reducing albedo. In turn, this would shift Southern Hemisphere climatic belts farther south, and thereby increasing poleward heat transport. Conversely, reduced NADW circulation would cool Antarctica.

Lowell *et al.* (1995) proposed that the forcing behind interhemispheric climatic synchroneity (their alpine ice advances) is due to cooler tropical SST's during stadials. Colder tropical temperatures are now recorded by a number of proxies, which seriously discredit the CLIMAP (1976) reconstruction of tropical SST's which indicated temperatures only slightly cooler than present. Guilderson *et al.* (1994) proposed that colder glacial SST's in tropical latitudes were caused by the inflow of colder subtropical waters into the region. The cooler tropical SST's lead to reduced evaporation, and, as a consequence, reduced water vapour in the Hadley circulation. The reduced water vapour leads to a net decrease in the long wave radiative forcing on both sides of the equator, and also reduced latent heat transport to higher latitudes. In this way a signal for climatic cooling can be transmitted to the Southern Hemisphere (Guilderson *et al.*, 1994).

Whether it is tropical atmospheric circulation or thermohaline circulation in the ocean (probably some combination of both) that could potentially lead to interhemispheric climatic synchroneity, there must be a driving force behind the oscillations. It was proposed in the previous section that internally forced oscillations in Laurentide ice sheet volume, and feedbacks in the ocean-atmosphere system, led to synchronous events in climate throughout the Northern Hemisphere at sub-orbital frequencies. Displacement of the Pacific's subarctic gyre farther south, and displacement of the stratus cloud decks farther south, would both have contributed to cooler tropical SST's via the meridional circulation, and NADW may have been reduced during Laurentide maxima, and then resumed after the Heinrich Events. Bender *et al.*, (1994) suggested reduced NADW might cause cooling around Antarctica. Therefore, prior to the Heinrich events, cooling of Southern Hemisphere subtropical SST's may have resulted in equatorward displacement of the Subtropical highs and expansion of

the Southern Hemisphere polar vortex, and northward displacement of storm tracks and oceanic gyre boundaries. Also, reduced upwelling around Antarctica would further amplify this effect by cooling the polar region. The result may have been sufficient cooling and displacement of precipitation belts in the Southern Hemisphere mid-latitudes to allow the glacier advances of Lowell *et al.* (1995). When the Laurentide ice sheet collapses the opposite sequence of events occurs in the atmosphere and strong thermohaline circulation returns. In response, Southern Hemisphere glaciers are forced to retreat shortly after the Heinrich events.

In summary, the previous conceptual model is somewhat speculative. GCM experiments that include a realistic reduction in ice height (?) at the time of the Heinrich events, or even include an ice sheet model, are needed to evaluate the importance of the proposed components of the conceptual model. It may be that the Laurentide ice sheet dominated climate oscillations in the late Pleistocene. However, apparent climatic oscillations in the absence of the Laurentide ice sheet (during isotope stage 5e, for example) recorded in the Greenland ice core, and some long pollen records, require a different origin. Furthermore, if future work shows that the higher frequency Dansgaard-Oeschger events were just as intense around the globe as the climatic warming after the Heinrich events appears to have been, then the climatic effects of massive ice sheet failure are subordinate to some other process, and superimposed on the Dansgaard-Oeschger cycles; it unlikely that the Laurentide ice sheet could collapse and grow fast enough to produce the required change in ocean-atmosphere configuration needed to transmit strong Dansgaard-Oeschger cycles to the west. For instance, MacAyeal's (1993) model produced a Heinrich event every ~7 ka, a considerably longer time period than occurs between Dansgaard-Oeschger cycles. If this is the case an alternate process might have its origins in the global thermohaline circulation, and its direct and indirect effects on the atmosphere, but such a mechanism will ultimately have to explain the progressive cooling of Dansgaard-Oeschger cycles.

This conceptual model, presented above, calls on processes in the Northern Hemisphere to be the driving force behind global climatic variability. It is possible, however, that processes in the Southern Hemisphere could be of primary importance. In the same way that the Laurentide ice sheet may have caused global climatic oscillations, internal

oscillations of the Antarctic ice sheet (MacAyeal, 1992) could also provide a means of synchronous interhemispheric climatic change. There could also be a sea level connection between the Laurentide ice sheet and the Antarctic ice sheet governing growth and collapse of both (Denton *et al.*, 1986). It has even been suggested that the strength of NADW circulation can be influenced from the southern Hemisphere (Toggweiler and Samuels, 1995). Therefore, there is a necessity for more long, high-resolution records from around the Southern Hemisphere in order to evaluate the behaviour of the Antarctic ice sheet and ocean circulation during the last glaciation.

6. The last interglacial period (marine isotope stage 5)

McMannus *et al.* (1994) show that there are 3 additional IRD layers in the North Atlantic sediments deposited during isotope stage 5, and like the first 6 Heinrich events, they can be correlated with GRIP stadials. If these events are of the same origin as the later Heinrich events then it suggests that perhaps there could be corresponding events in the North Pacific IRD record. However, as discussed previously in section III.3.i., there are diatomaceous layers deposited during the later half of stage 5 in the Gulf of Alaska cores, and it appears that these layers were deposited much quicker than the age model currently predicts. Not surprisingly, therefore, the correlation with the GRIP ice core deteriorates in this interval. There are, however, distinct IRD events with a spacing between them that appear to be proportional to that between stadials in the GRIP core. Given this, and given that clearer correlations between GRIP stadials-interstadials and IRD fluctuations can be made both before and after this interval, and since changes to the age model are expected, a tentative correlation is proposed here (Figure 16).

The last interglacial maximum (isotope stage 5e) is a time of global warmth, similar to the present. In the GRIP ice core, however, it is interrupted by two marked periods of climatic deterioration, separated by a warmer interval (Dansgaard *et al.*, 1993). Initially

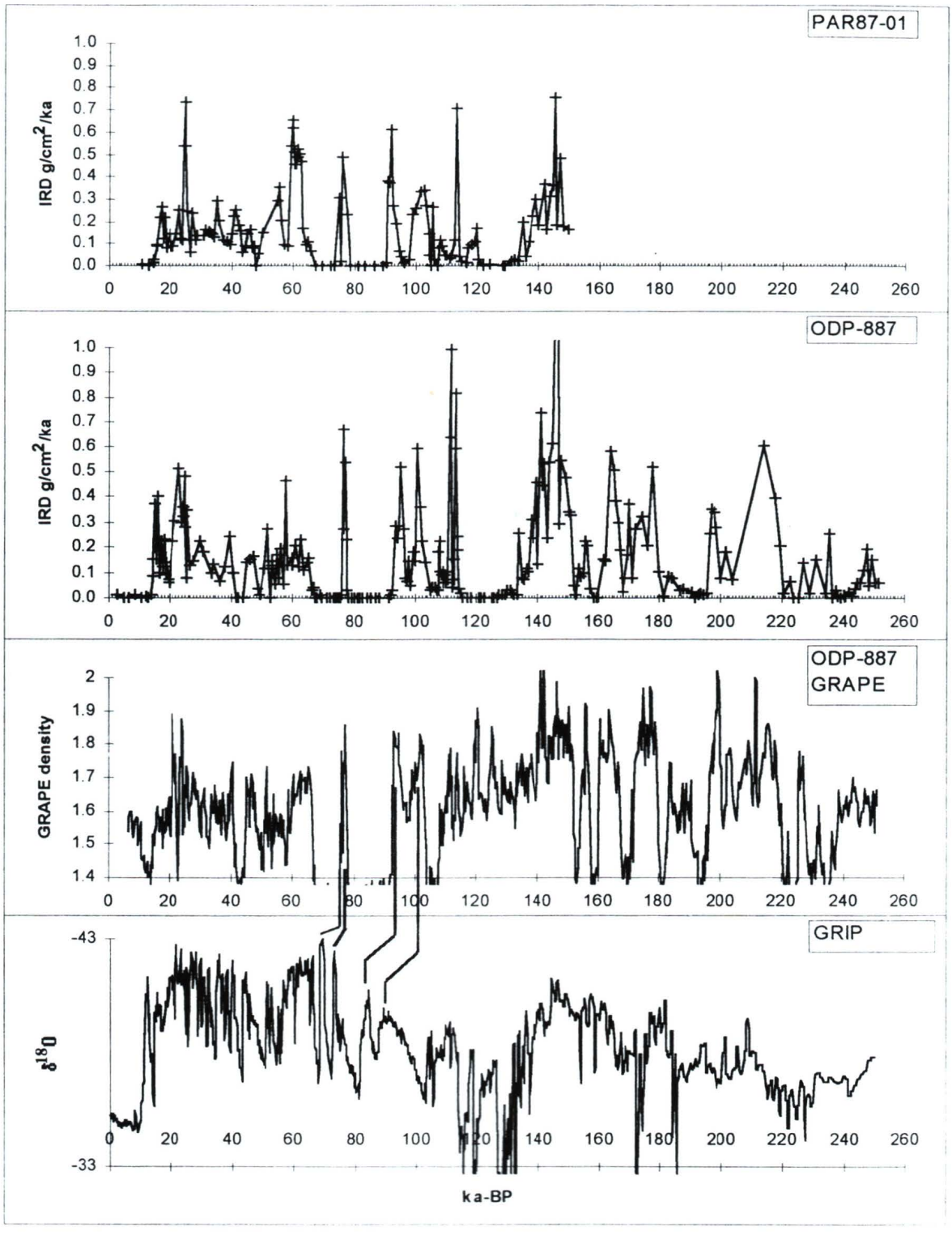

Figure 16. Correlation between IRD mass accumulation rate (and GRAPE density in ODP-887) with GRIP $\delta^{18}O$ during the last 250 ka-BP. The poor correlation during the later half of isotope stage 5 (65-90 ka-BP) is probably due to very high rates of sedimentation of thick diatomaceous layers during these intervals. Since the correlation between GRIP and the IRD record is clearer during intervals where the age control is better (see figure 12 also), a tentative correlation between the IRD events in this interval and stadials in the GRIP core is proposed (indicated by the solid tie-lines in GRIP).

there was doubt as to whether or not these oscillations were real or just an artifact of ice-layer deformation. Now it appears they are, indeed, real since they correlate with other paleoclimate records from northwestern Europe (Guiot *et al.*, 1993; Field *et al.*, 1994; Thouveny *et al.*, 1994; Cortijo *et al.*, 1994; Lauritzen, 1995).

The isotope stage 5e climatic oscillations cannot be caused by oscillations in ice elevation since there was presumably no Laurentide ice sheet in North America at that time. Perturbation of North Atlantic thermohaline circulation has been called upon to explain them. Wijfells *et al.* (1992) proposed that during higher sea level stands than present, there would be a greater flux of fresher water through the Bering Strait, into the Arctic, and then ultimately into Norwegian Sea; and that this could result in a more sensitive thermohaline circulation. Isotope stage 5e was such a time, and small perturbations in freshwater influx from the Arctic (Shaffer and Bendtsen, 1994), and/or an intensified 5e hydrological cycle (Weaver and Hughes, 1994), may have triggered the oscillations in the GRIP core through a reduction in deep sinking in the Norwegian Sea, and consequently the northward heat transport in the warm Norwegian Current.

Were these stage 5e oscillations global in nature? So far no paleoclimatic record outside the high latitudes of northwestern Europe or Greenland has suggested that they might be (McMannus *et al.*, 1994; Johnsen *et al.*, 1995). The events, especially the earlier one, are of long enough duration that they could conceivably cause Alaskan glaciers to advance, and also improve iceberg survivability, if the climate change associated with them was of global influence.

Only two of the cores investigated in this study penetrate to a depth inclusive of isotope stage 5e (PAR87A-01 and ODP 887). In PAR87A-01 there is, in fact, a small IRD peak that occurs at the same time as the later, shorter 5e stadial in the GRIP core (Figure 6), but not the earlier, longer one. On the other hand, there is only a very small amount of IRD in ODP 887 at any time during stage 5e. Von Huene *et al.*'s (1976) account of ice rafting in the North Pacific, although the chronology is not as rigorous as that used here, also indicates ice rafting during stage 5e (their figure 2). Evidently, climatic conditions in the North Pacific toward the end of the last interglacial were such that Alaskan glaciers advanced to the mouths of fjords, and temperatures were sufficiently cold, resulting in a greater flux of IRD

compared to the present interglacial period.

Unfortunately, there are presently no other suitably long, continuous, high-resolution records from the last interglacial Northeast Pacific with which to compare IRD flux. But in the low latitude western North Pacific, Linsley (1996) reports $\delta^{18}O$ data that contains an inferred cold period during isotope stage 5e. Like the IRD record only one stadial is identified, not two as in the GRIP core.

Whether or not the GRIP 5e stadials are transmitted to the North Pacific will have to wait until future records are available. Since the events appear to be subdued, or absent, outside northwestern Europe, however, it is unlikely they were strong in the North Pacific. Instead, this event in the IRD record is probably related to the reduced insolation at the time. Harrison *et al.*'s (1995) simulation of stage 5e climate was primarily a sensitivity study on the effect of insolation, rather than an attempt at a full climate simulation. Nevertheless, reduced insolation provided a colder climate at the end of stage 5e, when the IRD event occurs.

7. The last 800,000 years.

From the GRAPE density record (Figure 10) it is evident that ice-rafting in the Northeastern Pacific was variable at suborbital time scales throughout the last 800 ka-BP. If, as has been proposed here, Laurentide ice sheet volume controls the advance and retreat of Alaskan glaciers, then the high frequency oscillations in the GRAPE record suggest oscillations in the Laurentide ice sheet during glaciations have been a recurring phenomenon. van Kreveld *et al.* (1996) identified seven IRD layers in the North Atlantic, older than the Heinrich events, between 125-200 ka-BP. Several of these are characterized by detrital carbonate grains, like the Heinrich layers, suggesting they were deposited by Heinrich like events during the penultimate glaciation Although these seven events cannot all be as clearly correlated to IRD events in the North Pacific, there are, interestingly, seven major North Pacific IRD events in this same time interval (125-200 ka-BP in Figure 7)

i.) Correlation of the IRD record to the SPECMAP isotopic record

There are a number of long (~1 Ma) accounts of paleoclimatic change in the circum-North Pacific (Sancetta and Silvestri, 1986; Morley *et al.*, 1987, Hovan *et al.*, 1991; Ding *et al.*, 1995). The oceanic and atmospheric proxy records presented in these studies reveal dominant frequency in variability at periods corresponding to the major insolation cycles. Ding *et al.* (1995) compared a loess grain size record from China with the SPECMAP marine isotope record, and found that increased winter monsoon strength (larger eolian grain size) correlated with increased global ice volume. In particular a periodicity of 100,000 years dominated the grain size record, and the 41 and 23 ka periodicities were much weaker; the same pattern is seen in the SPECMAP stack (figure 9 in Ding *et al.*, 1995). They suggest this indicates the dominant role of northern hemisphere ice volume in controlling monsoon strength since the 41 ka and 23 ka orbital cycles (important cycles in controlling insolation) would otherwise have had a stronger effect on winter monsoon strength. The loess record of Porter and Zhisheng (1995), also from China, which they correlated with the Heinrich events, suggests Northern Hemisphere ice volume may have controlled winter monsoon strength at suborbital time scales as well.

The GRAPE record, presented here, also suggests a link exists between global ice volume and IRD flux in the Gulf of Alaska, at a 100,000 year periodicity. When the time series is smoothed with a 50 point running average, the resulting curve bares a distinct resemblance to the SPECMAP isotopic record of global ice volume (Figure 9). This suggests that Laurentide ice volume has controlled Alaskan glacier advances throughout the last 800 ka-BP, on both suborbital and 100,000 year time scales.

ii.) A mid-Brunhes climatic transition

There are a large number of long paleoclimatic records from around the world that contain evidence of a marked change in the intensity of glacial/interglacial contrasts after 0.4

Ma (review in Jansen *et al.*, 1986). It is also evident in the SPECMAP stack. After this "Mid-Brunhes climatic event" glacial periods in the Northern Hemisphere became colder, resulting in a greater contrast between glacial and interglacial periods. This transition has been noted in the North Pacific by (Sancetta and Silvestri, 1986; Morley *et al.*, 1987; Hovan *et al.*, 1991). Jansen *et al.* (1986) suggested this event might be related to a 500,000 year orbital cycle.

The smoothed GRAPE record also appears to exhibit a mid- Brunhes climatic transition around 400 ka-BP. In the early part of the record the transitional periods between glacial and interglacial conditions (peak GRAPE density versus minimum GRAPE density) appear more gradual than they do in the latter half of the record (Figure 9). Furthermore, the contrast between glacial and interglacial GRAPE values appears to increase after 400 ka-BP; i.e., GRAPE values do not decrease as much during the early Brunhes interglacials as they do in the late Brunhes interglacials. Also, peak GRAPE values are not as large in the early Brunhes during two of the three glacial periods between 400-700 ka; the one at ~690 ka-BP is of equal magnitude to those in the latter half of the record. According to the SPECMAP stack, global ice volume does not diminish to the same extent during interglacials prior to 400 ka-BP as it does after this time, and the IRD record (GRAPE and the visual estimate) indicated abundant IRD during these interglacials.

IV. CONCLUSIONS

This work has presented a high-resolution, 800,000 year account of the supply of ice-rafted debris (IRD) to the seafloor of the Northeast Pacific. The record was constructed from the mass accumulation rate of coarse lithic material (180 - 500 μm) in five cores, and also from Gamma Ray Attenuation Porosity Evaluator (GRAPE) density in one core. In addition, the petrology of ice-rafted grains was determined under a microscope. The major conclusions that emerge from the results are:

1. The petrology of IRD grains (500-5000 μm) in the four Gulf of Alaska cores is distinctly different from the petrology of grains in the core off Vancouver Island. IRD in the Gulf of Alaska is dominated by dark colored sedimentary and metasedimentary rock fragments (argillite, slate, silt and sandstone), whereas quartz grains dominate the IRD off Vancouver Island. This reflects the different continental source regions for the debris: the petrology of IRD grains in the Gulf of Alaska cores indicates southern Alaska (the Chugach and St. Elias mountains) as the dominant source. The petrology of grains in a core off northern Vancouver Island suggests granitic rocks in southeastern Alaska and northwestern British Columbia (Alexander Archipelago, Coast Mountains of British Columbia, Dixon Entrance, and Queen Charlotte Sound) were the chief source of this debris. At times of particularily high IRD accumulation, the concentration of debris from southeastern Alaska and western British Columbia was increased in the Gulf of Alaska cores relative to other grain types (there was a greater percentage of quartz + feldspar + granitic fragments). Such times are proposed to represent cold ocean conditions when more of the icebergs calved from eastern sources survived melting and reached the Gulf of Alaska core sites.

2. Periods of increased/decreased IRD flux are concurrent between the four Gulf of Alaska cores, but the magnitude of IRD accumulation rates, are often quite different. The close proximity of these four core sites probably precludes paleoclimatic/oceanographic factors in producing this variability. Instead it is proposed that this was a result of random iceberg behaviour: debris dumps off the top of icebergs are envisioned as being rather sporadically distributed, especially during times of low iceberg supply, and this results in the timing of entry and exit of IRD events (stadials) being less well defined in detail than they might otherwise be. The issue of random iceberg behaviour has not been addressed in the North Atlantic.

3. Periods of increased IRD flux are proposed to be intervals when both ice advance and colder ocean temperature resulting in an increased supply of IRD to the core sites in the Gulf of Alaska. On the other hand, the single IRD event in the core off Northern

Vancouver does not occur during a phase of glacial advance (and coldest ocean temperatures), but rather during the early stages of deglaciation of the shelf in that area. It is proposed that only at this time was ocean circulation favourable for transport of icebergs over this core site. Prior to deglaciation the Alaska Current originated farther south than this core site, and so debris was carried northward away from this core site; perhaps even over the core sites in the Gulf of Alaska. These cores do show an increase in debris more characteristic of the core off Southern Vancouver Island during times of especially high IRD accumulation.

4. It was found that periods of increased IRD flux are concurrent with well dated intervals of continental ice advance in southern Alaska and northwestern British Columbia. Extending beyond the range of radiocarbon dating, the IRD record presented in this work suggests many ice advance-retreat cycles during the late Quaternary, and provides a detailed chronology of these events through the last 800,000 years.

5. The IRD record was correlated with the $\delta^{18}O$ record in Greenland ice (the GRIP ice core). This correlation reveals that intervals of low IRD accumulation are concurrent with the especially long interstadials recorded the GRIP core. These are the same interstadials that follow the North Atlantic Heinrich events, and many of these are the same interstadials recorded in the Vostok ice core, and other long records. The shorter, higher frequency Dansgaard-Oeschger interstadials (that occur between the interstadials that follow the Heinrich events in the GRIP core and North Atlantic sediments) have no correlative North Pacific interstadials recorded in IRD accumulation. There is also no IRD event associated with Younger Dryas time.

6. A conceptual model was proposed to explain this apparent link between fluctuations in Northeast Pacific IRD accumulation and the North Atlantic Heinrich events, based mainly on the results of previously published GCM's. The model calls on the massive oscillations in Laurentide ice sheet height, that result in the Heinrich events, as a trigger forcing the climate system into a different configuration that results in a warmer climate

in Alaska, leading to glacier retreat, warmer waters, and hence reduced IRD accumulation. After the ice sheet surge, the regrowth in ice sheet volume causes a return to full glacial climate in Alaska, accompanied by ice advance, colder ocean temperatures, and hence increased IRD accumulation.

7. The shorter, High frequency Dansgaard-Oeschger cycles are missing in the Northeast Pacific IRD record because massive surging of the Laurentide ice sheet did not occur at these times (there are no detrital carbonate layers correlative with these events in the North Atlantic). These events are only clearly recorded in the North Atlantic, and are therefore probably greatly attenuated elsewhere in the world, whereas climate events associated with the Heinrich events appear to be global. The Younger Dryas, if indeed it did occur in the North Pacific region, is probably missing because it was not of long enough duration to cause a readvance of glaciers to fjord mouths to provide significant IRD to the cores sites.

8. There was a low, but significant quantity of IRD deposited in the North Pacific during some of the global interglacial episodes, but not the Holocene - so far. There is one such event at the end of isotope stage 5e, but in only one of the two cores that span this time. Nevertheless, it represents a period when glaciers were at fjord mouths, and ocean temperatures were probably colder than present, and also colder than earlier during stage 5e. This IRD event is roughly concurrent with the younger of the two stage 5e stadials recorded in the GRIP core, but there is no IRD event associated with the earlier, longer one. The forcing agent behind these IRD events must be something other than oscillations in Laurentide ice volume since there was no Luarentide ice sheet at the time. Decreasing insolation in the later half of stage 5e is a likely candidate.

9. The IRD record was correlated with the SPECMAP marine $\delta^{18}O$ record. This correlation shows that the 100,000 year cycle in ice volume that dominates the SPECMAP record is in phase with a 100,000 year cycle in IRD flux. A "mid-Bruhnes climate event" is also apparent at 400 ka-BP.

10. The correlations with $\delta^{18}O$ records in both the GRIP core and the SPECMAP stack suggest that fluctuations in Laurentide ice volume, and consequent forcing of the climate system, are what control the timing of ice advance (glaciations and stadials) in northwestern North America (and perhaps globally) on both 100,000 year time scales, and on suborbital time scales of around 10-15 kyr.

BIBLIOGRAPHY

Alley, N.F., and Chatwin, S.C. 1979. Late Pleistocene history and geomorphology, southwestern Vancouver Island, British Columbia. Canadian Journal of Earth Science. 16: 1645-1657.

Alley, R.B., Blankenship, D.D., Rooney, S.T., and Bentley, C.R. 1989. Sedimentation beneath ice shelves-the view from ice stream B. Marine Geology. 85: 101-120.

Barrie, J.V., and Bornhold, B.D. 1989. Surficial geology of Hecate Strait, British Columbia continental shelf. Canadian Journal of Earth Science. 26: 1241-1254.

Barrie, J.V., and Conway, K.W. 1993. Postglacial geology of Dixon Entrance northwestern British Columbia continental shelf. in Current Research, Part E: Geological Survey of Canada Paper 93-1E. p. 15-21.

Baumann, K-H., Lackshewitz, K.S., Mangerud, J., Spielhagen, R.F., Wolf-Welling, T.C.W., Henrich, R., and Kassen, H. 1995. Reflection of Scandinavian ice sheet fluctuations in Norwegian Sea sediments during the past 150,000 years. Quaternary Research. 43: 185-197.

Behl, R.J., and Kennett, J.P. 1996. Brief interstadial events in the Santa Barbara Basin, NE Pacific, during the past 60 kyr. Nature. 379: 243-246.

Bender, M., Sowers, T., Dickson, M-L., Orchardo, J., Grootes, P., Mayewski, P.A., and Meese, D.A. 1994. Climate correlation's between Greenland and Antarctica during the past 100,000 years. Nature. 372: 663-666.

Blaise, B., Clague, J.J., and Mathews, R.W. 1990. Time of maximum late Wisconsinan glaciation, west coast of Canada. Quaternary Research. 34: 282-295.

Blanchon, P., and Shaw, J. 1995. Reef drowning during the last deglaciation: Evidence for catastrophic sea-level rise and ice-sheet collapse. Geology. 23: 4-8.

Bobrowsky, P., and Rutter, N.W. 1992. The Quaternary geologic history of the Canadian Rocky Mountains. Geographie physique et Quaternaire. 46: 5-50.

Bond, G., Broecker, W.S., Johnsen, S., McManus, J., Labeyrie, L., Jouzel, J., and Bonani, G. 1993. Correlations between climate records from North Atlantic sediments and Greenland ice. Nature. 365: 143-147.

Bond, G., Heinrich, H., Broecker, W.S., and 11 others. 1992. Evidence for massive discharges of icebergs into the North Atlantic ocean during the last glacial period. Nature. 360: 245-249.

Bond, G.C., and Lotti, R. 1995. Iceberg discharges into the North Atlantic on Millennial times scales during the last glaciation. Science. 267: 1005-1010.

Bornhold, B.D. 1983. Ice-rafted debris in sediments form leg 71, southwest Atlantic Ocean. Initial Reports of the Deep Sea Drilling Project. LXXI: 307-316.

Bornhold, B.D., and Barrie J.V. 1991. Surficial sediments on the western Canadian continental shelf. Continental Shelf Research. 11: 685-699.

Boulton, G.S. 1978. Boulder shapes and grain-size distributions of debris as indicators of transport paths through a glacier and till genesis. Sedimentology. 25: 773-799.

Boulton, G.S., and Jones, A.S. 1979. Stability of temperate ice caps and ice sheets resting on beds of deformable sediment. Journal of Glaciology. 24: 29-43.

Brigham-Grette, J., and Hopkins, D.M. 1995. Emergent marine record and paleoclimate of the last interglaciation along the northwest Alaskan coast. Quaternary Research. 43: 159-173.

Broccoli, A.J., and Manabe, S. 1987a. The influence of continental ice, atmospheric CO_2, and land albedo on the climate of the last glacial maximum. Climate Dynamics. 1: 87-99.

Broccoli, A.J., and Manabe, S. 1987b. The effects of the Laurentide Ice Sheet on North American climate during the last glacial maximum. Geographie physique et Quaternaire. XLI(2): 291-299.

Broecker, W.S. 1994. Massive iceberg discharges as triggers for global climate change. Nature. 372: 421-424.

Broecker, W.S., Bond, G., and Klas, M. 1990. A salt oscillator in the glacial Atlantic? 1. The concept. Paleoceanography. 5: 469-477.

Budd, W.F., and McInnes, B.J. 1979. Periodic surging of the Antarctic ice sheet - an assessment by modeling. Hydrological Science Bulletin. 24(1): 95-104.

Carlson, P.R., Bruns, T.R., Molnia, B.F., Schwab, W.C. 1982. Submarine valleys in the northeastern Gulf of Alaska: Characteristics and probable origin. Marine Geology. 47: 217-242.

Clague, J.J. 1981. Late Quaternary Geology and Geochronology of British Columbia. Geological Survey of Canada Paper 80-35. 41p.

Clague, J.J. 1989. Cordilleran Ice Sheet. in Fulton, R.J., eds. Quaternary Geology of Canada and Greenland. Geological Society of America, The geology of North America, v. G-1: 40-62.

Clague, J.J., Armstrong, J.E., and Mathews, W.H. 1980. Advance of the Late Wisconsinan Cordilleran ice sheet in southern British Columbia since 22,000 Yr B.P. Quaternary Research. 13: 322-326.

Clark, P.U, and Bartlein, P.J. 1995. Correlation of Late Pleistocene glaciation in the western United States with North Atlantic Heinrich Events. Geology. 23: 483-486.

Clark, P.U. 1994. Unstable behavior of the Laurentide ice sheet over deforming sediment and its implications for climate change. Quaternary Research. 41: 19- 25.

CLIMAP project members. 1976. The surface of the Ice-Age Earth. Science, 191: 1131-1137.

COHMAP project members. 1988. Climatic Changes of the last 18,000 years: Observations and Model simulations. Science. 214: 1043-1052.

Cook, K.H. 1990. The atmosphere's response to the ice sheets of the last glacial maximum. Annals of Glaciology. 14: 32-38.

Cook, K.H., and Held, I.M. 1985. Stationary waves of the ice age climate. Journal of Climate. 1: 807-819.

Cortijo, E., Duplessy, J.C., Labeyrie, L., Leclaire, H., Duprat, J., and van Weering, T.C.E. 1994. Eemian cooling in the Norwegian Sea and North Atlantic ocean preceding continental ice-sheet growth. Nature. 372: 446-449.

Creagaer, J.S., and Scholl, D.W. et al. 1973. Initial Reports of DSDP. 19: 913.

Dansgaard, W., Johnsen, S.J., Clausen, H.B., Dahl-Jensen, D., Gundestrup, N.S., Hammer, C.U., Hvidber, C.S., Steffensen, J.P., Sveinbjörnsdottir, Jouzel, J., And Bond, G. 1993. Evidence for general instability of past climate from a 250- kyr ice core record. Nature. 364: 218-220.

Davis, P.T. 1994. Late-glacial moraines in American Cordillera of Younger Dryas age?: Geological Survey of America Abstracts with Programs. 26(7): A510.

Denton, G.H. 1974. Quaternary glaciations of the White River valley, Alaska, with a regional synthesis for the northern St. Elias Mountains, Alaska and Yukon Territory. Geological Society of America Bulletin. 85: 871-892.

Denton, G.H., Hughes, T.J., and Karlen, W. 1986. Global ice-sheet system interlocked by sea level. Quaternary Research. 26: 3-26.

Ding, Z., Liu, T., Rutter, N.W., Yu, Z., Guo, Z., and Zhu, R. 1995. Ice-volume forcing of East Asian winter monsoon variations in the past 800,000 years. Quaternary Research. 44: 149-159.

Domack, E.W., Anderson, J.B., and Kurtz, D.D. 1980. Clast shape as an indicator of transport and depositional mechanisms in glacial marine sediments: George V continental shelf, Antarctica. Journal of Sedimentary Petrology. 50: 813-820.

Dokken, T.M., and Hald, M. 1996. Rapid climatic shifts during isotope stages 2-4 in the Polar North Atlantic. Geology. 24: 599-602.

Dowdeswell, J.A., and Dowdeswell, E.K. 1988. Debris in icebergs and rates of glacial-marine sedimentation: Observations from spitzbergen and a simple model. Journal of Geology. 97: 221-231.

Drewry, D.J. and Cooper, A.P.R. 1981. Processes and models of Antarctic glaciomarine sedimentation. Annals of Glaciology. 2: 117-122.

Easterbrook, D.J. 1992. Advance and retreat of Cordilleran ice sheets in Washington, USA. Geographie physique et Quaternaire, 46: 51-68.

Engstrom, D.R., Hansen, G.S., and Wright, H.E., Jr. 1990. A possible Younger Dryas record in southeastern Alaska. Science. 250: 1383-1385.

Fanning, A.F., and Weaver, A.J. 1996. Deglacial meltwater episodes: A simulation of the Younger Dryas. Paleoceanography. submitted.

Field, M.H., Huntley, B., Muller, H. 1994. Eemian climate fluctuations observed in a European pollen record. Nature. 371: 779-783.

Fowler, A.C., and Johnson, C. 1995. Hydraulic run-away: A mechanism for thermally regulated surges of ice sheets. Journal of Glaciology. 41: 554-561.

Francois, R., and Bacon, M. 1994. Heinrich events in the North Atlantic: radiochemical evidence. Deep-Sea Research. 41: 315-334,

Fronval, T., Jansen, E., Bloemendal, J, and Johnsen, S. 1995. Oceanic evidence for coherent fluctuations in Fennoscandian and Laurentide ice sheets on millennium timescales. 374: 443-446.

Fulton, R.J., Armstrong, J.E., Fyles, J.G. 1976. Stratigraphy and Palynology of late Quaternary sediments in the Puget Lowland, Washington: Discussion and Reply. Geological Society of America Bulletin. 87:153-156.

Gehrels, G.E., and Berg, H.C. 1994. Geology of Southeastern Alaska. in Plafker, G., and Berg, H.C., eds. The geology of Alaska. Boulder, Colorado, Geological Society of America, The geology of North America. v. G-1: 451-467.

Goethcheus. 1995. Snapshots of the Pleistocene: two buried surfaces on the northern Seward Peninsula. Geological Society of America Abstracts with Programs, Cordilleran section. 27(5): 21.

Gosse, J.C., Evenson, E.B., Klein, J., Lawn, B., and Middleton, R. 1995. Beryllium-10 dating of the duration and retreat of the last Pinedale glacial sequence. Science. 268: 1329-1333.

Griggs, G.B., and Kulm, L.D. 1969. Glacial marine sediments from the northeast Pacific. Journal of Sedimentary Petrology. 39(3): 1142-1148.

Grimm, E.C., Jacobson, G.L., Watts, W.A., Jr., Hansen, B.C.S., Maasch, K.A. 1993. A 50,000-year record of climate oscillations form Florida and its temporal correlation with the Heinrich Events. Science. 261: 198-200.

Guilderson, T.P., Fairbanks, R.G., Rubenstone, J.L. 1994. Tropical temperature variations since 20,000 years ago: Modulating interhemispheric climate change. Science. 263: 663-665.

Guiot, J., de Beaulieu, J.L., Cheddadi, R., David, F., Ponel, P., and Reille, M. 1993. The climate in western Europe during the last glacial/interglacial cycle derived from pollen and insect remains. Palaeogeography, Palaeoclimatology, Palaeocology. 103: 73-93.

Gwiazda, R.H., hemming, S.R., and Broecker, W.S. 1996. Provenance of icebergs during Heinrich event 3 and the contrast to their sources during other Heinrich episodes. Paleoceanography. 11: 371-378.

Hall, N.M.J., Valdes, P.L., and Dong, B. 1996. The maintenance of the last great ice sheets: A UGAMP GCM study. Journal of Climate. 9: 1004-1019.

Haflidason, H., Serjup, H.S., Kristensen, D.K., and Johnsen, S. 1995. Coupled response of the late glacial climate shifts of northwest Europe reflected in Greenland ice cores: Evidence from the northern North Sea. Geology. 23: 1059-1062.

Hamilton, T. D. 1994. Late Cenozoic glaciation of Alaska, in Plafker, G., and Berg, H.C., eds. The geology of Alaska. Boulder, Colorado, Geological Society of America, The geology of North America, v. G-1: 813-842.

Harrison, S.P., Kutzbach, J.E., Prentice, I.C., Behling, P.J., Sykes, M.T. 1995. The response of Northern Hemisphere extratropical climate and vegetation to orbitally induced changes in insolation during the last interglaciation. Quaternary Research. 43: 174-184.

Hebda, R.J. 1983. Late-glacial and postglacial vegetation history at Bear Cove Bog, northeastern Vancouver Island, British Columbia. Canadian Journal of Botany. 61: 3172-3192.

Heinrich, H. 1988. Origin and consequence of cyclic ice rafting in the northeast Atlantic Ocean during the past 130,000 years. Quaternary Research. 29:143-152.

Heiser, P.A., Mann, D.H., and Hopkins, D.M. 1995. Testing alternative models of glacier extent in Beringia during the last glacial maximum. Geological Society of America Abstracts with Programs, Cordilleran section. 27(5): 25.

Herzer, R.H., and Bornhold, B.D. 1982. Glaciation and post-glacial history of the continental shelf off southwestern Vancouver Island, British Columbia. Marine Geology. 48: 285-319.

Heusser, C.J. 1972. Palynology and phytogeograhical significance of a late-Pleistocene refugium near Kalaloch, Washington. Quaternary Research. 2: 189-201.

Heusser, C.J. 1977. Quaternary palynology of the Pacific slope of Washington. Quaternary research. 8: 282-306.

Hicock, S.R. 1990. Last interglacial Muir Point formation, Vancouver Island, British Columbia. Geographie physique et Quaternaire. 44(3): 337-341.

Hicock, S.R., Hebda, R.J., and Armstrong, J.E. 1982. Lag of Fraser glacial maximum in the Pacific Northwest: Pollen and macrofossil evidence from western Fraser Lowland, British Columbia. Canadian Journal of Earth Science. 19: 2288-2896.

Hovan, S.A., Rea, D.K., and Pisias, N.G. 1991. Late Pleistocene continental climate and oceanic variability recorded in northwest Pacific sediments. Paleoceanography. 6(3): 349-370.

Howes, D.E. 1981. Late Quaternary sedimentation and geomorphic history of north-central Vancouver Island. Canadian Journal of Earth Science. 18: 1-12.

Howes, D.E. 1983. Late Quaternary sedimentation and geomorphic history of northern Vancouver Island. Canadian Journal of Earth Science. 20: 57-65.

Hu, F.S., Brubaker, L.B., and Anderson, P.M. 1995. Postglacial vegetation and climate change in the northern Bristol Bay region, southwestern Alaska. Quaternary Research. 43: 382-392.

Hughes, T. 1983. On the disintegration of ice shelves: the role of fracture. Journal of Glaciology. 29(101): 98-117.

Hughes, T. 1992. Theoretical calving rates from glaciers along ice walls rounded in water of variable depths. Journal of Glaciology. 38(192): 282-294.

Hunter, L.E., Powell, R.D., and Lawson, D.E. 1996. Flux of debris transported by ice at three Alaskan tidewater Glaciers. Journal of Glaciology. 12(140): 123-134.

Jackson, L.E., Rutter, N.W., Hughes, O.L., and Clague, J.J. 1989. Glaciated fringe (Quaternary stratigraphy and history, Canadian Cordillera). in Fulton, R.J., eds. Quaternary Geology of Canada and Greenland. Geological Society of America, The geology of North America, v. G-1. p. 63-68.

Jansen, J.H., Kuipers, A., and Troelstra, S.R. 1986. A mid-Brunhes climatic event: long-term changes in global atmosphere and ocean circulation. Science. 232: 619-622.

Johnsen, S.J., Clausen, H.B., Dansgaard, W., Gundestrup, N.S., Hammer, C.U., and Tauber, H. 1995. The Eem stable isotope record along the GRIP ice core and its interpretation. Quaternary Research. 43: 117-124.

Josenhans, H.W., Barrie, J.V., Conway, K.W., Patterson, R.T., Mathews, R.W., and Woodsworth, G.J. 1993. Surficial geology of the Queen Charlotte Basin: evidence of submerged proglacial lakes at 170 m on the continental shelf of western Canada. in Current Research, Part A: Geological Survey of Canada Paper 93-1A. p. 119-127.

Jouzel, J., Vaikmae, R., Petit, J.R., Martin, M., Duclos, Y., Stievenard, M., Lorius, C., Toots, M., Mélières, M.A., Burckle, L.H., Barkov, N.I., Kotlyakov, V.M. 1995. The two-step shape and timing of the last deglaciation in Antarctica. Climate Dynamics. 11: 151-161.

Kaufman, D.S., Forman, S.L., Lea. P.D., and Wobus, C.W. 1996. Age of Pre-late-Wisconsinan glacial-esturine sedimentation, Bristol Bay, Alaska. Quaternary Research. 45: 59-72.

Keany, J., Ledbetter, M., Watkins, N., Huang, T. 1976. Diachronous deposition of ice-rafted debris in sub-Antarctic deep-sea sediments. Geological Society of America Bulletin. 87: 873-882.

Kent, D., Odpyke, N.D., and Ewing, M. 1971. Climate change in the North Pacific using ice- rafted detritus as a climatic indicator. Geological Society of America Bulletin. 82: 2741-2754.

Kline, J.T., and Bundtzen, T.K. 1986. Two glacial records from west-central Alaska. in Hamilton, T.D., Reed, K.M., and Thorson, R.M., eds. Glaciation in Alaska: The geologic record. Alaska Geological Society. p. 123-150.

Kotilainen, A.T. and Shackleton, N.J. 1995. Rapid climate variability in the North Pacific Ocean during the past 95,000 years. Nature. 377: 323-326.

Kulm, L.D. and others. 1973. Site 172. Initial reports of the DSDP. XVIII: 15-30.

Kunz, M.L., and Reiner, R.E. 1994. Paleoindians in Beringia: Evidence form Arctic Alaska. Science. 263: 660-662.

Kutzbach, J.E., and Guetter, P.J. 1986. The influence of changing orbital parameters and surface boundary conditions on climate simulations for the past 18,000 years. Journal of Geophysical Research. 43: 1727-1759.

Lauritzen, S-E. 1995. High-resolution paleotemperature proxy record for the last interglaciation based on Norwegian speleothems. Quaternary Research. 43: 133-146.

Lea, P.D., Elias, S.A., and Short, S.K. 1991. Stratigraphy and paleoenvironments of Pleistocene nonglacial deposits in southern Nushagak lowland, southwestern Alaska, U.S.A. Arctic and Alpine Research. 23 (4): 375-391.

Licht, K.J., Jennings. A.E., Andrews, J.T., and Williams, K.M. 1996. Chronology of Late Wisconsinan ice retreat form the western Ross Sea, Anarctica. Geology. 24: 223-226.

Linsley, B.K. 1996. Oxygen-isotope record of sea level and climate variations in the Sulu Sea over the past 150,000 years. Nature. 380: 234-237.

Liu, T., Broecker, W.S., Hajdas, I., and Bonani, G. 1996. North Atlantic climatic changes correlated with rock varnish microlaminae in the Death Valley region, southwestern USA. Geology. submitted.

Lowell, T.V., Heusser, B.G., Anderson, P.I., Moreno, A. H., Heusser, L.E., Schluchter, C., Marchant, D.R., and Denton, G.H. 1995. Interhemispheric correlation of Late Pleistocene glacial events. Science. 269: 1541-1548.

Luternauer, J.L., and Murray, J.W. 1983. Late Quaternary morphologic development and sedimentation, central British Columbia continental shelf. Geological Survey of Canada Paper 83-21. p.31.

Luternauer, J.L., Conway, K.W., Barrie, J.V., Blaise, B., and Mathews, R.W. 1989a. Late Pleistocene terrestrial deposits on the continental shelf of western Canada: Evidence for rapid sea-level change at the end of the last glaciation. Geology. 17: 357-360.

Luternauer, J.L., Conway, K.W., Clague, J.J., and Blaise, B. 1989b. Late Quaternary Geology and Geochronology of the central shelf of western Canada. Marine Geology. 89: 57-68.

MacAyeal, D.R. 1992. Irregular oscillations of the West Antarctic ice sheet. Nature. 350: 29-32.

MacAyeal, D.R. 1993. Binge/purge oscillations of the Laurentide Ice Sheet as a cause of the North Atlantic's Heinrich Events. Paleoceanography. 8(6): 775-784.

MacDonald, D. 1996. M.Sc. Thesis. University of British Columbia. Department of Oceanography. In preparation.

Manabe, S., and Broccoli, A.J. 1985. The influence of continental ice sheets on climate of an ice age. Journal of Geophysical Research. 90(D1): 2167-2190.

Mann, D.E., and Peteet, D.M. 1994. Extent and timing of the last glacial maximum in southwestern Alaska. Quaternary Research. 42: 136-148.

Mann, D.H. 1986a. Wisconsinan and Holocene glaciation of southeast Alaska. in Hamilton, T.D., Reed, K.M., and Thorson, R.M., eds. Glaciation in Alaska: The geologic record. Alaska Geological Society. p. 237-265.

Mann, D.H. 1986b. Reliability of a fjord glacier's fluctuations for paleoclimatic reconstructions. Quaternary Research. 25: 10-24.

Mathews, R.W., Heusser, L.E., and Patterson, R.T. 1993. Evidence for a Younger Dryas-like cooling event on the British Columbia coast. Geology. 21: 101-104.

McMannus, J.F., Bond, G.C., Broecker, W.S., Johnsen, S., Labeyrie, L., and Higgins, S. 1994. High-resolution climate record form the North Atlantic during the last interglacial. Nature. 371: 326-329.

Mickelson, D.M., Acomb, L.J., and Bentley, C.R. 1981. Possible mechanism for the rapid advance and retreat of the Lake Michigan lobe between 13 000 and 11 000 years BP (abstract only). Annals of Glaciology. 2: 185-186.

Molnia, B.F. 1986. Glacial history of the northeastern Gulf of Alaska - A synthesis. in Hamilton, T.D., Reed, K.M., and Thorson, R.M., eds. Glaciation in Alaska-The geologic record. Alaska Geological Society. p. 193-218.

Moore, T.C. 1973. Late Pleistocene-Holocene oceanographic changes in the Northeastern Pacific. Quaternary Research. 3: 99-109.

Morley, J.J., Pisias, N.G., and Leinen, M. 1987. Late Pleistocene time series of atmospheric and oceanic variables recorded in sediments form the subarctic Pacific. Paleoceanography. 2(1): 49-62.

Oppo, D.W., and Lehman, S.J. 1994. Suborbital timescale variability of North Atlantic Deep Water. Paleoceanography. 10: 901-910.

Orelemans, J. 1993. Evaluating the role of climate cooling in iceberg production and Heinrich events. Nature. 364: 783-786.

Patterson, T.R., Guilbault, J., Thomson, R.E., and Luternauer, J.L. 1995. Foraminiferal evidence of the Younger Dryas age cooling on the British Columbia shelf. Geographie physique et Quaternaire. 49: 409-428.

Phillips, F.M., Campbell, A.R., Smith, G.I., and Bischoff, J.L. 1994. Interstadial climate cycles: A link between western North America and Greenland? Geology. 22: 1115-1118.

Plafker, G., Moore, J.C., and Winkler, G.R. 1994. Geology of the southern Alaska margin. in Plafker, G., and Berg, H.C., eds. The geology of Alaska. Boulder, Colorado, Geological Society of America, The geology of North America. v. G-1: 389-449.

Porter, S.C., and Zhisheng, A. 1995. Correlation between climate events in the North Atlantic and China during the last glaciation. Nature. 375: 3053-308.

Powell, R. D. 1984. Glacialmarine processes and inductive lithofacies modeling of ice shelf and tidewater glacier sediments based on Quaternary examples. Marine Geology. 57: 1-52.

Powers, M.C. 1953. A new roundness scale for sedimentary particles. Journal of Sedimentary Petrology. 23: 117-119.

Ramnathan, V., Cess, R.D., Harrison, E.F., Minnis, P., Barkstrom, B.R., Ahmad, E., and Artman, D. 1989. Cloud-radiative forcing of climate: Results from the Earth radiation Budget Experiment. Science. 267: 57-63.

Rea, D., and ODP leg 145 members. 1993. Paleoceanographic record of North Pacific quantified. EOS transaction. AGU. Sept 7. 1993.

Rea, D., and Schrader, H. 1985. Late Pliocene onset of glaciation: Ice-rafting and diatom stratigraphy of North Pacific DSDP cores. Paleogeography, Plaeoclimatology, Paleoecology. 49: 313-325.

Reasoner, M.A., Osborn, G., and Rutter, N.W. 1994. The age of the Crowfoot moraine system in the Canadian Rocky Mountains: A glacial event coeval with the Younger Dryas oscillation. Geology. 439-442.

Rind, D. 1987. Components of the Ice Age circulation. Journal of Geophysical Research. 92: 4241-4281.

Sancetta, C., and Silvestri, S. 1986. Pliocene-Pleistocene evolution of the North Pacific ocean-atmosphere system, interpreted form fossil diatoms. Paleoceanography. 1(1): 163-180.

Schmoll, H.R., Szabo, B.J., Rubin, M., and Dobrovolny, E. 1972. Radiometric dating of marine shells from the Bootlegger Cove Clay, Anchorage area, Alaska. Geological Society of America Bulletin. 83: 1107-1113.

Shaffer, G., and Bendtsen, J. 1994. Role of the Bering Strait in controlling North Atlantic ocean circulation and climate. Nature. 367: 354-357.

Shaw, J. 1989. Drumlins, subglacial meltwater floods, and ocean responses. Geology. 17: 853-856.

Sirocko, F., Garbe-Schönberg, D., McIntyre, A., and Molfino, B. 1996. Teleconnections between the Subtropical Monsoons and high-latitude climates during the last deglaciation. Science. 272: 526-529.

Sowers, T., and Bender, M. 1995. Climate records covering the last deglaciation. Science. 269: 210-214.

Thomson, J., Higgs, N.C., and Clayton, T. 1995. A geochemical criterion for the recognition of Heinrich events and estimation of their depositional fluxes by the $(^{230}Th_{excess})_0$ profiling method. Earth and Planetary Science Letters. 135: 41-56.

Thorson, R.M. 1986. Late Cenozoic glaciation of the northern Nenana River valley. in Hamilton, T.D., Reed, K.M., and Thorson, R.M., eds. Glaciation in Alaska: The geologic record. Alaska Geological Society. p. 99-121.

Thouveny, N., de Beaulieu, J.L., Bonifay, E., Creer, K.M., Guiot, J., Icole, M., Johnsen, S., Jouzel, J., Reille, M., Williams, T., and Williams, D. 1994. A high resolution record of the last climate cycle in western Europe from magnetic susceptibility in Maar Lake sequences. Nature: 371: 503-506.

Thunnell, R.C., and Mortyn, G.P. 1995. Glacial climate instability in the Northeast Pacific Ocean. Nature. 376: 504-506.

Toggweiler, J.R., and Samuels, B. 1995. Effect of Drake Passage on the global thermohaline circulation. Deep-Sea Research. 42: 477-500.

van Kreveld, S.A., and Knappertsbusch, M., Ottens, J., and Ganssen, G.M., and van Hinte, J.E. 1996. Biogenic carbonate and ice-rafted debris (Heinrich layer) accumulation in deep-sea sediments from a Northeast Atlantic piston core. Marine Geology. 131: 21-46.

Von Huene, R., Crouch, J. and Larson, E. 1976. Glacial advance in the Gulf of Alaska area implied by ice-rafted material. Geological Society of America Memoirs. 145: 411-422.

Von Huene, R., Larson, E., and Crouch, J. 1973. Preliminary study of ice-rafted erratics as indicators of glacial advances in the Gulf of Alaska. Initial Reports of the DSDP. 18: 835-842.

Warner, B.G., Clague, J.J., and Mathews, R. 1984. Geology and Paleoecology of a Mid-Wisconsinan peat from the Queen Charlotte islands, British Columbia, Canada. Quaternary Research. 21: 337-350.

Warnke, D.E. 1970. Glacial erosion, ice rafting, and glacial-marine sediments: Antarctica and the Southern Ocean. American Journal of Science. 269: 276- 294.

Watts, W.A., Jr., Hansen, B.C.S. 1994. Pre-Holocene and Holocene pollen records of vegetation history from the Florida peninsula and their climatic implications. Palaeogeography, Palaeoclimatology, Palaeoecology. 109: 163-176.

Weaver, A.J., and Hughes, T.M.C. 1994. The ocean as a source for rapid interglacial climate fluctuations. Nature. 367: 447-450.

Weertman, J. 1974. Stability of the junction of an ice sheet and ice shelf. Journal of Glaciology. 13: 3-11.

Wijffels, S.E., Schmitt, R.W., Bryden, H.L., Stigebrandt, A. 1992. Transport of freshwater by the oceans. Journal of Physical Oceanography. 22: 155-162.

Zhan, R., Pedersen, T.F., Bornhold, B.D., and Mix, A.C., 1991. Water mass conversion in the glacial subarctic Pacific (54N,148W): Physical constraints and benthic-planktonic stable isotope record. Paleoceanography. 6: 543-560.

Appendix A: Mass of IRD (lithic debris in the size range 180-500 mm) in ODP-887.

Depth m	grams IRD	volume cc	Depth m	grams IRD	volume cc	Depth m	grams IRD	volume cc
0.12	0.02	10	3.39	0.05	10	6.16	0	10
0.22	0	10	3.46	0.02	10	6.26	0	10
0.32	0	10	3.55	0.16	10	6.36	0	10
0.42	0.03	10	3.62	0.38	10	6.46	0	10
0.52	0	10	3.66	0.16	10	6.55	0	10
0.58	0.01	10	3.72	0	10	6.76	0	10
0.62	0	10	3.74	0.18	10	6.81	0.02	10
0.67	0.01	10	3.76	0.2	10	6.86	0.04	10
0.72	0.07	10	3.82	0.08	10	6.91	0.39	10
0.77	0.15	10	3.86	0.24	10	6.96	0.32	10
0.82	0.36	10	3.91	0.11	10	7.01	0.37	10
0.86	0.15	10	3.96	0.27	10	7.06	0.67	10
0.92	0.4	10	4.01	0.08	10	7.11	0.36	10
0.97	0.1	10	4.06	0.67	10	7.16	0.1	10
1.02	0.22	10	4.11	0.2	10	7.21	0.09	10
1.065	0.11	10	4.19	0.28	10	7.26	0.19	10
1.12	0.22	10	4.21	0.23	10	7.31	0.06	10
1.17	0.09	10	4.26	0.37	10	7.36	0.24	10
1.22	0.16	10	4.31	0.22	10	7.41	0.19	10
1.28	0.08	10	4.36	0.41	10	7.46	0.77	10
1.31	0.09	10	4.42	0.19	10	7.52	0.47	10
1.375	0.29	10	4.46	0.25	10	7.57	0.29	10
1 42	0.52	10	4.52	0.28	10	7.66	0.12	10
1.52	0.75	10	4.56	0.05	10	7.86	0.02	10
1.58	0.31	10	4.61	0.08	10	7.96	0.03	10
1.61	0.31	10	4.63	0	10	8.06	0.03	10
1.67	0.16	10	4.66	0	10	8.16	0.02	10
1.72	0.24	10	4.71	0.02	10	8.22	0.02	10
1.78	0.14	10	4.74	0	10	8.26	0.12	10
1.81	0.04	10	4.84	0	10	8.32	0.15	10
1.85	0.41	10	4.94	0	10	8.365	0.07	10
1.94	0.21	10	5.06	0	10	8.42	0.06	10
2.01	0.24	10	5.16	0	10	8.46	0.07	10
2.14	0.37	10	5.21	0	10	8.52	0.04	10
2.21	0.3	10	5.25	0	10	8.565	0.06	10
2.36	0.16	10	5.31	0	10	8.64	0.04	10
2.41	0.22	10	5.36	0.01	10	8.72	0.05	10
2.53	0.12	10	5.43	0.61	10	8.77	0.07	10
2.61	0.23	10	5.46	0.25	10	8.86	0.66	10
2.71	0.27	10	5.49	0.49	10	8.92	0.42	10
2.81	0.1	10	5.55	0.21	10	8.97	0.03	10
2.89	0	10	5.6	0.03	10	9.02	0.05	10
2.96	0	10	5.66	0	10	9.06	0.1	10
3.06	0	10	5.76	0	10	9.11	0.54	10
3.13	0.19	10	5.86	0	10	9.16	0.39	10
3.23	0.21	10	5.96	0	10	9.22	0.16	10
3.3	0.23	10	6.06	0	10	9.26	0.14	10

Appendix B: Mass of IRD (lithic debris in the size range 180-500 mm) in PAR87A-01.

Depth m	grams IRD	volume cc	Depth m	grams IRD	volume cc	Depth m	grams IRD	volume cc
0.04	0.04	16	2.38	0	16	5.86	0.75	16
0.12	0	16	2.45	0.15	16	5.91	0.54	16
0.22	0.04	16	2.55	0.4	16	5.97	0.22	16
0.26	0.03	16	2.82	0.8	16	6.01	0.07	16
0.32	0.16	16	2.86	0.96	16	6.07	0	16
0.36	0.18	16	2.89	0.54	16	6.14	0.33	16
0.42	0.42	16	2.95	0.25	16	6.18	0.03	16
0.485	0.49	16	3.02	0.27	16	6.29	0	16
0.53	0.22	16	3.09	0.91	16	6.4	0.16	16
0.58	0.41	16	3.12	0.69	16	6.44	0.26	16
0.63	0.18	16	3.17	0.82	16	6.48	0.19	16
0.68	0.34	16	3.21	0.64	16	6.55	0.11	16
0.72	0.21	16	3.23	0.54	16	6.59	0.11	16
0.775	0.26	16	3.29	0.48	16	6.66	0.07	16
0.82	0.47	16	3.34	0.65	16	6.7	0.11	16
0.875	0.7	16	3.38	0.64	16	6.76	0.26	16
0.92	0.25	16	3.4	0.59	16	6.8	1.81	16
0.96	0.24	16	3.51	0.59	16	6.87	0.16	16
0.98	0.74	16	3.56	0.58	16	6.91	0.08	16
1.03	0.7	16	3.6	0.52	16	6.96	0.07	16
1.08	0.66	16	3.62	0.61	16	6.98	0.4	16
1.13	0.45	16	3.66	0.36	16	7.01	0.43	16
1.23	0.18	16	3.7	0	16	7.06	0.27	16
1.26	0.75	16	3.78	0	16	7.08	0.43	16
1.3	0.36	16	3.91	0	16	7.12	0.11	16
1.35	0.41	16	3.98	0	16	7.18	0.02	16
1.45	0.43	16	4.11	0.63	16	7.22	0.04	16
1.47	0.5	16	4.15	0.04	16	7.33	0	16
1.52	0.49	16	4.21	0.98	16	7.35	0	16
1.57	0.47	16	4.31	0.51	16	7.44	0.07	16
1.59	0.45	16	4.39	0	16	7.51	0.08	16
1.61	0.41	16	4.575	0	16	7.56	0.07	16
1.66	0.94	16	4.77	0	16	7.63	0.61	16
1.705	0.68	16	4.95	0	16	7.685	0.13	16
1.77	0.41	16	5.135	0	16	7.75	0.39	16
1.82	0.33	16	5.18	0.02	16	7.79	0.77	16
1.87	0.24	16	5.24	0.59	16	7.85	0.99	16
1.91	0.35	16	5.3	0.78	16	7.89	0.61	16
1.95	0.46	16	5.35	1.48	16	7.99	1.22	16
2	0.55	16	5.4	0.63	16	8.04	0.54	16
2.05	0.48	16	5.47	0.42	16	8.08	0.96	16
2.1	0.41	16	5.53	0.27	16	8.13	0.72	16
2.14	0.16	16	5.56	0.16	16	8.18	1.52	16
2.19	0.24	16	5.6	0.06	16	8.24	0.37	16
2.23	0.36	16	5.65	0.11	16	8.29	1.25	16
2.28	0.46	16	5.69	0.95	16	8.36	0.59	16
2.31	0.22	16	5.75	1.08	16	8.44	0.54	16
2.36	0.22	16	5.8	1.06	16			

Appendix C: Mass of IRD (lithic debris in the size range 180-500 μm) in PAR87A-02

Depth m	grams IRD	volume cc
0.015	0.02	16
0.065	0	16
0.115	0	16
0.165	0	16
0.215	0	16
0.265	0	16
0.31	0	16
0.365	0	16
0.415	0	16
0.465	0.11	16
0.515	0.26	16
0.565	0.29	16
0.615	0.51	16
0.665	0.62	16
0.715	0.7	16
0.815	0.17	16
0.865	0.24	16
0.915	0.42	16
0.965	0.42	16
1.015	0.33	16
1.065	0.45	16
1.115	0.28	16
1.165	0.65	16
1.215	0.7	16
1.265	1.13	16
1.315	1.49	16
1.365	1.13	16
1.415	0.58	16
1.47	0.39	16
1.515	0.43	16
1.57	0.29	16
1.615	1.24	16
1.665	1	16
1.765	1.32	16
1.815	0.6	16
1.885	0.43	16
1.915	0.93	16
1.965	1.61	16
2.015	0.55	16

Appendix D: Mass of IRD (lithic debris in the size range 180-500 mm) in PAR87A-10.

Depth m	grams IRD	volume cc	Depth m	grams IRD	volume cc	Depth m	grams IRD	volume cc
0.04	0.03	16	2.18	0.9	16	4.73	0	16
0.07	0.02	16	2.21	0.37	16	4.77	0	16
0.1	0.01	16	2.27	0.13	16	4.82	0	16
0.135	0	16	2.31	0.35	16	4.87	0	16
0.165	0.02	16	2.38	0.69	16	4.91	0.14	16
0.19	0.02	16	2.43	0.47	16	5	0.33	16
0.23	0.02	16	2.47	0.28	16	5.02	0.58	16
0.28	0.05	16	2.5	0.36	16	5.06	0.56	16
0.32	0	16	2.56	0.18	16	5.14	0.16	16
0.37	0	16	2.6	0.27	16	5.2	0	16
0.41	0	16	2.63	0.41	16	5.25	0	16
0.46	0	16	2.69	0.01	16	5.3	0	16
0.5	0.03	16	2.75	0.02	16	5.35	0	16
0.55	0	16	2.79	0	16	5.4	0	16
0.56	0	16	2.84	0	16	5.46	0	16
0.59	0.04	16	2.9	0	16	5.51	0	16
0.64	0.13	16	2.95	0.04	16	5.55	0	16
0.68	0.24	16	3.01	0.7	16	5.59	0	16
0.73	0.2	16	3.05	0.24	16	5.64	0	16
0.74	0.41	16	3.16	0.27	16	5.69	0	16
0.77	0.52	16	3.23	0.05	16	5.77	0	16
0.79	0.26	16	3.29	0	16	5.82	0	16
0.81	0.42	16	3.35	0.12	16	5.87	0	16
0.83	0.52	16	3.39	0.45	16	5.92	0	16
0.87	0.32	16	3.45	0.85	16	5.96	0	16
0.9	0.38	16	3.48	0.55	16	6.01	0.36	16
0.92	0.31	16	3.54	0.45	16	6.05	1.39	16
1.02	0.2	16	3.58	0.14	16	6.11	1.15	16
1.06	0.12	16	3.62	0.51	16	6.18	0.38	16
1.08	0.29	16	3.66	0.64	16	6.2	0.52	16
1.11	0.21	16	3.72	0.64	16	6.23	0.51	16

Appendix D continued

Depth m	grams IRD	volume cc	Depth m	grams IRD	volume cc	Depth m	grams IRD	volume cc
0.79	0.26	16	3.29	0	16	5.82	0	16
0.81	0.42	16	3.35	0.12	16	5.87	0	16
0.83	0.52	16	3.39	0.45	16	5.92	0	16
0.87	0.32	16	3.45	0.85	16	5.96	0	16
0.9	0.38	16	3.48	0.55	16	6.01	0.36	16
0.92	0.31	16	3.54	0.45	16	6.05	1.39	16
1.02	0.2	16	3.58	0.14	16	6.11	1.15	16
1.06	0.12	16	3.62	0.51	16	6.18	0.38	16
1.08	0.29	16	3.66	0.64	16	6.2	0.52	16
1.11	0.21	16	3.72	0.64	16	6.23	0.51	16
1.14	0.11	16	3.76	0.37	16	6.27	0.22	16
1.17	0.16	16	3.83	0.72	16	6.29	1.43	16
1.21	0.08	16	3.9	0.54	16	6.33	0.63	16
1.24	0.05	16	3.93	0.69	16	6.39	1.13	16
1.37	1.95	16	3.97	0.55	16	6.43	2.18	16
1.4	0.64	16	4.06	0.53	16	6.49	0.31	16
1.47	0.72	16	4.1	0.49	16	6.53	0.04	16
1.505	0.89	16	4.15	0.55	16	6.6	0	16
1.585	0.34	16	4.21	0.56	16	6.64	0.4	16
1.63	0.38	16	4.25	0.3	16	6.69	0	16
1.66	0.29	16	4.31	0	16	6.73	0.1	16
1.71	0.23	16	4.36	0	16	6.79	0.26	16
1.855	0.4	16	4.41	0	16	6.83	0.11	16
1.91	0.55	16	4.45	0	16	6.88	0.11	16
1.94	0.25	16	4.49	0	16	6.92	0.33	16
1.98	0.32	16	4.53	0	16	6.98	0.18	16
2.03	0.74	16	4.63	0	16	7.02	0.39	16
2.09	0.57	16	4.68	0	16			
2.13	0.86	16	4.72	0	16			

Appendix E: Mass of IRD (lithic debris in the size range 180-500 μm) in PAR85-01.

Depth m	grams IRD	volume cc	Depth m	grams IRD	volume cc	Depth m	grams IRD	volume cc
0	0	8	4.35	0	8	8.69	0.01	8
0.5	0	8	4.55	0	8	8.84	0.02	8
0.6	0	8	4.65	0	8	8.89	0.01	8
0.7	0	8	4.72	0	8	8.99	0	8
0.71	0	8	4.85	0	8	9.09	0.01	8
0.8	0	8	4.95	0.03	8	4.65	0	8
0.9	0	8	5.25	0	8	9.19	0.03	8
0.98	0	8	5.35	0	8	9.29	0.01	8
0.99	0	8	5.41	0	8	9.35	0.02	8
1	0	8	5.45	0	8	9.39	0	8
1.1	0	8	5.48	0	8	9.49	0	8
1.2	0	8	5.58	0	8	9.59	0	8
1.4	0	8	5.68	0	8	9.64	0.01	8
1.5	0.03	8	5.78	0	8	9.69	0	8
1.6	0.1	8	5.88	0	8	9.79	0	8
1.7	0	8	5.98	0	8	9.89	0	8
1.8	0.07	8	6.08	0	8	9.99	0.01	8
1.9	0	8	6.28	0	8	10.17	0.01	8
2	0	8	6.38	0	8	10.27	0	8
2.1	0	8	6.48	0	8	10.37	0.01	8
2.2	0	8	6.58	0	8	10.42	0.02	8
2.22	0	8	6.68	0	8	10.47	0	8
2.3	0.04	8	6.79	0	8	10.57	0.01	8
2.4	0	8	6.81	0	8	10.67	0	8
2.52	0	8	6.88	0	8	10.77	0.02	8
2.6	0	8	6.98	0	8	10.87	0	8
2.72	0	8	7.01	0.03	8	10.97	0	8
2.82	0	8	7.09	0	8	11.07	0	8
2.92	0.07	8	7.21	0	8	11.17	0	8
3.02	0.18	8	7.31	0	8	11.27	0	8
3.12	0	8	7.41	0	8	11.37	0	8
3.2	0	8	7.61	0	8			
3.22	0	8	7.63	0	8			
3.32	0.61	8	7.71	0	8			
3.42	0.04	8	7.81	0.01	8			
3.52	0.24	8	7.91	0	8			
3.62	0	8	8	0	8			
3.72	0	8	8.01	0	8			
3.82	0	8	8.11	0	8			
3.92	0	8	8.21	0.01	8			
4.04	0	8	8.31	0	8			
4.05	0.02	8	8.42	0	8			
4.15	0.02	8	8.51	0.01	8			
4.25	0	8	8.59	0.02	8			

Appendix F: Petrology of IRD grains (500-5000 μm) in ODP-887

ODP 887	NUMBER OF GRAINS								
Depth (m)	Quartz grains	Plutonic rocks	Feldspar grains	Basalt	Other Volcanics	Slate & Argillite	Sand Stone	Quartzite	Total # of grains
0.82	23	0	3	6	19	35	31	15	**132**
0.92	46	3	3	5	11	56	20	16	**160**
1.02	39	0	6	7	12	30	19	13	**126**
1.12	31	2	6	6	15	45	19	13	**137**
1.22	15	3	3	0	8	37	21	8	**95**
1.375	27	3	4	9	18	83	56	22	**222**
1.42	83	1	8	10	23	120	52	34	**331**
1.58	40	2	4	9	21	80	57	24	**237**
1.61	31	0	1	9	9	87	36	18	**191**
1.67	19	1	1	0	0	45	31	13	**110**
1.72	12	0	1	3	12	53	33	17	**131**
1.81	21	0	0	2	7	79	33	12	**154**
2.14	49	0	2	4	12	46	54	20	**187**
2.21	29	0	2	3	5	29	25	11	**104**
2.71	13	0	0	0	4	25	32	12	**86**
3.62	36	2	1	3	6	21	24	11	**104**
3.86	23	2	3	6	9	27	16	15	**101**
4.06	46	4	1	3	15	53	31	20	**173**
4.11	25	3	2	7	8	40	28	18	**131**
4.19	76	3	6	7	22	151	67	24	**356**
4.21	22	2	1	2	10	64	40	15	**156**
4.36	61	3	3	4	22	91	94	22	**300**
4.42	25	3	1	7	6	47	16	12	**117**
4.46	48	1	4	7	12	70	88	18	**248**
4.52	31	1	1	3	8	53	41	19	**157**
5.46	20	2	0	4	10	32	50	25	**143**
5.49	53	2	2	9	13	90	85	50	**304**
5.55	17	3	1	0	11	32	46	12	**122**
6.91	58	1	3	3	9	75	35	22	**206**
6.96	23	2	2	1	10	37	31	17	**123**
7.06	43	1	6	2	12	33	57	13	**167**
7.11	39	2	2	4	15	18	27	16	**123**
7.36	37	2	2	5	3	16	48	26	**139**
7.52	45	2	1	2	11	48	47	17	**173**
8.86	48	0	2	2	7	35	39	24	**157**
8.92	32	0	3	1	10	32	25	16	**119**
9.06	41	2	2	1	21	39	42	31	**179**
9.11	60	5	3	3	20	87	102	30	**310**
9.16	38	0	3	0	8	59	52	16	**176**
10.76	53	4	4	1	8	31	64	23	**188**

Appendix G: Petrology of IRD grains (500-5000 μm) in PAR87A-10

PAR87A-10	NUMBER OF GRAINS			
Depth (m)	Quartz grains	Feldspar grains	Other grains	Total # of grains
0.68	16	1	88	**105**
0.77	23	2	82	**107**
0.83	34	3	119	**156**
0.87	19	2	81	**102**
1.08	23	2	104	**129**
1.11	21	2	118	**141**
1.4	46	4	219	**269**
1.47	50	4	233	**287**
1.505	45	5	250	**300**
1.585	25	3	154	**182**
1.66	21	3	153	**177**
1.71	16	2	112	**130**
1.855	27	3	163	**193**
1.91	31	3	135	**169**
2.09	52	2	106	**160**
2.13	76	4	212	**292**
2.18	60	4	177	**241**
2.21	24	2	80	**106**
2.31	20	1	75	**96**
2.38	63	3	164	**230**
2.43	42	2	101	**145**
2.63	34	2	94	**130**
3.01	50	3	144	**197**
3.39	35	2	68	**105**
3.45	80	4	150	**234**
3.48	43	2	104	**149**
3.54	55	3	130	**188**
3.62	55	4	235	**294**
3.66	81	7	366	**454**
3.72	62	6	351	**419**
3.76	64	4	194	**262**
3.83	77	6	325	**408**
3.9	68	5	263	**336**
3.97	48	5	303	**356**
4.1	55	5	242	**302**

Appendix H: Petrology of IRD grains (500-5000 μm) in PAR85-01

PAR85-01	NUMBER OF GRAINS								
Depth (m)	Quartz grains	Plutonic rocks	Feldspar grains	Basalt	Other Volcanics	Slate & Argillite	Sand Stone	Quartzite	Total # of grains
1.6	18	0	0	0	0	1	5	2	**26**
1.8	11	0	0	0	2	0	1	2	**16**
2.3	14	0	0	1	0	0	3	2	**20**
3.02	17	2	0	0	4	0	5	2	**30**
3.32	184	33	3	8	11	8	19	28	**294**
3.52	39	3	0	0	3	0	5	6	**56**
3.72	0	0	0	0	0	0	0	1	**1**
6.78	1	1	0	0	0	1	0	0	**3**
8.41	0	0	0	0	0	0	1	0	**1**
9.18	2	0	0	0	0	0	1	0	**3**
10.41	4	0	0	0	0	0	1	1	**6**

VITA

Surname: Hewitt Given Names: Antony Trevor

Place of Birth: Belfast, Northern Ireland

Educational Institutions Attended:

University of Victoria	1988 to 1994
University of Victoria	1994 to 1996

Degrees Awarded:

B.Sc.	University of Victoria	1994

PARTIAL COPYRIGHT LICENSE

I Hereby grant the right to lend my thesis to users of the University of Victoria Library, and to make single copies only for such users or in response to a request from the Library or any other university, or similar institution, on its behalf or for one of its users. I further agree that permission for extensive copying of this thesis for scholarly purposes may be granted by me or a member of the University designated by me. It is understood that copying or publication of this thesis for financial gain shall not be allowed without my written permission.

Title of Thesis:

A high resolution record of ice-rafting in the Northeast Pacific

Authour [redacted]
Antony Trevor Hewitt
September 30, 1996